Synthesis of Carotenoid-Containing Polyesters and Protein Engineering to Improve Synthetic Efficiency of *Pseudomonas fluorescens* Esterase

A DISSERTATION SUBMITTED TO THE
GRADUATE SCHOOL OF THE UNIVERSITY OF
MINNESOTA
BY

Yun Jiang

IN PARTIAL FULFILLMENT OF THE
REQUIREMENTS FOR THE DEGREE OF
DOCTOR OF PHILOSOPHY

Romas Kazlauskas, Advisor

October 2009

ACKNOWLEDGEMENTS

These doctoral projects would not accomplished without many people's help. First, I thank my advisor, Professor Romas Kazlauskas, for his continuous encouragement, guidance and support on my research and writing. I would like to thank other members of my thesis committee: Professor Claudia Schmidt-Dannert, Professor Michael Sadowsky, Professor Mark Distefano and Professor Alex Lange, who gave insightful comments and reviewed my work.

I am also grateful for Yuk Sham, a computational structural biology consultant, and Zheng Jin Tu, a computational structural biology consultant. They guide me to use many softwares to solve problems in my projects. I also thank Thomas Kirk, Senior Scientist and Manager in the Center for Mass Spectrometry and Proteomics, who helps me to run samples on LC-MS.

I am grateful to all the members who have been worked or are working in the Kazlauskas lab. Christopher Savile and Paul Mugford gave me a lot of help in the beginning of my PH. D research, so that I can get familiar with everything in the lab. Krzysztof Okrasa, Adrian Katona, Qing Jing and Johnathan Gorke gave me a lot of help about solving the GC, HPLC computer problem. Johnathan Gorke also discusses with me about our polyester synthesis project and gave me suggestions. Ryota Fujii, Santosh Kumar Padhi, Tyler Yin and Graig Legatt also gave me useful suggestions about my research and writing.

Finally, I am grateful to my husband and parents for their understanding, endless patience and encouragement when it was most required.

ABSTRACT

The conjugated double bonds in carotenoids central chain make these compounds potential building blocks for conductive polymers. Bixin and crocetin's capability of forming carboxylester bonds at end are used to synthesis polyesters. Among 20 esterases and lipases, *Candida antarctica* Lipase B (CalB) is the only enzyme that catalyzes bixin esterification reaction with linear alcohols. None of these enzyme catalyzes crocetin esterification reaction. *Candida antarctica* Lipase B added alcohols, such as, *n*-propanol, polyethylene glycol 400 and 1, 10- decanediol to bixin to make bixin diesters, which worked as initiators and were added into ε-caprolactone to synthesis polyesters. The corresponding polymers had the MW 10,600, 12,900 and 11,100.

Esterases/lipases and some acyltransferases share a Ser-His-Asp catalytic triad and similar mechanisms. Comparison of the x-ray structures of these structurally related esterases/lipases with acyltransferases reveals a different conformation of the oxyanion loop. In esterases/lipases this loop adopts a type II β turn conformation with C=O of the main chain facing the active site. In acyltransferases this loop adopts a type I β turn with the N–H of the main chain facing the active site. The x-ray crystal structure of *Pseudomonas fluorescens* esterase containing a sulfonate transition state analog shows the C=O facing active site activate via a bridging water molecule to the attacking water molecule. While in acyltransferases an opposing interaction with the N–H may deactivate the attacking water molecule.

Oxyanion turn GWLL of *Pseudomonas fluorescens* esterase (PFE) was engineered in order to switch to a type I β turn and favor acyltransfer reaction. Replacing GWLL with acyltransferases oxyanion turn peptides yielded several mutants with only PFE-GLRA soluble. However PFE-GLRA doesn't show activity. Saturation mutagenesis at position W28 and L29, yielded mutants L29I, L29T, L29V, L29W, with acyltransfer/hydrolysis (A/H) ratios 2.2, 2.5, 2.5, 4 fold of that of the wild type. Some of these mutants might contain type I β turns.

TABLE OF CONTENTS

Acknowledgements i

Abstract ii

Table of Contents iii

List of Tables v

List of Figures vi

List of Abbreviations viii

Chapter 1. Introduction 1

- 1. Biocatalysis 1
- 2. Protein Engineering 6
- 3. Esterases/Lipases of α/β hydrolase superfamily 10
- 4. Research overview 18
- References 19

Chapter 2. Biosynthesis of carotenoid-containing polyesters 22

- 1. Introduction 23
- 2. Methods 25
- 3. Results 30
- 4. Discussion 40
- References 42

Chapter 3. Active site loop orientation differs in esterases/lipases and acyltransferases: molecular basis for controlling the reactivity of water 43

- 1. Introduction 44
- 2. Methods 50
- 3. Results 57
- 4. Discussion 82
- References 87

Chapter 4. Protein engineering to improve PFE acyltransfer/hydrolysis ratio by deactivating nucleophilic water 99

- 1. Introduction 100

- 2. Methods 103
- 3. Results 108
- 4. Discussion 110
- References 121

Comprehensive references 123

List of Tables

Chapter 2
Table 1. Enzymes used for carotenoid ester bond hydrolysis 26
Table 2. Enzymatic hydrolysis of ethyl sorbate and bixin 31
Table 3. Molecular weight of bixin-containing polyesters 39
Chapter 3
Table 1. Data-collection and refinement statistics 56
Table 2. Conformation of the oxyanion turn in thirty-one GX-class hydrolases within the α/β-hydrolase superfamily 62
Table 3. Conformation of the oxyanion turn in eight acyltransferases within the α/β-hydrolase superfamily 67
Chapter 4
Table 1. Primers for PFE mutagenesis 105
Table 2. A/H ratio of PFE Trp28X and Leu29X variants catalyzed phenyl acetate and benzyl alcohol reaction 113
Table 3. A/H ratio of PFE Leu29X mutants catalyzed isopropenyl acetate and *n*-propanol reaction 115

List of Figures

Chapter 1

Fig 1. Chemical synthesis and biosynthesis of simvastatin 3

Fig 2. Biodiesel synthesis from plant oils or animal fats 4

Fig 3. Lipase catalyzed polyester synthesis 5

Fig 4. X-ray crystal structure of α/β hydrolase family protein PFE 11

Fig 5. Mechanism for esterases/lipases catalyzed hydrolysis of an ester 13

Fig 6. Catalytic mechanisms of α/β hydrolase family esterases/lipases obtained activity 17

Chapter 2

Fig 1. HPLC analysis of CalB catalyzed bixin and ethanol reaction 32

Fig 2. TLC analysis of crocin esterification reaction 33

Fig 3. HPLC analysis of bixin initiator synthesis 35

Fig 4. CalB catalyzed bixin initiator polymerizations with ε-caprolactone 38

Scheme I. Substrates used in this article 29

Scheme II: CalB catalyzed bixin and ethanol reaction 32

Chapter 3

Fig 1. Acyltransferases catalyze the transfer of an acyl group from a donor (ester or thioester) to an acceptor (alcohol in this example) 45

Fig 2. Acyltransferases catalyze key steps in antibiotic synthesis 46

Fig 3. Acyltransferases follow a ping-pong bi-bi mechanism 48

Fig 4. β-turns 58

Fig 5. Dihedral angles of the oxyanion residue (*i* + 1 in the turn) in hydrolases and acyltransferases 69

Fig 6. X-ray crystal structure of hFAS TE 71

Fig 7. 6-Deoxymethynolide B synthase thioesterase domain catalyzes a macrolactonization to form precursor of the macrolactide antibiotic erythromycin 73

Fig 8. X-ray crystal structure of pikromycin thioesterase containing a covalently bound phosphonate transition state analog 73

Fig 9. Synthesis of *p*-nitrophenyl ester of racemic butane-2-sulfonic acid 75
Fig 10. X-ray crystal structure of a sulfonate transition state analog bound to the catalytic serine of esterase from *Pseudomonas fluorescens* 77
Fig 11. The different conformation of the oxyanion loop in esterases and acyltransferases can activate or deactivate the attacking water via a second water molecule 81
Chapter 4
Fig 1. Primer pair of Gly27Ala mutation 104
Fig 2. PFE catalyzed phenyl acetate and benzyl alcohol reaction 106
Fig 3. PFE catalyzed isopropenyl acetate and *n*-propanol reaction 107
Fig 4. PFE wild type catalyzed phenyl acetate and benzyl alcohol assay 109
Fig 5. PFE Leu29X mutant A/H ratios in both reactions compared to wild type 114
Fig 6. Substrates of *Mycobacterium tuberculosis* Antigen 85C 116

List of Abbreviations

TBDS	*tert*-butyldimethylsilyl
FAME	fatty acid methyl ester
FAEE	fatty acid ethyl ester
PCR	polymerase chain reaction
E.coli	*Escherichia coli*
GC	Gas chromatography
HPLC	High performance liquid chromatography
CASTing	Combinatorial active-site saturation testing
CalB	*Candida antarctica* lipase B
PFE	*Pseudomonas fluorescens* esterase
Td1	Transition state 1
Td2	Transition state 2
CPO-F	Chloroperoxidase F
EchA	*Agrobacterium radiobacter* expoxide hydrolase
Me	Methyl
MW	Molecular Weight
APCI	atmospheric pressure chemical ionization
MS	Mass spectrometry
TLC	Thin layer chromatography
PEG400	Polyethylene Glycol 400
KCl	Potassium chloride
GPC	Gel permeation chromatography
RF	Retention factor
KD	Kilo Dalton
HTA	Homoserine *O*-acetyltransferase
SrfTE	Surfactin thioesterase
LB	Luria-Bertani
NMR	Nuclear magnetic resonance
VAST	The vector alignment search tool
SCOP	Structural classification of proteins

THF	Tetrahydrofuran
DESB TE	6-Deoxymethynolide B synthase thioesterase
Hi HAT	*Haemophilus influenzae* homoserine acyltransferase
Li HAT	*Leptospira interrogans* homoserine acyltransferase
BES	*N, N*-Bis(2-hydroxyethyl)-2-aminoethanesulfonic Acid
ACP	acyl-carrier protein
RdmC	Aclacinomycin methylesterase
hFAS TE	Human fatty acid synthase thioesterase
pikTE	Pikromycin thioesterase
6-APA	6-amino-penicillanic acid

Chapter 1. Introduction

1 Biocatalysis

With the development of industry during the last century, there has been much debate about environmental problems, which were mainly generated in the chemical industry. In 1998, Anastas and Warner proposed the concept of green chemistry to guide the design of environmentally benign products and processes [1]. The principles of green chemistry are: conserve energy and resources and avoid waste and hazardous materials [1]. Biocatalysis is one of the techniques developed to fulfill this goal. Biocatalysis is the use of enzymes, which are robust natural catalysts, to catalyze chemical transformations. Compared to traditional chemical conversions, enzyme-catalyzed reactions have many advantages: robust catalytic activity, avoiding the use of toxic reagents and extreme reaction conditions, environmentally benign, high regio- and stereo- selectivity. Currently biocatalysis is used widely in the synthesis of chemical intermediates for pharmaceuticals, agrochemicals and insecticides [2], fuels [3] and polymers [4].

Biocatalysis can use free enzymes without immobilization, immobilized enzymes or whole cells of different organisms. The immobilized enzymes are enzymes linked to an inert, insoluble carrier. This technique can enhance an enzyme's stability to extremes of pH and temperature. After the reaction, enzyme can be easily separated and recycled. Sometimes immobilized enzyme can also gain improved catalytic activity and selectivity. There are several kinds of immobilization techniques that are frequently used: noncovalent adsorption or convalent attachment to outside of inert materials, entrapment of enzyme in insoluble beads or membrane, and covalently binding of enzyme to matrix, also called cross-linking [5].

Whole cell catalysts are normally microbial cells expressing the desired enzymes. Compared to isolated enzymes, whole cell catalysts are much cheaper and the enzymes in cells are more stable than isolated ones. It is not necessary to add expensive cofactors, because the cell can provide them. Sometimes, microorganisms contain the individual enzymes or the whole pathways required for the biosynthesis of desired products. If the catalysts are not present, organisms can be developed to express foreign proteins by using recombinant DNA techniques. *E. coli* and yeast are the most widely used model organisms for recombinant DNA techniques. Filamentous fungi are good for expressing eukaryotic proteins due to their similar protein glycosylation systems to animal cells. Lactic acid bacteria have been used for the production of fermentated food for a long time and are healthy for humans. Therefore they are also preferable host cells [6].

1.1 Biocatalysis in pharmaceutical synthesis.

Biocatalysis play an important role in pharmaceutical synthesis processes. The most obvious advantage of using enzymes in these processes is their excellent regioselectivity and enantioselectivity. For pharmaceutical compounds of bigger size and more complex structures, enzymes can resolve chiral compounds and also catalyze reactions specifically on desired positions. This saves multiple steps of protection and deprotection from traditional chemical process.

One example is the synthesis of simvastatin, which is a cholesterol-lowering compound. The traditional chemical synthesis starts from natural product lovastatin, which has a structure similar to simvastatin, except that lovastatin contains a α-methylbutyryl group while simvastatin contains a α-dimethylbutyryl group. Theoretically, hydrolyzing this acyl group to release Monacolin J and adding α-dimethylbutyryl group would yield simvastatin. However, it is not practical in chemical synthesis because there are several hydroxyl groups in Monacolin J. Hence multiple steps of protection and

deprotection are required to convert Monacolin J to simvastatin. There are five steps, four of which, lactonization, silylation, hydrolysis of TBSO and lactone ring opening are protection and deprotection steps [7]. Recently, a one step, whole cell biocatalysis from monacolin J directly to simvastatin was achieved by using a recombinant *E.coli* expressing acyltransferase LovD, which shows strict regioselectivity and transfers the acyl group only to the desired hydroxyl group [8, 9] (Fig .1).

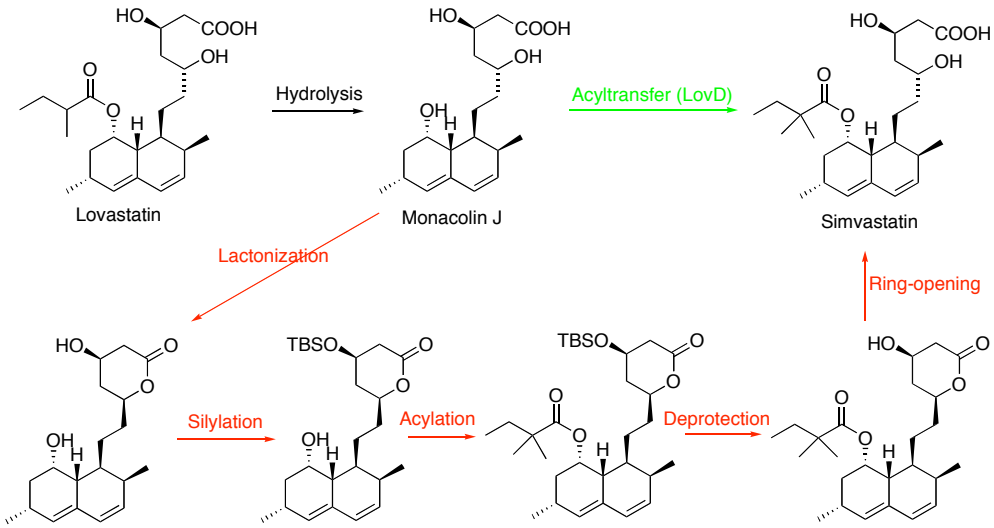

Figure 1. Chemical synthesis and biosynthesis of simvastatin. The first step is common for both pathways: natural product lovastatin hydrolyzes to Monacolin J. Then in the chemical pathway (shown in red arrows), there are steps of lactonization, silylation to protect the hydroxyl group, acylation, hydroxyl group deprotection and lactone ring opening. There is only one step in the biocatalysis pathway (shown in green): acyltransferase LovD transfers α-dimethylbutyryl group to monacolin J and generates simvastatin.

1.2. Biocatalysis in biodiesel synthesis

Research on generating CO_2-neutral renewable fuels is attracting considerable attention these days because of global warming concerns, high oil prices and the depletion of petroleum reserves. Vegetable oils and animal fats are renewable fuels, however they cannot be directly used in diesel

engines due to their high viscosity, free fatty acid content and high melting temperatures, which leads to freezing in cold weather. Biodiesel is produced from plant oils, animal fats and waste cooking oil by transforming triglycerides and fatty acids into fatty acid methyl ester (FAME) or ethyl esters (FAEE) [10] (Fig .2). Lipases catalyze the hydrolysis of ester bonds of lipids in water, that transfer the acyl group from esters to water molecules. In organic solvent, lipases preserve their catalytic activity. However they transfer free carboxylic acid or acyl group of ester to alcohol and the corresponding process is called esterification or transesterification. These lipases are used to transfer fatty acid moiety of vegetable oil to produce biodiesel. Comparing to the alkali-catalyzed transesterification reaction, which also requires high temperature, biocatalysis process saves energy and is easier for glycerol byproduct recovery.

In transesterification, water competes with alcohols for the acyl group and generates a fatty acid side product which decreases the yield [11]. Some lipases obtain higher acyltransfer over hydrolysis activity than others. *Candida rugosa* lipase, *Pseudomonas cepacia* lipase, *Pseudomonas fluorescens* lipase and *Candida antarctica* lipase B show excellent performance in biodiesel synthesis [3]. *Rhizopus oryzae* lipase can catalyze biodiesel synthesis even in a high water content system [12]. Substrate specificity is also a concern about the lipase properties. There are three ester bonds in triglycerides and to gain 100% yield, all the three fatty acid moieties have to be converted into FAME or FAEE. *Rhizopus oryzae* lipase shows 1, 3-specific toward triglyceride reaction. Adding a nonspecific enzyme like *Candida rugosa* lipase creates a more efficient synthesis [13].

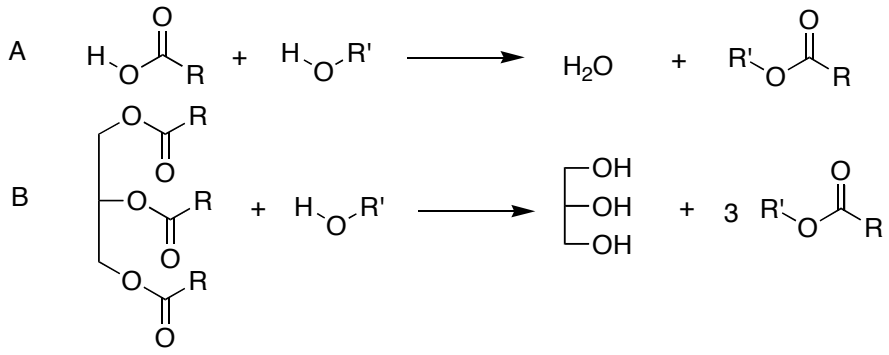

Figure 2. Biodiesel synthesis from plant oils or animal fats. R' represents methyl or ethyl group and R represents long alkyl group. A. Esterification reaction of fatty acid. B. Transesterification reaction of triglyceride. The RC(O)OR' is biodiesel.

1.3 Biocatalysis in polyester synthesis

Polymers for biomedical applications include diverse polymers, but polyesters attract the most attention due to their biodegradable, biocompatible properties [14]. There are several ways to produce polyesters: using organo metallic catalysts, biosynthetic pathway in bacteria and *in vitro* synthesis using individual lipases. The enzyme catalyzed synthesis has several advantages over chemical reaction, e.g., mild reaction condition and able to catalyze large-size lactone ring opening reactions [15]. Polyester synthetases are a class of enzymes isolated from a wide range of bacteria and some archaea. These enzymes synthesize polyesters as insoluble cytoplasmic inclusions to serve as reserve carbon source for the bacteria.

There has been a rapid development in *in vitro* lipase-catalyzed polyester synthesis in the last decade. The advantages of lipase catalyze transesterification and esterification in organic solvents as mentioned in last section also apply in polyester synthesis (Fig .3). The lipases have broad substrate specificity, high thermostability and can be immobilized for reuse.

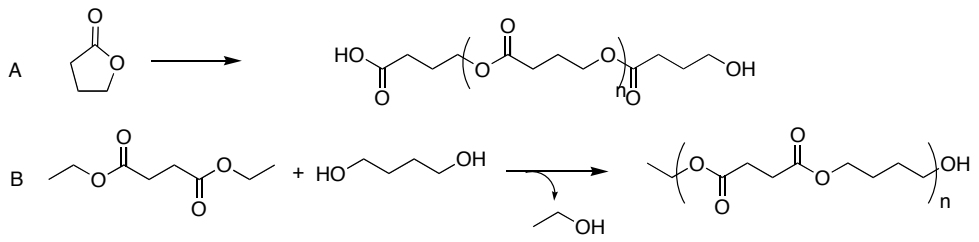

Figure 3. Lipase catalyzed polyester synthesis reaction. A. Polyester synthesis by ring-opening polymerizing from lactone. B. Polyester synthesis by condensation polymerization of diester and diol.

2. Protein engineering

In many cases, natural enzymes are not suitable to perform targeted reactions due to their poor catalytic activity, thermostability, substrate specificity, enantioselectivity or regioselectivity. It is then necessary to improve these enzymes' properties. The process of developing useful or valuable protein is called protein engineering. There are two strategies often used for protein engineering: rational design and random mutagenesis.

2.1 Rational design

Rational design is also called structural-based design, which is based on in depth knowledge of the relationship between protein structure and function. The advantages of this method are that it requires making only a few mutants and it is easy to obtain the mutants in a short time. However, there are also drawbacks: protein structural and catalytic mechanism information might be unavailable, our current understanding of protein structure/function is very limited and the effects of mutations are hard to predict. Sometimes our predicted mutations might cause protein folding and solubility problems.

2.2 Random mutagenesis

Random mutagenesis, also called directed evolution, is widely used in the lab. In this process a large pool of protein variants is generated and the pool is screened for those with desired catalytic properties. The advantage of

random mutagenesis is that the protein structure and detailed knowledge of the catalytic mechanism are not required. However directed evolution requires generating a mutant pool, which is large and complex enough to contain our desired mutants and having a rapid and effective screening method. Generally, mutations are introduced either by error-prone PCR or DNA shuffling. PCR, (polymerase chain reaction), is the use of heat-stable DNA polymerase and thermal cycling to exponentially amplify DNA fragment. Error-prone PCR is the modification of standard PCR method, in which genes are amplified with higher error rates to generate variations. To obtain an appropriate level of mutation, error rate are normally controlled at 1~5 nucleotides per 1 kb [15]. DNA shuffling is also a PCR based process. A group of homologous genes is chopped into fragments by enzymes. These fragments are combined and reassembled using PCR reactions. During PCR, DNA fragments are separated into single strand and some of these fragments will bind to other fragments that share complementary DNA regions. These complementary DNA regions serve as primer binding areas and the following elongation step mixes the DNA fragments from different genes together, which results in chimeras [16]. Generally, the whole PCR process generating an intact gene, screening the library for desired mutants, sequencing and amplifying identified variants are termed a "round" of directed evolution for either error prone PCR or DNA shuffling. Most experiments will perform more than one round to generate a big mutant pool. For example, *Escherichia coli* D-Neu5Ac (N-acetylneuraminic acid, D-sialic acid) aldolase catalyzes the reversible adolation reaction from N-acetyl-D-neuraminic acid (D-sialic acid). After 5 rounds of error-prone PCR D-Neu5Ac (N-acetylneuraminic acid, D-sialic acid) aldolase reversed its enantioselectivity to L-3-deoxy-manno-2-octulosonic acid [17].

Screening methods are often a rate-limiting step for directed evolution experiments. Screening methods are divided into three classes. The first class is the colony screening, which is based on the changed cell phenotypes

introduced by the target protein variants. Enzyme activities are linked to cell viability or colony colors in these assays. These assays are potentially high-throughput methods, however not all enzyme activities relate to cell phenotypes, these assays are not applicable for most experiments. The second class uses chromogenic and fluorogenic assays performed in microplates and is the most popular method. The third class relies on analytic instruments such as GC, HPLC to detect reaction products quantitatively and is the most time consuming method.

2.3 Semi-rational approach

Directed evolution generates mutations through all the peptide sequence. Because some positions affect the desired protein properties more than the others, a lot of mutations are 'wasted' in uninteresting positions and some important positions cannot generate enough variation to obtain the desired beneficial change. Thus, if the protein structural information is available, rational design combined with directed evolution can be used in protein engineering, which is called "semi-rational approach".

Saturation mutagenesis, where all the 20 different protein generic amino acids are tested at a specific position, is used widely. Saturation mutagenesis focusing on the active site should get a better result than random mutagenesis because residues in active site have more effects on enzyme properties. Random mutagenesis generates mutations evenly through out the whole peptide sequences and only a small number of residues are located at active site, therefore a lot of mutations occur in remote areas [18, 19]. However, sometimes the remote mutations did show dramatic improvement in enzyme catalytic activity and enantioselectivity, which cannot be explained by our current knowledge [20]. Saturation mutagenesis is combined with random mutagenesis to get better results. Random mutagenesis can identify important positions throughout the protein peptide sequences, the saturation mutagenesis can find best mutations at these positions and therefore generate better

mutants than random mutagenesis alone. Multiple rounds of random and saturation mutagenesis reversed the enantioselectivity of *Burkholderia gladioli* esterase EstB, the protein was subject to error-prone PCR and saturation mutagenesis [21].

Combinatorial active-site saturation testing (CASTing) was introduced by Reetz and coworkers to change the enzyme substrate specificity. Amino acids in the active site, which are spatially close to each other, might have synergistic conformational effects. Five amino acid pairs in *Pseudomonas aeruginosa* lipase active site were picked and subjected to saturation mutagenesis. Several single and double mutants were identified to hydrolyse esters with bulky acyl group much faster than the wild type enzyme. Some of the largest improvements are observed only in double mutants [22].

2.4 Other mutagenesis methods

Not all enzyme properties are readily applicable to develop a high-throughput screening method and not every existing protein scaffold is readily modified to obtain a desired property, which limits the application of directed evolution.

Rational design and random mutagenesis generate mainly amino acid substituted mutants and don't change the protein folding and topology. Lipases of α/β hydrolase superfamily are divided into GX and GGGX classes according to their oxyanion hole conformation. Lipases of the GGGX class are excellent catalysts for esters of bulky secondary and tertiary alcohols. However, lipases of GX class show poor performance in this reaction because of the steric hindrance of the peptide backbone of the oxyanion hole [23]. The peptides of GX class lipase are shorter than GGGX class lipase. Amino acid substitution can hardly remove this steric hindrance. Moreover direct insertion mutation might result in insoluble protein.

Candida antarctica lipase B is a very useful catalyst with high catalytic activity and thermostability, however as a GX class enzyme, it cannot catalyze esters of tertiary alcohols. Circular permutations were introduced to broaden the active site of *Candida antarctica* lipase B by relocating the termini to release the structural constraints. The original termini are connected by a 6-amino acid peptide and breaking of existing peptide bond throughout the entire protein sequence creates new N and C termini. Most functional variants have the new termini at the cap region, which is responsible for substrate interaction. The best mutant CP283, which has the new termini at position 283, showed a specific activity higher than 175 fold that of CalB wild type toward 6,8-difluoro-4-methylumbelliferyl octanoate [24].

3. Esterases/lipases of α/β hydrolase superfamily

Among the most popular enzymes used in biocatalysis are members of the α/β hydrolase superfamily. Proteins in this family have a similar catalytic domain despite of their low sequence similarity. Structural features include: a core of 8 mostly parallel β strand; each β strand forms a twisted plane at the center; two layers of α helixes are packing at both sides of the β sheet; loops of diverse lengths and conformations connect α helixes and β strands. (Fig 4) However, its members are classified into several groups corresponding to divergent functions: esterases/lipases, epoxide hydrolase, hydroxynitrile lyase, haloalkane dehalogenase, haloperoxidase, peptidase, acyltransferases.

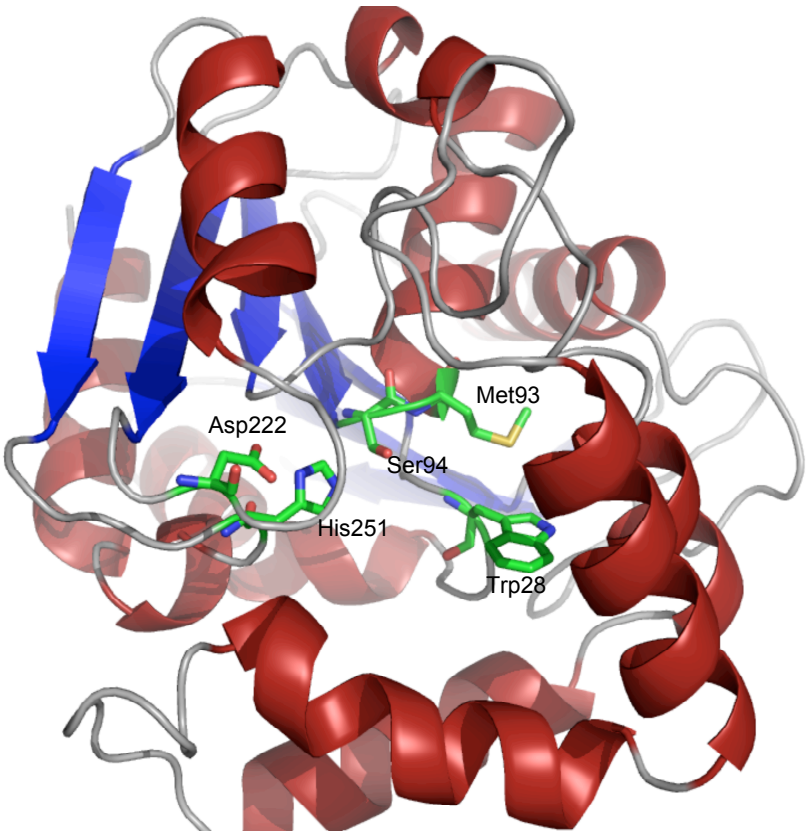

Figure 4. X-ray crystal structure of α/β hydrolase family protein PFE. β sheet is shown in blue at the center. α helixes are shown in fire brick red flanking β sheet. Loops are shown in light gray connecting β strands and α helixes. Catalytic triad Ser94-His251-Asp222 and oxyanion residues Met93, Trp28 are shown in stick.

Lipases/esterases (E.C 3.1.1) are the most common in this superfamily, which catalyze the hydrolysis of triglycerides and other carboxylic acid esters. The catalytic triad is Ser- His- Acid (Asp/Glu). The nucleophile residue is located at a conserved position: a structure motif called nucleophile elbow (Gly-X-nucleophile-X-Gly), a tight turn between a central β sheet and the following α helix. Because of their broad substrate specificity, high regio-, stereoselectivity and thermostability, lipases/esterases are widely used for kinetic resolution of optically active compounds. The structure and function relationship of these enzymes have been intensively investigated. Besides the triad, the catalytic machinery also includes two or three oxyanion residues.

One of the oxyanion residues is next to the C terminal of nucleophilic Ser and the other locates at a turn at N-terminal of the protein. In the first step of the catalysis, the oxyanion hole hydrogen bonds to the carbonyl oxygen of the ester and the nucleophilic Ser attacks carbonyl carbon to form the first tetrahedral intermediate; then the alcohol group is released to generate the acyl-enzyme intermediates, then a water attacks the acyl-enzyme intermediate to form the second tetrahedral intermediate followed by the release of carboxylic acid (Fig .5). The lipase-engineering database summarizes esterases/lipases properties [25, 26].

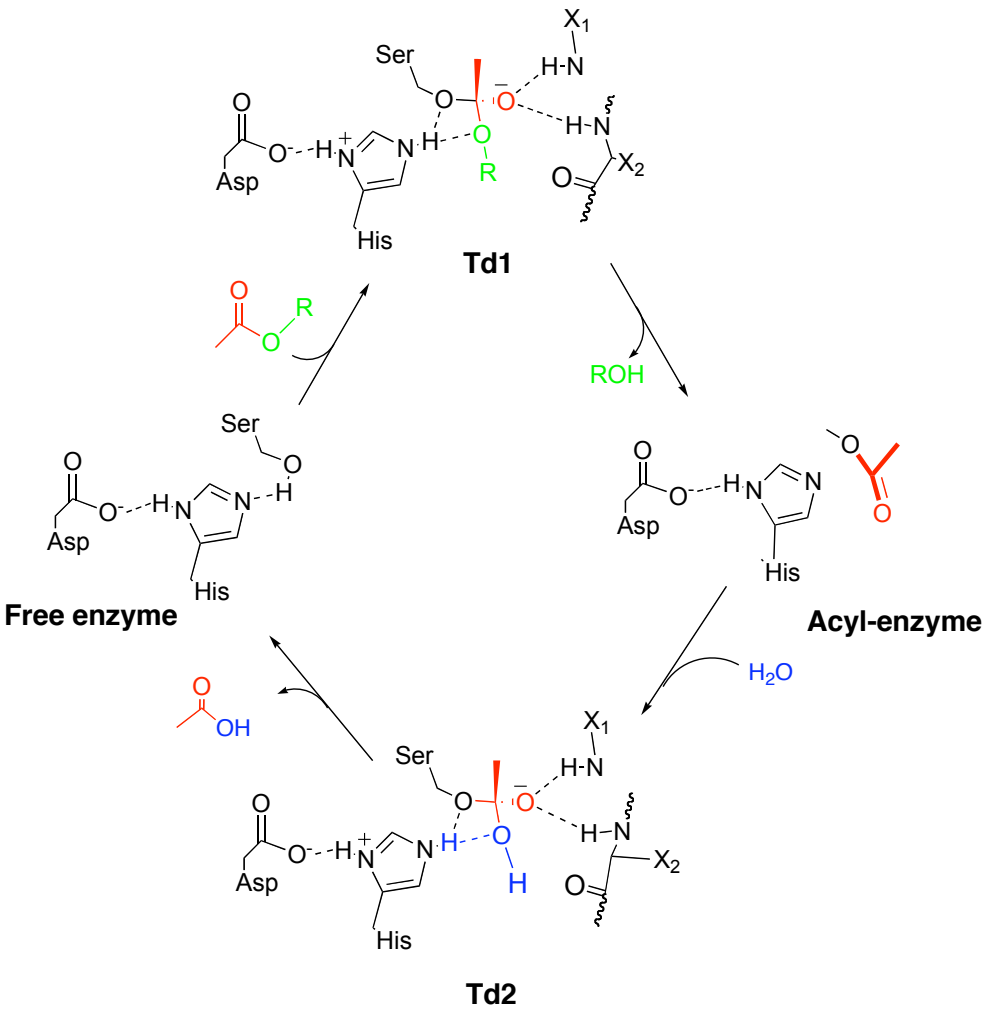

Figure 5. Mechanism for esterases/lipases catalyzed hydrolysis of an ester. The catalytic machinery contains catalytic triad, which is composed of Ser-His-Asp, and oxyanion hole, which is formed by two residues. The catalytic Ser attacks carbonyl group of the ester and forms the first tetrahedral intermediate (Td1), which is stabilized by oxyanion hole. The alcohol group of the ester is broken from this tetrahedral intermediate, which turns into an acyl-enzyme intermediate. A nucleophilic water molecule attacks this acyl-enzyme intermediate to form the second tetrahedral intermediate (Td2), followed by the formation of the carboxylic acid product and releases of the free enzyme.

3.2 Existing lipase promiscuity and the gain of new functions by protein engineering

Enzyme promiscuity is the ability of one enzyme to catalyze more than one type of chemical transformation. Some enzymes of the α/β hydrolase superfamily that catalyze different reactions not only share a similar structure and active site, but also mechanisms. For example, lipases/esterases, perhydrolase, protease/amidases and acyltransferases of this family use the same catalytic triad Ser-His-Asp/Glu and oxyanion hole. The transition states of these reactions are also similar. Therefore, it is of particular interest to explore what are the structural differences that distinguish one type of enzyme from the other, e.g., lipases versus perhydrolases. Moreover some lipases catalyze more than one type of reaction, e.g., CalB catalyze both ester and amide bond hydrolysis reactions with the same catalytic triad [27]. Understanding the structural bases between these proteins will help to design proteins with new functions in lipases and expand their applications. Perhydrolases catalyze the acyl group transferred from a carboxylic acid to hydrogen peroxide to form peracid, which can be used in bleach as an oxidant. *Pseudomonas fluorescens* lipase (PFE) shows similar peptide sequence to perhydrolase (CPO-F) but has a very low perhydrolase activity. Amino acids that are conserved in perhydrolases but are different in PFE were substituted to the perhydrolase equivalent residues. One of the resulting mutant PFE L29P showed a dramatic increase in perhydrolase activity with the specificity of perhydrolysis over hydrolysis 2600 fold of the wild type protein. The following structural model of PFE L29P indicates a different oriented Trp28 backbone carbonyl group in the PFEL29P activates hydrogen peroxide more efficiently with the H-bond between Trp28 carbonyl oxygen and peroxide hydroxy group 2.7 Å and for wilde type this distance is 3.2 Å [28] (Fig .6A).

Amidases use exactly the same catalytic machinery as that of lipases. Lipases with amidase activity can be used to resolve chiral amides. *Pseudomonas aeruginosa* lipase is engineered by using random mutagenesis

and saturation mutagenesis to enhance amidase activity. Amino acid at position 252, which is next to the catalytic His, affects amidase activity significantly and the triple mutant F207S/A213D/M252F exhibited amidase activity (k_{cat}/K_M) 28-fold higher than that of the wild-type lipase. The kinetic assay indicates the improved k_{cat} is because of the efficient protonation of the leaving group by the catalytic His251. The structural model shows that residue at 252 is very close to the leaving group and promote the catalytic His ability of protonation the leaving group [29].

Reactions of dramatic different mechanisms can occur in the same protein scaffold. Aldol addition and Michael addition are two carbon-carbon bond formation reactions in chemical synthesis. Aldol addition involves a nucleophilic enolate adding to the electrophilic carbonyl carbon of an aldehyde to form a β-hydroxy ketone, or "aldol" (aldehyde + alcohol) and Michael addition is the nucleophilic addition of a carbanion to the β carbon of α, β unsaturated carbonyl compound. CalB catalyzes aldol addition of hexanal at least 10 fold faster than a catalytic antibody with aldolase activity, even though this activity is 10^5 times slower than its lipase activity. Although the catalytic mechanism is not clear yet, it is proposed that the oxyanion hole and the catalytic His contribute to the transition state stabilization. The nucleophilic Ser for hydrolysis activity is not required here and the Ser105Ala mutant increases aldolase activity nearly two fold [30] (Fig .6B) CalB also catalyze Michael addition via the similar mechanism as aldol addition [31] (Fig .6C).

Introducing critical catalytic residues of new reactions into an old enzyme can create new functions for this enzyme. Epoxide hydrolases with α/β hydrolase folding contain a catalytic machinery of Asp-His-Asp catalytic triad and two Tyr residues, which protonate the epoxide oxygen during catalysis. (Fig 6D) PFE was subjected to protein engineering by substituting a few amino acids to obtain the epoxide hydrolase catalytic machinery.

However, these mutants didn't show any epoxide hydrolase activity. A further study of the protein structures identified a loop in PFE block the supposed substrate entrance. In epoxide hydrolases, this loop stay at one side of the entrance, and hence, the whole loop in PFE mutant containing epoxide hydrolase catalytic machinery was replaced to the corresponding peptide of *Agrobacterium radiobacter* epoxide hydrolase and resulted in a chimera showing some hydrolysis activity towards *p*-nitrostyrene oxide[32].

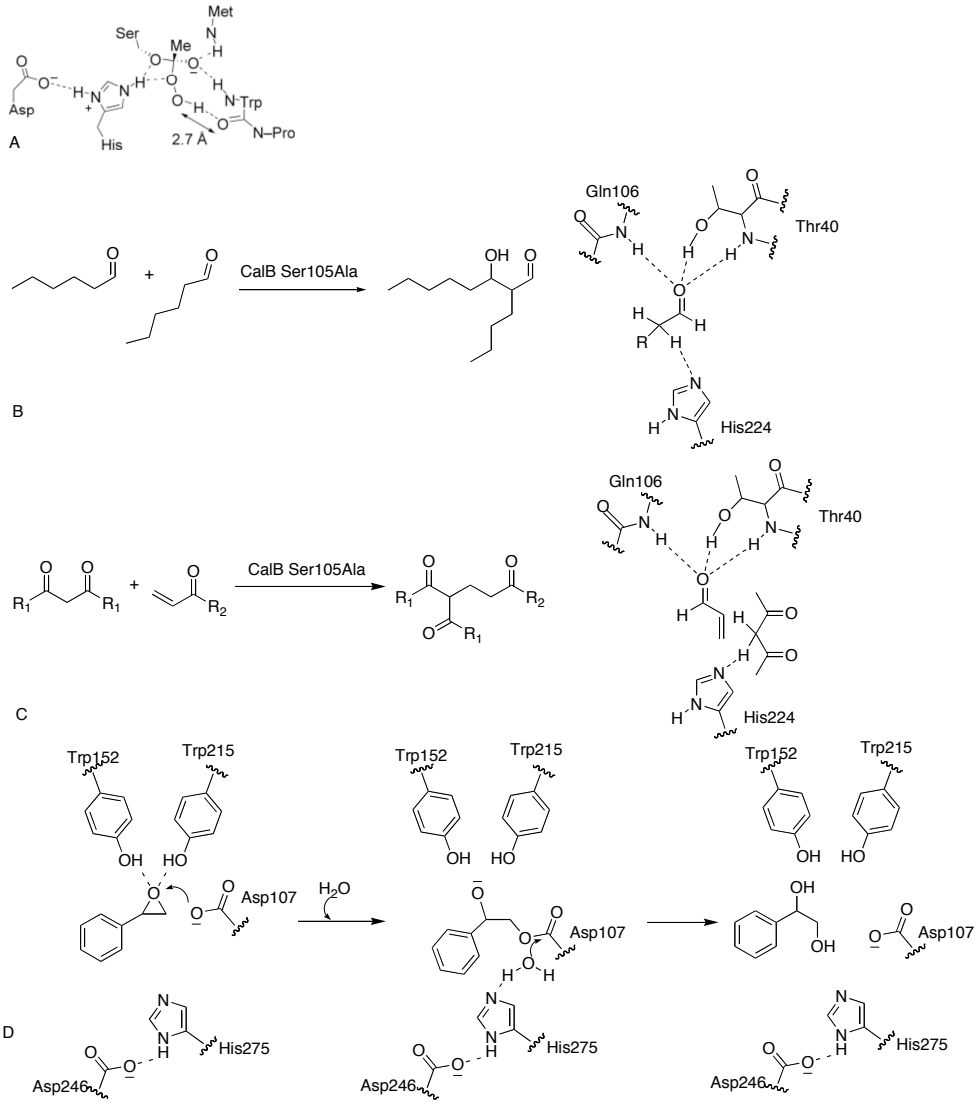

Figure 6. Catalytic mechanisms of α/β hydrolase family esterases/lipases obtained activity. A. Proposed molecular basis of perhydrolase activity in PFE: the formation of the second tetrahedral intermediate (after nucleophilic attack by the substrate peroxide) is facilitated and subsequently stabilized by a key hydrogen bond in the Leu 29 Pro mutant. [25] B. Proposed mechanism of CalB catalyzed aldol addition. The reaction is shown at left and the mechanism at right. R represents butyl group. C. Proposed mechanism of CalB catalyzed Michael addition. The reaction is shown at left and the mechanism at right. R1 represent Me or OMe group, R2 represent H, Me or OMe group. D Machanism of *Agrobacterium radiobacter* epoxide hydrolase (EchA) catalyzed styrene oxide reaction. [33]

4. Research overview

My research focuses on the synthesis of carotenoid-containing polyesters by using sterases/lipases catalyzed acyltransfer reaction and protein engineering to improve the enzyme acyltransfer efficiency.

Carotenoids are natural pigments found in plants, animals and algae. The main chain of carotenoids is a polyene chain and the two ends are oxygen-containing functional groups. The alternating single and double bonds of the main chain make the compound potentially conductive. Incorporation of carotenoids into polyester might create conductive polymers. Esterases/lipases are widely used for the biosynthesis of polymers as described previously. However, esterases /lipases prefer hydrolysis reactions rather than acyltransfer reactions and the trace amount of water in an organic solvent can decrease the synthetic efficiency. These esterases/lipases belong to α/β hydrolase superfamily. Some natural acyltransferases contain homologus structures and catalytic mechanism to these esterases/lipases. These acyltransferases catalyze the transfer of acyl group in aqueous solution. However, these acyltransferases have very narrow substrate specificity and low catalytic capability. In theses studies, I tried to identify the structural differences between these two classes of enzymes and improve the acyltransfer/hydrolysis ratio of esterases/lipases through protein engineering.

References

1. Anastas, P.T., Warner, J.C. (1998). *Green Chemistry: Theory and Practice.* Oxford University Press, USA
2. Theil, F. (1995). Lipase-supported synthesis of biologically active compounds. *Chem. Rev.* 95, 2203-2227.
3. Shimada, Y., , Watanabe, Y., Samukawa, T., Sugihara, A., Noda, H., Fukuda, H., Tominaga, H. (1999). Conversion of vegetable oil to biodiesel using immobilized *Candida antarctica* lipase. *J. Am. Oil Chem. Soc.* 76, 789-793.
4. Chaudhary, A.K., Beckman, E.J., Russell, A.J. (1997). Biocatalytic polyester synthesis: Analysis of the evolution of molecular weight and end group functionality. *Biotechnol Bioeng.* 55, 227-239.
5. Bornscheuer, U.T. (2003). Immobilizing enzymes: how to create more suitable biocatalysts. *Angew. Chem. Int. Ed. Engl.* 42, 3336-3337.
6. Ishige, T., Honda, K., Shimizu, S. (2005). Whole organism biocatalysis. *Curr. Opin. Chem. Biol.* 9, 174-180.
7. Tao, J., Xu, J. H. (2009). Biocatalysis in development of green pharmaceutical processes. *Curr. Opin. Chem. Biol.* 13, 43-50.
8. Xie, X., Tang, Y. (2007). Efficient synthesis of simvastatin by use of whole-cell biocatalysis. *Appl. Environ. Microbiol.* 73, 2054-2060.
9. Xie, X., Watanabe, K., Wojcicki, W. A., Wang, C. C., Tang, Y. (2006). Biosynthesis of lovastatin analogs with a broadly specific acyltransferase. *Chem. Biol.* 13, 1161-1169.
10. Akoh, C.C., Chang, S. W., Lee, G. C., Shaw, J. F. (2007). Enzymatic approach to biodiesel production. *J. Agric. Food Chem.* 55, 8995-9005.
11. Kaiedaa, M., Samukawaa, T., Kondoa, A., Fukuda, H., (2001). Effect of methanol and water contents on production of biodiesel fuel from plant oil catalyzed by various lipases in a solvent-free system. *J. Biosci. Bioeng.* 91, 12-15.
12. Kaiedaa, M., Samukawaa, T., Matsumotoa, T., Ban, K., Kondoa, A., Shimadac, Y., Nodad, H., Nomotoe, F., Ohtsukae, K., Izumotof, E., Fukudab, H. (1999). Biodiesel fuel production from plant oil catalyzed by *Rhizopus oryzae* lipase in a water-containing system without an organic solvent. *J. Biosci. Bioeng.* 88, 627-631.
13. Lee, J.H., Lee, D. H., Lim, J. S., Um, B. H., Park, C., Kang, S. W., Kim, S. W. (2008). Optimization of the process for biodiesel production using a mixture of immobilized *Rhizopus oryzae* and *Candida rugosa* lipases. *J. Microbiol. Biotechnol.* 18, 1927-1931.
14. Duda, A., Kowalski, A., Penczek, S., Uyama, H., Kobayashi, S (2002). Kinetics of the ring-opening polymerization of 6-, 7-, 9-, 12-, 13-, 16-, and 17-membered lactones. Comparison of chemical and enzymatic polymerizations *Macromolecules* 35, 4266-4270.

15. Patrick, C.C., Kimberly, M. M., Umeno, D. (2008). Generating mutant libraries using error-prone PCR. *Direct evolution library creation: Methods and Protocols.* Humana Press, 1st edition *231*, 3-9.
16. Cohen, J. (2001). How DNA shuffling works. *Science* 293, 237.
17. Hsu, C.C., Hong, Z., Wada, M., Franke, D., Wong, C. H. (2005). Directed evolution of D-sialic acid aldolase to L-3-deoxy-manno-2-octulosonic acid (L-KDO) aldolase. *Proc. Natl. Acad. Sci. U. S. A.* 102, 9122-9126.
18. Horsman, G.P., Liu, A. M., Henke, E., Bornscheuer, U. T., Kazlauskas, R. J. (2003). Mutations in distant residues moderately increase the enantioselectivity of *Pseudomonas fluorescens* esterase towards methyl 3bromo-2-methylpropanoate and ethyl 3phenylbutyrate. *Chemistry* 9, 1933-1939.
19. Park, S., Morley, K. L., Horsman, G. P., Holmquist, M., Hult, K., Kazlauskas, R. J. (2005). Focusing mutations into the P. *fluorescens* esterase binding site increases enantioselectivity more effectively than distant mutations. *Chem. Biol.* 12, 45-54.
20. Schmidt, M., Hasenpusch, D., Kähler, M., Kirchner, U., Wiggenhorn, K., Langel, W., Bornscheuer, U. T. (2005). Directed evolution of an esterase from *Pseudomonas fluorescens* yields a mutant with excellent enantioselectivity and activity for the kinetic resolution of a chiral building block. *Chembiochem* 7, 805-809.
21. Ivancic, M., Valinger, G., Gruber, K., Schwab, H. (2007). Inverting enantioselectivity of *Burkholderia gladioli* esterase EstB by directed and designed evolution. *J. Biotechnol.* 129, 109-122.
22. Reetz, M.T., Bocola, M., Carballleira, J. D., Zha, D. X., Vogel, A., (2005). Expanding the range of substrate acceptance of enzyme: combinatorial active-site saturation test. *Angew. Chem. Int. Ed. Engl.* 44, 4192-4196.
23. Kourist, R., María, P., Bornscheuer, U. T. (2008). Enzymatic synthesis of optically active tertiary alcohols: expanding the biocatalysis toolbox. *Chembiochem* 9, 491-498.
24. Qian, Z., Fields, C. J., Lutz, S. (2007). Investigating the structural and functional consequences of circular permutation on lipase B from *Candida antarctica*. *Chembiochem* 8, 1989-1996.
25. Pleiss, J., Fischer, M., Peiker, M., Thiele, C., Schmid, R. D. (2000). Lipase engineering database - Understanding and exploiting sequence-structure-function relationships. *J. Mol. Catal. B: Enzym.* 10, 491-508.
26. Fischer, M., Pleiss, J. (2003). The lipase engineering database: a navigation and analysis tool for protein families. *Nucleic. Acids. Res.* 31, 319-321.
27. Torres-Gavilán, A., Castillo, E., López-Munguía, A. (2006). The amidase activity of *Candida antarctica* lipase B is dependent on specific structural features of the substrates. *J. Mol. Catal. B: Enzym.* 41, 136-140.

28. Bernhardt, P., Hult, K., Kazlauskas, R. J. (2005). Molecular basis of perhydrolase activity in serine hydrolases. *Angew. Chem. Int. Ed. Engl.* 44, 2742-2746.
29. Nakagawa, Y., Hasegawa, A., Hiratake, J., Sakata, K. (2007). Engineering of *Pseudomonas aeruginosa* lipase by directed evolution for enhanced amidase activity: mechanistic implication for amide hydrolysis by serine hydrolases. *Protein Eng., Des. Sel.* 20, 339-346.
30. Bornscheuer, U., Kazlauskas, RJ. (2004). Catalytic promiscuity in biocatalysis: using old enzymes to form new bonds and follow new pathways. *Angew. Chem. Int. Ed. Engl.* 43, 6032-6040.
31. Svedendahl, M., Hult, K., Berglund, P. (2005). Fast carbon-carbon bond formation by a promiscuous lipase. *J. Am. Chem. Soc*. 127, 17988-17989.
32. Jochens, H., Stiba, K., Savile, C., Fujii, R., Yu, J. G., Gerassenkov, T., Kazlauskas, R. J., Bornscheuer, U. T. (2009). Converting an esterase into an epoxide hydrolase. *Angew. Chem. Int. Ed. Engl.* 48, 3532-3535.

Chapter 2. Biosynthesis of carotenoid-containing polyesters

The polymer analysis on the HPLC GPC column and the molecular weight calculations were done by Johnathan Gorke.

Carotenoids contain a conjugated double bond in the central backbone, which make them potential building blocks for conductive polymers. Bixin and crocetin are used to synthesize polyesters by enzymatic reaction. Around 20 esterases and lipases were screened for carotenoid esterification activity. *Candida antarctica* Lipase B (CalB) is the only enzyme that catalyzes bixin esterification reaction with linear alcohols. None of the enzyme catalyzed crocetin esterification reaction. *Candida antarctica* Lipase B can either add *n*-propanol to bixin to get bixin diester or add diols, like polyethylene glycol 400 and 1, 10- decanediol, to bixin to get bixin diol. These bixin diester and bixin diols were then used as initiator and added into ε-caprolactone to synthesis polyesters catalyzed by CalB. The bixin-ε-caprolactone polymers had a MW of 10,600. The bixin-PEG400-ε-caprolactone polymers had a MW of 12,900.The bixin-1, 10-decanediol-ε-caprolactone polymers had a MW of 11,100.

1. Introduction

Carotenoids are a class of natural pigments wildly distributed in plants, marine animals, algae, and photosynthetic bacteria [1-4]. The common structural feature of carotenoids is: isoprenoid units repeated in the center of molecule to make the conjugated double bond throughout the chain. The ends of the carotenoids chain vary. For example, torulene has hydrocarbon ends, alloxanthin has alcohol ends, zeaxanthin has cyclic end group, bixin and crocin have ester end.

The unique structures of alternative double and single bond of the central chain, which allows electron transfer, provide carotenoids many biological functions. The ability of carotenoids absorption of lights not only makes itself a chromophore and colors the organism, but also play a critical role in photosynthesis by transferring energy. The stable carotenoid radicals make them good antioxidants[5].

I plan to use the electron transfer feature of carotenoids to synthesis conductive polymers. Conductive polymers are organic polymers, which conduct electricity. Their ability of conducting relies on their conjugated double bond structure of the polymer backbone. Conductive polymers have several advantages over metal, such as, low weight, a less corrosive nature and processibility. Conductive polymers can be used to make sensors to detect air quality and this application takes the advantage that the conductive polymers are the material of macromolecules, which allow gas enter their interior and the conductivity changes accordingly [6].

Carotenoids contain conjugated double bond in their main chain and therefore are potentially conducting electricity. Furthermore carotenoids are natural carbon hydroxy compounds, they are considered renewable. Recently, metabolic engineering was applied to amplify the biosynthesis of carotenoids

in plants and microorganisms [7, 8]. Schmidt-Danner's group expressed gene clusters involved in carotenoids biosynthetic pathways in *E. coli* and can synthesis C30 carotenoid structures [9].

Caroteoids able to form ester bond in the end, that is, have carboxylic acid, alcohol or carboxylic ester group in both ends, can be used to synthesis polyesters. Bixin, crocin and crocetin are good candidates. Bixin is a C25 carotenoid extracted from annatto seeds, with one end carboxylic acid and the other end methyl ester. Bixin is not heat sensitive. During the high-temperature pigment extract process, bixin can be degraded into small fragments of C17 and *m*-xylene and also other products and also all-*trans*-bixin. Crocetin is a C20 carotenoid with carboxylic acid at both ends. Crocin is the diester form of crocetin.

Carotenids are sensitive to heat, oxidants, light and extreme pHs. Therefore, traditional chemical reactions are not suitable for synthesis carotenoids polyesters. Lipases/esterase catalyzed esterification reaction in organic solvent provides a mild environment for carotenoids. In this research, we are going to use lipases/esterases to synthesis carotenoid polymers.

2. Methods

2.1 Chemicals and enzymes

Bixin was from ChromaDex (Irvine, CA). Crocin and crocetin were obtained from TCA America (Portland, OR). All other reagents were purchased from Sigma-Aldrich (St. Louis, MO). Around 20 enzymes were used to screen for bixin and carotenoid ester bonds hydrolysis activity (Table 1). *Pseudomonas fluorescens* esterase was purified and lyophilized in our lab. Immobilize CalB (Novo 435) was bought from Sigma (St. Louis, MO), which contains 1% weight of enzyme [11]. Other enzymes were gained from Altus (Burlington, Ma) and were numbered.

2.2 Screening of lipases and esterases with ethyl sorbate hydrolysis activity

All the enzymes listed in Table 1 were used for this reaction. Reactions were performed by adding 1mg enzymes and ethylsorbate to a final concentration 100mM in a solvent of 40 µl water and 160 µl t-butanol mixture. After incubating at 35 ºC, at 600 rpm for 2 hours, samples were taken for HPLC analysis by using Zorbax C18 reverse phase column. HPLC method for analysising ethyl sorbate hydrolysis reaction starts from water 60% and acetonitrile 40%, then a linear gradient of acetonitrile to 75% (0~20min); followed by a linear gradient of acetonitrile to 100% (20~20.1min); then keep using 100% acetonitrile (20.1~24min). The retention time of sorbic acid was 3.5 minutes and ethyl sorbate was 7.8 minutes.

Table 1: Enzymes used for carotenoid ester bond hydrolysis

Altus number	Enzyme name
Altus 2	*Pseudomonas cepacia* Lipase
Altus 3	Porcine Pancreatic Lipase
Altus 4	*Candida rugosa* Lipase
Altus 5	α-Chymotrypsin
Altus 6	Penicillin Acylase
Altus 7	Aspergillus niger Lipase
Altus 11	*Candida antarctica* Lipase A
Altus 12	*Candida* lypolytica Lipase
Altus 13	*Candida antarctica* Lipase B
Altus 14	*Humicola lanuginosa* Lipase
Altus 15	*Bacillus stearothermophilus* Protease
Altus 23	*Rhizopus delemar* Lipase
Altus 25	*Rhizopus oryzae* Lipase
Altus 26	*Chromobacterium viscosum* lipase
Altus 27	*Alcaligenes species* Lipase
Altus 29	*Mucor javanicus* Lipase
Altus 30	*Aspergillus Oryzae* Protease
Altus 31	*Candida rugosa* Esterase
Altus 45	*Aspergillus melleus* Protease
Altus 50	*Psuedomonas sp.* (*aeruginosa)* lipase, immobilized on Celite.
Altus 52	*Bacillus lentus* Protease
Altus 54	*Thermomyces lanuginosus* Lipase
Altus 55	*Penicillium roqueforti* Lipase
	Pseudomonas fluorescens esterase

2.3 Bixin hydrolysis and transesterification reaction

Enzymes with ethyl sorbate hydrolysis activity were used for bixin hydrolysis activity screening. Reactions were performed by adding enzymes 1mg, bixin 0.1mg in the solvent of 40 μl water and 160 μl t-butanol. After incubating at 35 ºC, 600 rpm for 2 hours, samples were taken out for HPLC analysis by using Zorbax C18 reverse phase column.

Immobilized CalB was used for transfer reaction. Reactions were carried out by mixing bixin 0.1mg, CalB beads 1mg and alcohol (ethanol or 1-butanol) 40 μl or 5 mg dihydroquinone or 1, 4-diaminobenzene with t-butanol 200 μl. The mixtures were incubated at 60ºC, with shaking at 700 rpm for 24 hours, and analyzed by HPLC using Zorbax C18 reverse phase column. The new product was analyzed by LC-positive ion atmospheric pressure chemical ionization (APCI)-MS to determine the molecular weight.

HPLC method for bixin reactions started with 75% water and 25% acetonitrile, then a linear gradient of acetonitrile to 100%(0~25min); followed by 100% acetonitrile (25~29min). The retention time of bixin was 11.8 minutes and that of norbixin was 7.8 minutes.

2. 4 Screening of lipases and esterases with crocin hydrolysis activity

For each crocin hydrolysis reaction, 1mg enzyme and 0.5 mg crocin were added into a mixture of 20 μl water and 180 μl t-butanol. Reactions were carried out at 35 ºC, with shaking at 600 rpm for 24 hours in amber vials. There were two control reactions, 'Con1' was the control reaction without enzyme and 'Con2' was the same mixture as con1 but not carried out at 35 ºC, with shaking at 600 rpm for 24 hours. Thin layer chromatography (TLC) was used to detect the reaction. The mobile phase is the mixture of acetonitrile and water with the ratio 80:20 (v/v).

2. 5 CalB catalyzed transesterification reaction to synthesis bixin initiators

CalB catalyzed bixin and alcohol, diols and diamine reactions are performed by mixing 1 mg bixin, 20 mg CalB and 500 µl toluene and the corresponding alcohol, diol or diamine (1, 7- diaminoheptane 20 µl, *n*-propanol 20 µl, polyethylene glycol 400 (PEG 400) 20 µl, 1, 10- decanediol 40mg). After incubating at 60 ºC, with shaking at 800 rpm for 72 hours and 144 hours, 80 µl reaction samples are taken out and mixed with 200 µl acetonitrile for HPLC analysis. Reactions were stopped by filter through cotton to remove enzyme. *n*-propanol is removed by air-evaporating all the solvent. PEG 400 is removed by washing the solvent with KCl saturated water. 1, 10- decanediol is not soluble in toluene in room temperature and is removed by cotton.

2.6 Polymerization synthesis with bixin initiators

All the bixin initiators gathered from 144 hours of last step of the reactions were mixed with 1 or 10 mg CalB (10 mg for bixin n-propanol diester and 1 mg for two bixin-diol initiators), 400 µl ε-caprolactone and 2 ml toluene, and incubate at 60 ºC, with shaking at 800 rpm. After 72 hours and 144 hours days, samples are taken out for HPLC analysis to determine molecular weight and yield. Reactions were stopped by filter through cotton to remove enzyme. Polymers are precipitated by adding 10-fold methanol, followed by filter through Grade P8 filter paper to remove solvent and then dried. Dried product was weighted and dissolved in chloroform with 1% iron liquid 1-butyl-3-methylimidazolium bis(trifluoromethane)sulfonimide. The chloroform was evaporated at 60 ºC and the ionic liquid-polymer mixture was washed three times with methanol to remove any non-entrained ionic liquid.

2. 7 HPLC methods for bixin polymer initiators and polymers

An ACE C18 reverse phase column was used for bixin transesterification reaction analysis. Solvent A was acetonitrile and solvent B

was pure water with 10% methanol. The method start with solvent A at 75% and solvent B at 25% for 10 minutes, then a linear gradient to 100% solvent A (10 -25 minutes) and keep solvent A 100% (25 -30 minutes) at a rate of 1 ml per minute. Compounds are detected at 450 ± 50 nm.

2. 8 MW calculation by using GPC (gel permeation chromatography) column

The synthesized polymers were analyzed by using GPC column with tetrahydrofuran as the solvent to separate polymer compounds.

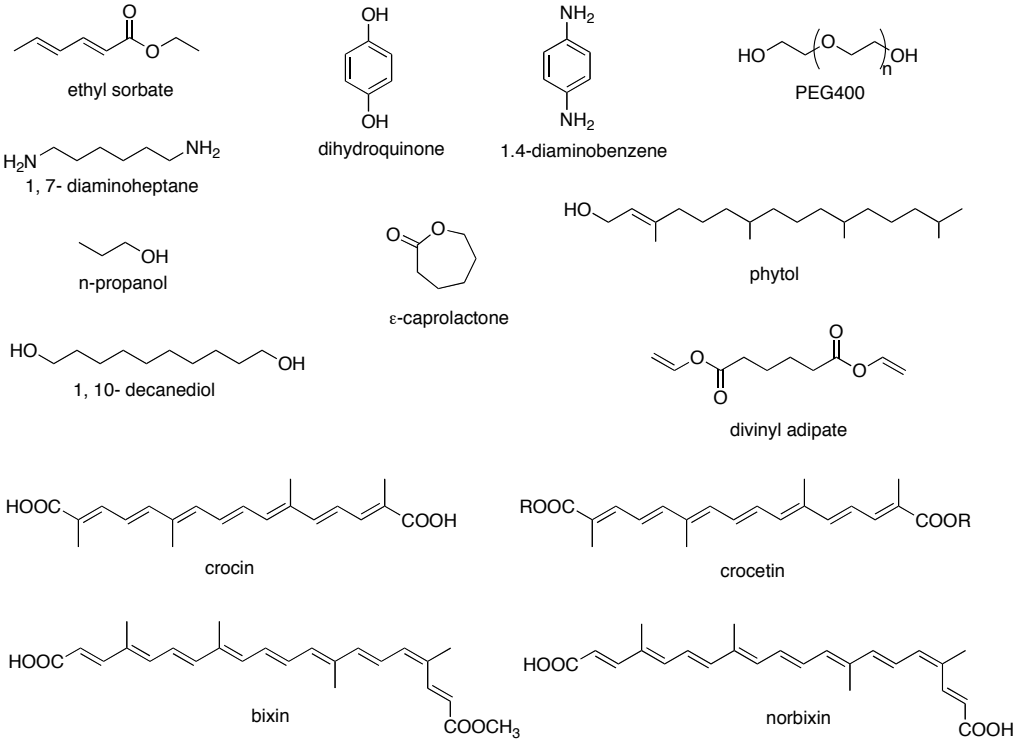

Scheme I. Substrates used in this article

3. Results

3.1 CalB catalyzed bixin hydrolysis and transesterification reaction

Pure bixin is expensive, therefore I started with ethyl sorbate to screen for a suitable catalyst. Ethyl sorbate has a similar structure around a carboxyl ester bond to that of bixin. Around 20 Altus enzymes were screened for the ethyl sorbate hydrolysis activity, among which Altus enzyme 2, 4, 13, 23, 26, 27, 31 and PFE hydrolyzed ethyl sorbate to sorbic acid. Positive reactions showed a sorbic acid peak at 3.5 min in HPLC analysis, which was confirmed by using standard sorbic acid. These enzymes were then used to hydrolyze bixin and the results are shown in Table1. Bixin has a methyl ester at one end, which can be hydrolyzed to a carboxylic acid, and a carboxylic acid at the other end. The hydrolyzed bixin with both ends carboxylic acids norbixin, which was shown in Scheme I. Only three reactions showed norbixin conversions, but two of them, Altus 27 and PFE, had very low conversions with the yield of 0.17% and 0.25%. CalB was the best catalyst among these enzymes, which show 80% conversion in the reaction.

CalB was used to catalyze bixin transesterification reaction. Five different alcohols were used: ethanol, 1-butanol, phytol, dihydroquinone and 1, 4-diaminobenzene. CalB catalyzed bixn with ethanol and 1-butanol reaction show hydrophobic products on HPLC analysis. The former reaction generated new products at ~14min and ~23 min with molecular weights of 408 and 436 from LC-positive ion APCI-MS analysis. This implied transesterification and esterification products. (Fig 1 and Scheme II) The conversion to transesterification product was very high, which was the major bixin compound in the reaction mixiture. The later reaction had a product with MW 436, which corresponded to transesterification product. (DATA not shown) CalB catalyzed bixin with phytol, dihydroquinone and 1, 4-diaminobenzene reactions didn't show new peaks on HPLC.

Table 2. Enzymatic hydrolysis of ethyl sorbate and bixin.

enzyme	Ethyl sorbate hydrolysis (48h)	Bixin hydrolysis (12h)
Control (none)	none	0
Altus2	8.5%	0
Altus 4	1.8%	0
CalB	58.2%	80%
Altus23	2.2%	0
Altus26	3.4%	0
Altus27	7.5%	0.17%
Altus31	3.4%	0
PFE	1.5%	0.25%

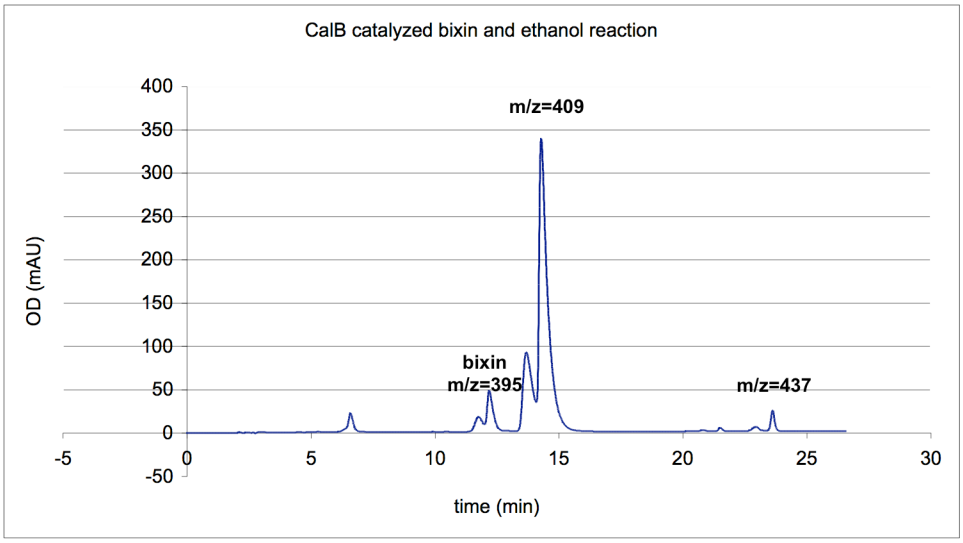

Figure 1. HPLC analysis of CalB catalyzed bixin and ethanol reaction. The retention time for bixin is 12 min. Two peaks around this area represent two bixin isomers (*cis* and *trans*). The m/z=395, which is one more than the bixin MW 394 due to the added proton during ionization. Accordingly, the product at around 14minutes has the MW 408 and the product at 23 minutes has the MW 436.

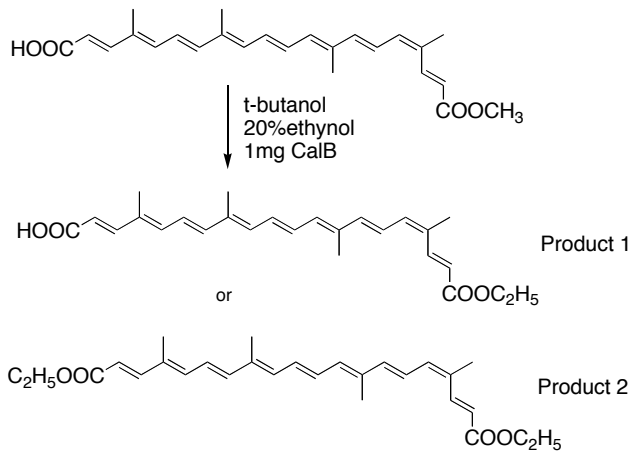

Scheme II: CalB catalyzed bixin and ethanol reaction. The product1 is the transesterification product with the MW 408. The product2 is the continuous esterification product of product1 with the MW 436.

3.2 Screening of lipases and esterases with crocin hydrolysis activity

Crocin is also a carotenoid compound with ester bond at the end, but it has a methyl side chain at C_{β}, which does not exist in in bixin and ethyl sorbate. This might make a different structural requirement for the catalyst. Thus I used all the esterase/lipases to hydrolyze crocin. Both the crocin and crocetin are hydrophilic compounds and the crocin has complex R groups (different types and numbers of sugar moieties), which shows multiple peaks on HPLC and is hard to separate from crocetin peaks. Their separation on TLC was good. Crocin showed mainly three spots on TLC with the RF 0.58, 0.72 and 0.74. Crocetin moved faster than crocin and had an RF 0.84. Con1 and Con2 were the same mixture as the enzyme catalyzed reactions except that no enzyme was added. Con1 was treated the same way as enzyme catalyzed reaction. Con2 was kept at 4 ºC in the dark. TLC showed the same pattern for Con1 and Con2, which indicated 35 ºC treatment of the reaction won't degrade the substrate. Enzyme-catalyzed reactions were also detected on TLC. The compositions of these results were the same as controls and didn't show the crocetin product. (Fig 2.)

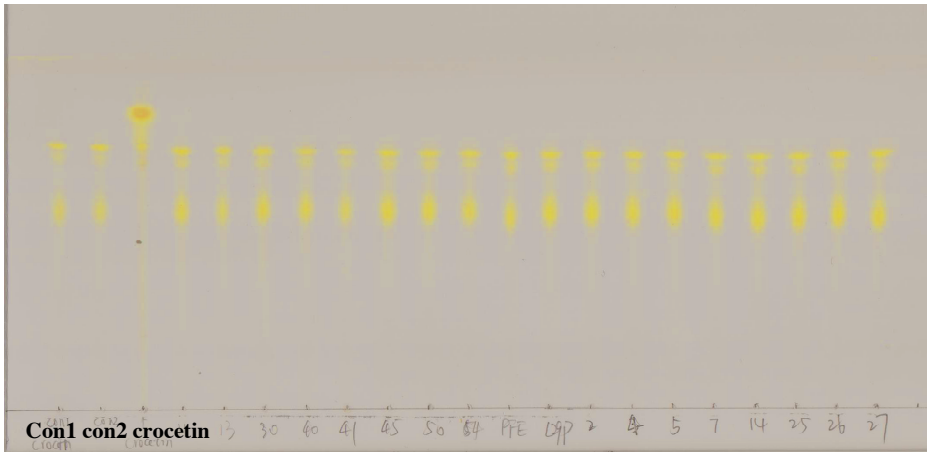

Figure 2. TLC analysis of crocin esterification reaction. For Crocin, there are 3 spots with RF: 0.58, 0.72 and 0.74. For the crocin, there is only one main spot with RF 0.84. The beginning 3 samples are Con1, Con2 and crocetin respectively and the rests are all enzyme-catalyzed reactions.

3. 3 CalB catalyzed bixin transesterification reaction for polymer initiator

Bixin contains a carboxylic acid end and the esterification of which is harder than transesterification reaction of the other end. Therefore we used *n*-propanol to make bixin diesters before the polymerization reaction. Bixin diester can react with ε-caprolactone when catalyzed by CalB. However, this was a very slow reaction. CalB catalyzed ε-caprolactone polymerization reaction much faster than bixin esterification, or a transesterification reaction and may generate polymers without bixin. To avoid this problem, we made bixin initators by adding 1, 10-decanediol, PEG400 and 1, 7- diaminoheptane, which are long chain diols or diamine. CalB can directly transfer ε-caprolactone on these diol or diamine ends and reactions are much faster than directly working on bixin end.

CalB catalyzed bixin and n-propanol reaction showed new compounds after 72 hours. (Fig 3A)The split peaks at ~12 min was bixin. New compounds had the retention time around 15 min, 22 min and 26 min, which are more hydrophobic than bixin as we expected. Major compound come out at 15 minutes. After a 144-hour reaction, nearly all the bixin was converted into the compound of 26 minutes. The peak at 15minutes might be bixin transesterification product, in which n-propanol replaced the methanol group at the ester end. The peak at 22 minutes might be bixin esterification product, in which n-propanol was added to the carboxylic acid end. The peak at 26 minutes might be bixin diesters with both ends *n*-propanol.

PEG400 is a very hydrophilic compound and I expected that its bixin esters were more hydrophilic than bixin itself. CalB catalyzed bixin and PEG400 reaction showed new compounds after 72 hours(Fig 3B). New compounds had the retention time around 4.8 and 6.5 min. After 144 hours reaction, nearly all the bixin was converted into 4.8 minutes compound, which

might be bixin-PEG400 diesters because it was the most hydrophilic product and the yield was increasing during the reaction.

It was hard to determine if 1, 10-decanediol was more hydrophilic or hydrophobic than bixin. CalB catalyzed bixin and 1, 10-decanediol reaction generated new compounds with the retention times before and after bixin, which were 8, 17, 25 and 30 minutes respectively. (Fig 3C) With the reaction going on (from 72 hours to 144 hours), bixin was converted to the 30 minutes compound, which might be bixin-1, 10-decanediol diesters.

CalB catalyzed bixin and 1, 7- diaminoheptane didn't show any products. (Data not shown)

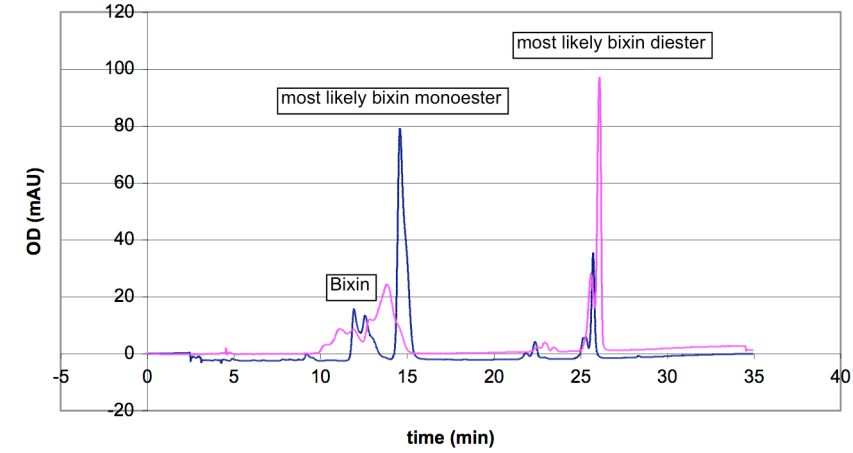

A

B

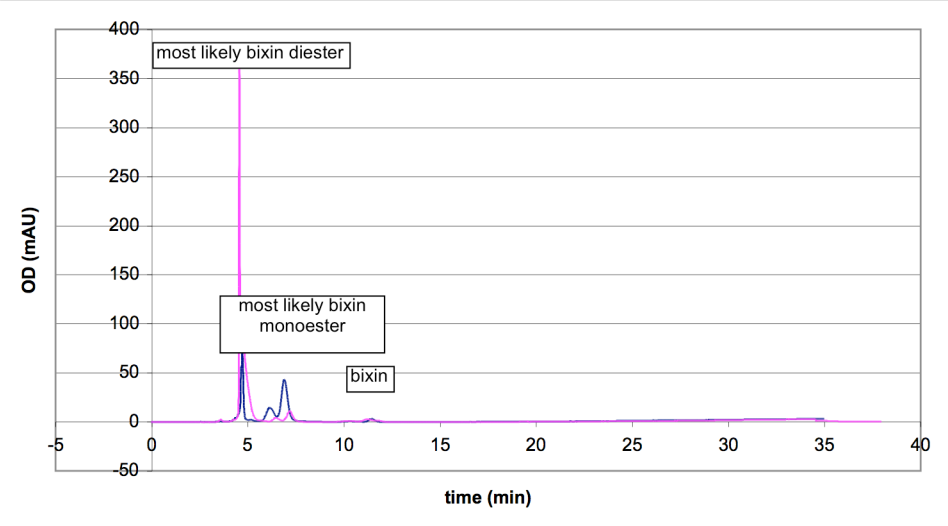

C

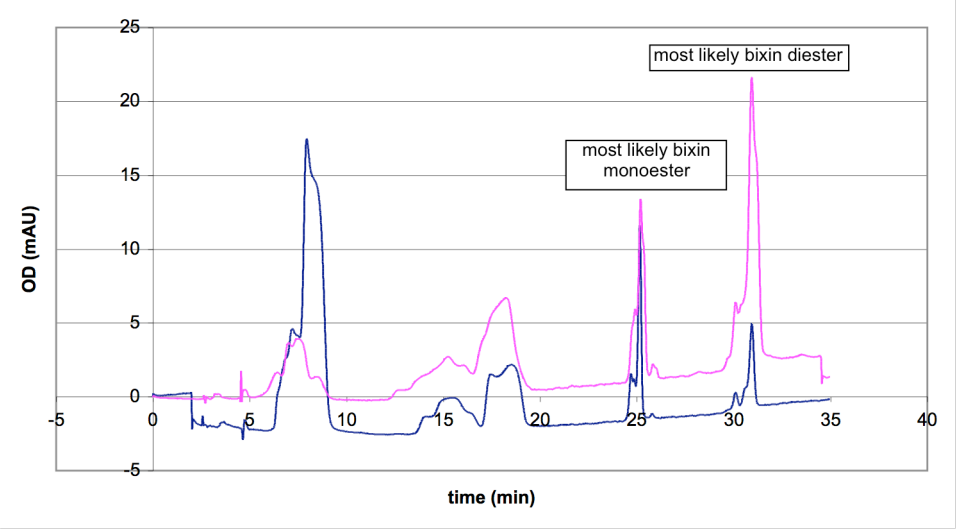

Figure 3. HPLC analysis of Bixin initiator synthesis. A, CalB catalyzed bixin and *n*-propanol reaction. B. CalB catalyzed bixin and PEG400 reaction. C. CalB catalyzed bixin and 1, 10-decanediol reaction. For each reaction, blue lines represent 72 hours reaction and pink lines represent 144 hours reaction.

3. 5 CalB catalyzed Bixin initiator and ε-caprolactone polymerization.

The bixin initiators purified from last step was used for polymerization reactions as described in method section. The polymerization products were detected by using GPC column to determine their molecular weights. (Fig 4 and Table 3.) Bixin-n-propyl diester and ε-caprolactone polymerization was a slow reaction compared to the other two reactions as we expected. The reaction shows a main peak at 16.9 min and a shoulder at 19.2 min after 72 hours. In GPC analysis, molecules are separated according to their size, smaller molecules move slower and came out later. The compound eluting at 19.2 min was the unreacted initiator and compound comes out at 16.9 minutes is the polymer of peak average molecular weight 10,600 g mol^{-1}. Bixin-PEG400 and ε-caprolactone reaction shows only one peak at 16.7 minutes after 72 hours indicating peak average molecular weight 12,900 g mol^{-1}. Bixin-1, 10-decanediol and ε-caprolactone reaction also shows only one peak at 16.85 minutes after 72 hours with average molecular weight 11,100 g mol^{-1}, the increase very little after 144 hours with a peak at 16.3 min with average molecular weight 19,100 g mol^{-1}.

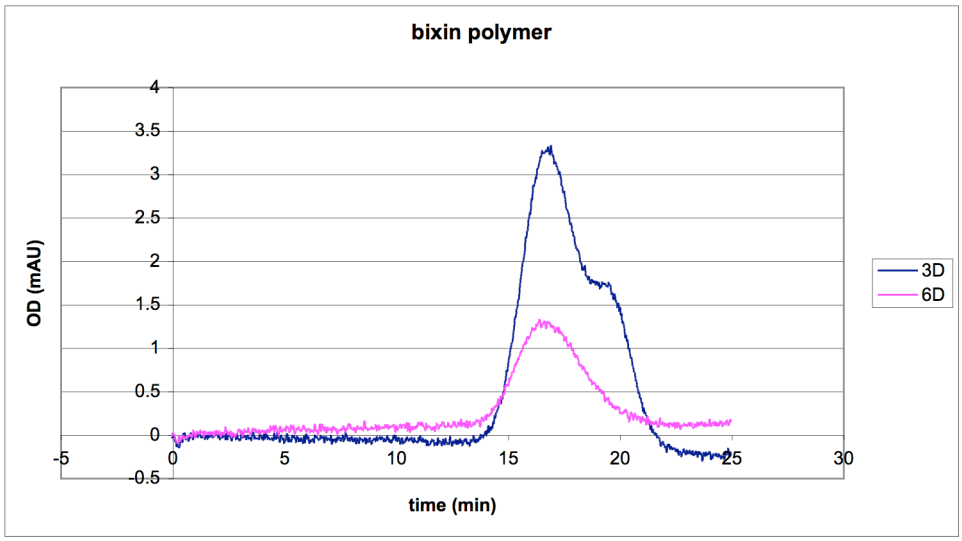
bixin polymer
OD (mAU)
time (min)
3D
6D

A

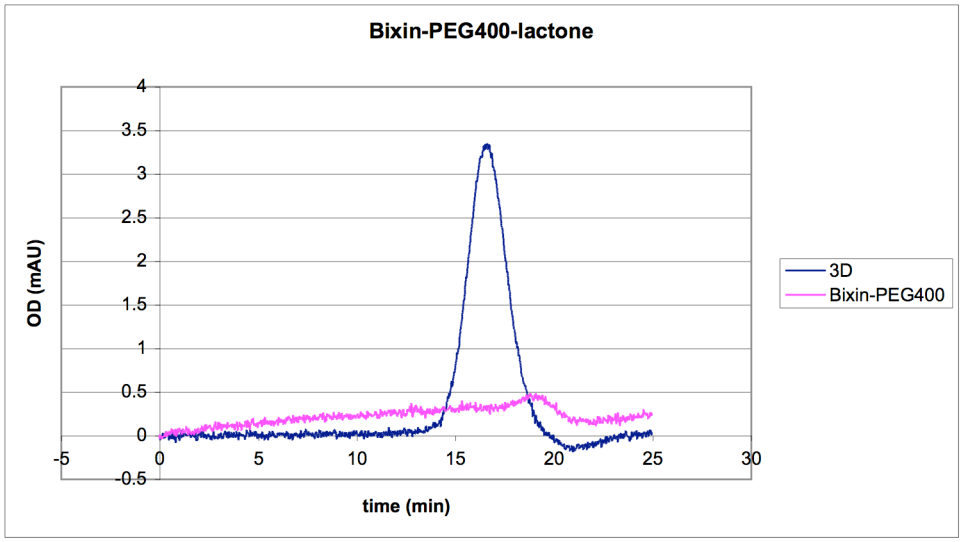
Bixin-PEG400-lactone
OD (mAU)
time (min)
3D
Bixin-PEG400

B

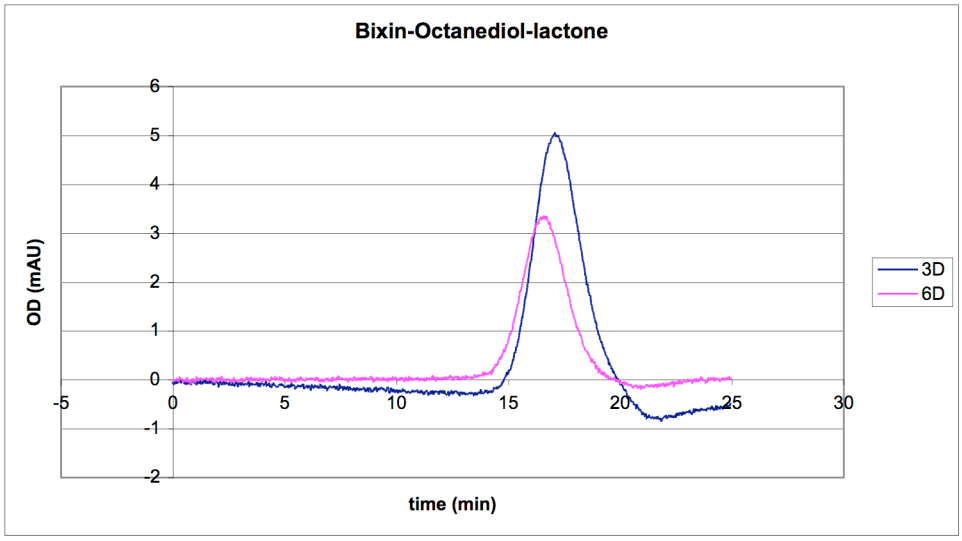
Bixin-Octanediol-lactone
OD (mAU)
time (min)
3D
6D

C

Figure 4. CalB catalyzed bixin initiators polymerizations with ε-caprolactone. A. Bixin-*n*-propanol-ε-caprolactone synthesis. B. Bixin-PEG400-ε-caprolactone synthesis. C. Bixin-1, 10-decanediol-ε-caprolactone synthesis. Blue lines indicate 72 hours reaction in A, B and C. Pink lines indicate 144 hours reaction in A and C and indicate the bixin initiator (starting material) in B.

Table 3. Molecular weight of bixin-containing polyesters.

Polymer	Yield (start from 0.9mg bixin and 400 µl ε-caprolactone)	Retention time (minutes)	MW
Bixin-ε-caprolactone	0.33 g	16.9	10,600
Bixin-PEG400-ε-caprolactone	0.28g	16.7	12,900
Bixin-1, 10-decanediol-ε-caprolactone	0.28 g	16.9	11,100

4. Discussion

Among the 20 esterases and lipases, CalB was identified to be the only catalyst for the bixin hydrolysis reaction. None of the enzyme hydrolyzed crocin. It might be because the sugar moieties at the end of crocin structure are bulky and hydrophilic, which cannot fit into the esterases and lipases hydrophobic active site. CalB also catalyzed bixin esterification or transesterification with substrates of linear chains, like ethanol, *n*-propanol, 1-butanol, 1, 10-decanediol and PEG400. Substrates with side chains, like phytol and dihydroquinone, cannot be condensed with bixin. Though CalB was the only only enzyme that catalyzes bixin reaction, CalB was a very poor catalyst for this reaction. In the reactions, we added CalB (MW 33KD) 20 mg, which contains 0.2 mg enzyme, and bixin (MW 394) 1mg, with molar concentration ratio only 1:400, but it took 72 hours to convert all the bixin, that is, one CalB molecule converted one bixin molecule every 648 seconds. The alternating single and double bonds in bixin mainchain can make this molecule rigid and it makes the molecule hard to fit into CalB active site and positions itself to the productive conformation. CalB can be subjected to protein engineering to improve its catalytic activity towards bixin.

Amide bond is considered more stable than ester bond. Though CalB has amidase activity [10], it doesn't catalyze bixin and 1,4 benznediamine or 1, 7- diaminoheptane transfer reaction and I was not able to synthesis bixin amide initiator.

The synthesized bixin diesters with *n*-propanol, 1, 10-decanediol and PEG400 were used as initiators to synthesis polymers. The CalB catalyzed polymerization reaction on bixin- *n*-propanol was a slow reaction compared to the other two reactions, because 10 mg immobilized CalB, that is 0.1 mg enzyme, catalyze this reaction for 72 hours and still cannot convert all the bixin diester into polymer, which can be seen from the shoulder in Fig4A.

CalB catalyzed bixin diol polymerization is much faster and 1 mg immobilized CalB can convert the initiator into polymer in 72 hours reaction. The diols have very long chains and CalB might work directly on these chains without too much interaction with bixin moiety, so the reactions are more efficient.

These polymerization reactions are our primary tests for carotenoids-containing polyester synthesis and they demonstrate that we can use lipase-catalytized reaction to synthesis these polymers. There are still more to explore: the catalytic efficiency can be improved by changing reaction temperature, substrate to solvent ratio and different lactones; carotenoids-containing polyester with bixin and diols, such as divinyl adipate (Scheme I), alternating in the main chain can be tried by manipulate substrates ratios; CalB can be engineered to improve the catalytic activity towards bixin reaction.

References

1. Del Campo, J.A., García-González, M., Guerrero, M.G. (2007) Outdoor cultivation of microalgae for carotenoid production: current state and perspectives. *Appl. Microbiol. Biotechnol.* 74, 1163-1174.
2. Maoka, T. (2009) Recent progress in structural studies of carotenoids in animals and plants. *Arch. Biochem. Biophys.* 483, 191-195.
3. Suhnel, S., Lagreze, F., Ferreira, J.F., Campestrini, L.H., Maraschin, M. (2009) Carotenoid extraction from the gonad of the scallop *Nodipecten nodosus* (Linnaeus, 1758) (Bivalvia: Pectinidae). *Braz. Biol.* 69, 209-215.
4. Yurkov, V.V., Beatty, J.T. (1998) Aerobic anoxygenic phototrophic bacteria. *Microbiol. Mol. Biol. Rev.* 62, 695-724.
5. Britton, G. (1995) Structure and properties of carotenoids in relation to function. *FASEB J.* 9, 1551-1558.
6. Janata, J., josowicz, A. (2003) Conducting polymers in electronic chemical sensors. *Nat. Mater.* 2, 19-24.
7. Das, A., Yoon, S.H., Lee, S.H., Kim, J.Y., Oh, D.K., Kim, S.W. (2007) An update on microbial carotenoid production: application of recent metabolic engineering tools. *Appl. Microbiol. Biotechnol.* 77, 505-512.
8. Zhu, C., Naqvi, S., Capell, T., Christou, P. (2009) Metabolic engineering of ketocarotenoid biosynthesis in higher plants. *Arch Biochem. Biophys.* 483, 182-190.
9. Mijts, B.N., Lee, P.C., Schmidt-Dannert, C. (2005) Identification of a carotenoid oxygenase synthesizing acyclic xanthophylls: combinatorial biosynthesis and directed evolution. *Chem. Biol.* 12, 453-460.
10. Torres-Gavilán, A., Castillo, E., López-Munguía, A. (2008) The amidase activity of *Candida antarctica* lipase B is dependent on specific structural features of the substrates. *J. Mol. Catal. B: Enzym.* 41, 136.
11. Faber, K. Bitransformations in organic chemistry. Springer 2004. p434

Chapter 3. Active site loop orientation differs in esterases/lipases and acyltransferases: molecular basis for controlling the reactivity of water

X-ray crystallographic data for the structure of *Pseudomonas fluorescens* esterase bound to (*R*)-butane-2-sulfonate has been deposited in the Protein Data Bank as accession number 3ia2.

Krista Morley and Josehh Schrag did the *Pseudomonas fluorescens* esterase crystalization and solved the crystal structure.

This chapter is going to be submitted to Chembio. It is slightly modified for this thesis.

Both esterases/lipases and some acyltransferases transfer acyl groups use a Ser-His-Asp catalytic triad and similar mechanisms. Acyltransferases transfer the acyl group to an acceptor alcohol, while esterases/lipases transfer the acyl group to water. Comparison of the x-ray structures of structurally related esterases/lipases with acyltransferases reveals a different conformation of the oxyanion loop within the active site. In esterases/lipases this loop adopts a type II β turn conformation with carbonyl oxygen of the main chain amide facing the active site. In acyltransferases this loop adopts a type I β turn with the N–H of the main chain amide facing the active site. To identify the mechanistic significance of this different structure, we solved the x-ray crystal structure of *Pseudomonas fluorescens* esterase containing a sulfonate transition state analog bound the active site serine. This structure mimics the transition state for the attack of water on an acyl enzyme intermediate. The structure shows a carbonyl oxygen in the oxyanion loop hydrogen bonding via a bridging water molecule to the attacking water molecule. This interaction

may activate the water molecule for attack to promote hydrolysis. I hypothesize that in acyltransferases the lack of this interaction and an opposing interaction with the N–H deactivates the attacking water molecule. This insight main shows how main chain interactions, which may not be identified by sequence comparison, can direct the reaction path in these two important classes of enzymes.

1. Introduction

Acyltransferases (Enzyme Commission number 2.3) catalyze the transfer an acyl group from donor, usually an ester or thioester, to an acceptor, usually an alcohol or amine thereby forming esters or amides, Figure 1. Some acyltransferases are called thioesterases for their homology to fatty acyl thioesterases. In fatty acid biosynthesis these thioesterases catalyze hydrolysis, but the thioesterase domains in polyketide biosynthesis and nonribosomal peptide biosynthesis may catalyze either hydrolysis or acyl transfer. The acyl transfer reaction is similar to the hydrolysis reaction catalyzed by carboxyesterases and lipases (Enzyme Commission number 3.1.1). The difference is that acyl transfer involve transfer to an acceptor, while in hydrolysis the acceptor is water. Acyl transfer is kinetically controlled; the thermodynamically favored product is hydrolysis.

Acyltransferases catalyze critical steps in antibiotic biosynthesis and other pathways such as amino acid biosynthesis.[1] Both polyketide biosynthesis and non-ribosomal peptide synthesis uses acyltransferases to catalyze macrocyclization or acylation, Figure 2. Macrocyclization reduces conformational freedom to ensure complementary with biological target and reduces susceptibility to proteases. Acylation, usually with a hydrophobic acyl group, of the aglycone or sugar moiety allow the antibiotics to interact with hydrophobic targets such as cell membranes. Acyltransferases also catalyze key steps in amino acid biosynthesis. Homoserine *O*-acetyltransferase (HTA)

from *Haemophilus influenzae* catalyzes the transfer of the acetyl group from acetyl-CoA to L-homoserine to form *O*-acetylhomoserine Figure 2.[2,3]

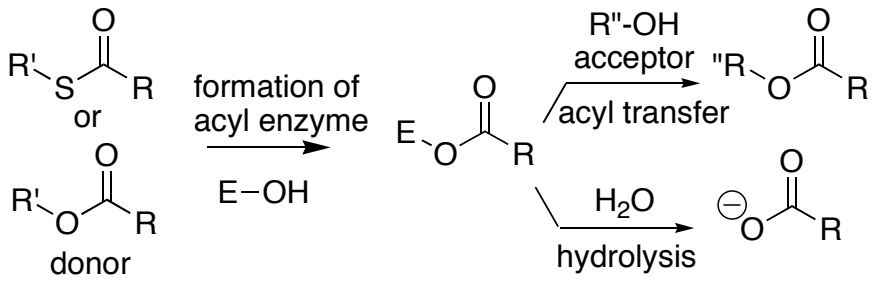

Figure 1. Acyltransferases catalyze the transfer of an acyl group from a donor (ester or thioester) to an acceptor (alcohol in this example). Both hydrolases and acyltransferase form an acyl enzyme intermediate, but hydrolases transfer the acyl group to water, while acyltransferases transfer it to an acceptor.

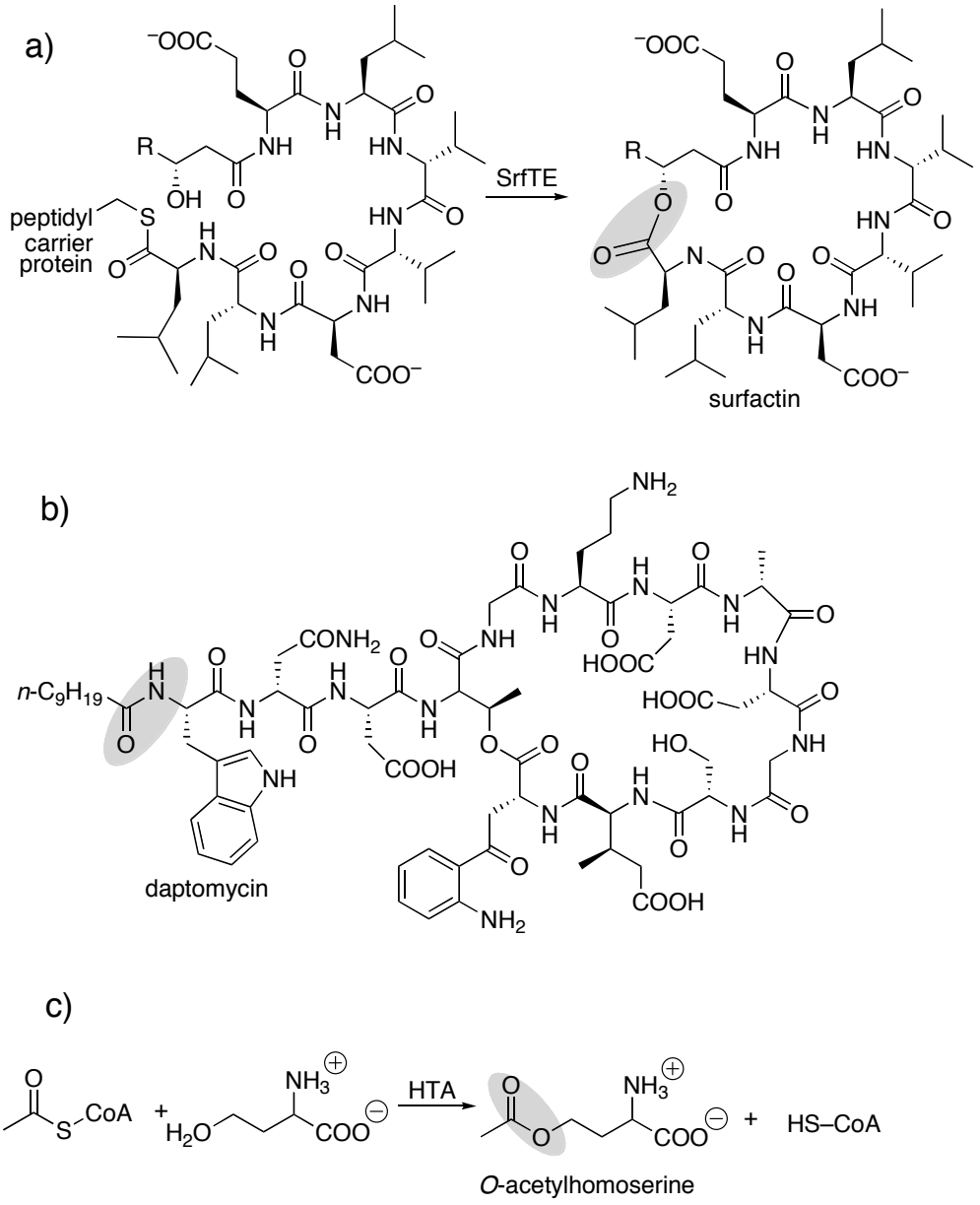

Figure 2. Acyltransferases catalyze key steps in antibiotic synthesis. a) Surfactin synthase thioesterase domain (SrfTE) catalyzes intramolecular cyclization of peptidyl carrier protein thioester to form macrolactone cyclic heptapeptide. b) Biosynthesis of daptomycin involves *N*-acylation of the tryptophan moiety, but the details are not yet clearly established. c) As part of methionine biosynthesis homoserine *O*-acetyltransferase (HTA) catalyzes the transfer of the acetyl group from acetyl-CoA to L-homoserine to form *O*-acetylhomoserine.

Acyltransferases also catalyze critical steps in the synthesis of bacterial polyesters, triacylglycerols and wax esters. Many bacteria store excess carbon as insoluble granules of poly-β-hydroxybutyrate. The elongation step of this polyester synthesis involves an acyl transfer of the growing polyester chain to an added monomer.[4] In triacylglycerol or wax ester synthesis, acytransferases add the acyl group from acyl-coenzyme A to a diacylglycerol to make a triacylglycerol or to a long chain alcohol to make a wax ester.[5] Cholesterol transport and lipoprotein assembly also involves acyltransferases.

Acyltransferases are also used in biocatalysis for the chemoenzymatic synthesis of natural product analogs. For example, Kohli et al. used a cloned thioesterase to catalyze the macrocylization of peptides to create small libraries of macrolactams.[6] Such reactions would have yielded mixtures of different cyclization products without an enzyme. Later the same group used a different thioesterase to regioselectively acylate vancomycin or teicoplanin variants.[7] In another acylation example, Tang's group used the acyltransferase LovD for a regioselective acylation in the gram-scale chemoenzymatic synthesis of simvastatin - a cholesterol lowering drug, which is a semi-synthetic analog of the natural product lovastatin. This procedure allowed use of water as the solvent and avoided multiple protection and deprotection steps.[8]

Esterases/lipases and acyltransferases catalyze both hydrolysis and acyl transfer, but esterases/lipases favor hydrolysis (transfer of the acyl group to water), while acyltransferases favor transfer to an acceptor other than water. In non-aqueous solvents, esterases and lipases favor acyl transfer to an acceptor over hydrolysis. Lyophilized powders of esterases or lipases suspended in non aqueous solvents, typically ionic liquids or non polar organic solvents, catalyze acyl transfer.[9] Examples include resolution of

alcohols by enantioselective acylation, regioselective acylation of sugars, and synthesis of polymers by ring-opening polymerization of lactones.

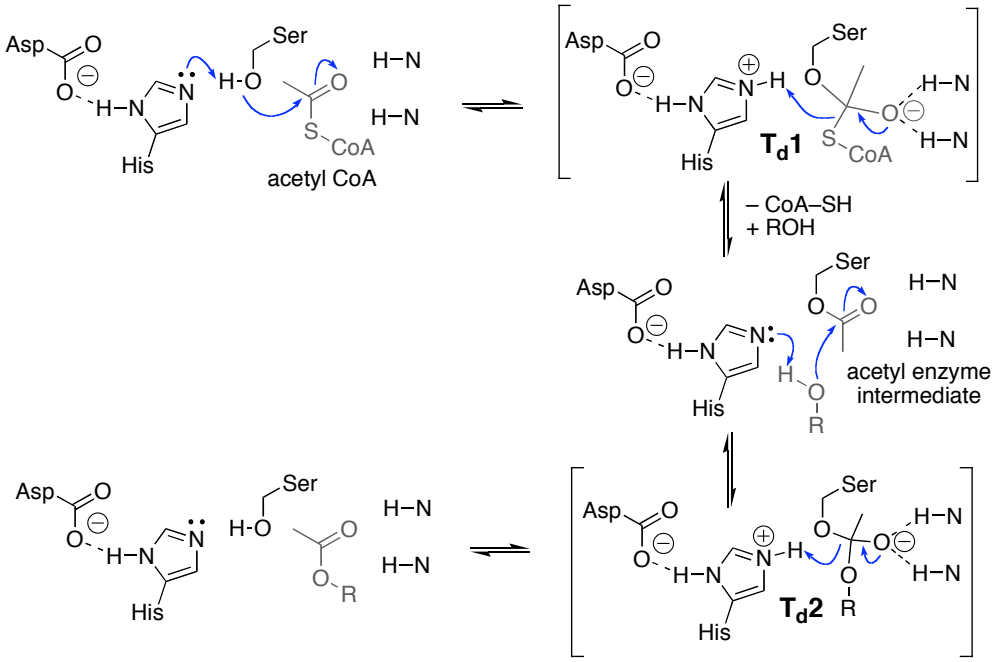

Figure 3. Acyltransferases follow a ping-pong bi-bi mechanism to transfer an acetyl group from acetyl CoA to an acceptor, ROH. The serine nucleophilic attacks carbonyl carbon of acetyl-CoA and forms the first tetrahedral intermediate, T_d1. Release of CoA-SH from this intermediate form the acetyl enzyme intermediate. The acceptor, ROH, attacks the carbonyl carbon of the acetyl enzyme intermediate and forms the second tetrahedral intermediate, T_d2. Release of the serine residue from this intermediate forms the product. Hydrolysis occurs when R = H; acyl transfer occurs when R is an alkyl or aryl group. Two main chain amide N-H (called the oxyanion hole) hydrogen bond to the oxyanion intermediates. The bottom N-H is on the oxyanion loop and occurs first in the linear amino acid sequence, so it will be called the first oxyanion residue.

Hydrolysis is a common side reaction of acyltransferases, especially in the absence of an acceptor. For example, ~30% hydrolysis accompanied macrocyclization of natural peptide catalyzed by Srf TE domain in vitro.[10] Homoserine acetyltransferase and DEBS TE catalyze hydrolysis of acetyl CoA and N-acetylcysteamine thioester derivatives in the absence of an acceptor. [5,11] Some in vitro experiments use thioesterases excised from large multidomain complexes and show more hydrolysis than expected. Addition of solvents and surfactants also influences the relative amount of hydrolysis. Researchers have not identified the reasons for these changes.

This overlapping catalytic activity in esterases/lipases and acyltransferases is due to their similar three-dimensional structures and similar catalytic machinery. Both adopt the α/β-hydrolase fold.[12] Both esterases/lipases and acyltransferases contain a Ser-His-Asp catalytic triad, an oxyanion hole and follow a ping-pong bi-bi reaction mechanism involving an acyl-serine enzyme intermediate, Figure 3. In both cases, catalysis starts by the serine nucleophile attacking the substrate's carbonyl carbon and formation of an acyl-enzyme intermediate. The next step differs in the two enzyme classes: in esterases/lipases: a water nucleophile attacks acyl-enzyme intermediate, while in acyltransferases an alcohol nucleophile (or other acyl acceptor) attacks acyl-enzyme intermediate.

Despite the x-ray crystal structures of eight acyltransferases, including structures with bound substrate analogs, the molecular basis of acyltransferase activity versus hydrolysis remains elusive. The key difference between these reaction is choosing between water and alcohol (or amine) as the nucleophile, see Scheme 1 above. There are two ways to favor acyltransfer over hydrolysis: first, decrease the ability of water to act as a nucleophile or second, increase the ability of alcohol to act as a nucleophile. Both approaches can work simultaneously. In two cases crystallographers suggested that the

active site of acyltransferases is hydrophobic and excludes water (Srf TE, *Mycobacterium* antigens), but in some three cases (*Hi*HAT, *Li*HAT, fengycin TE) crystallographers did not mention any evidence for a water-excluding mechanism. Most structures show evidence for specific interactions between the alcohol and acyltransferase, but these differ for each enzyme because the alcohols differ.

My hypothesis is that there is a common mechanism for deactivation of water as a nucleophile in acyltransferases. Nucleophile substrate binding also contributes to the preference for alcohol over water as a nucleophile. However, this will differ for each acyltransferase as each nucleophile differs. The common feature in acyltransferases may be deactivation of water. Our approach is to compare the x-ray crystal structures of related hydrolases and acyltransferases to identify the structural differences, especially in the active site region that binds the nucleophilic water or alcohol. We found a difference in the main chain orientation of the oxyanion loop in the active site and propose a mechanism of how this different orientation can deactivate water as a nucleophile

2. Methods

2.1 General.

All chemicals were purchased from Sigma-Aldrich (Oakville, ON). LB media was obtained from Difco Laboratories (Detroit, MI). Gas chromatography was carried out with a Chromopak Chiralsil-Dex CB column (25 m x 0.25 mm, Raritan, NJ). ^{1}H NMR and ^{13}C NMR spectra were acquired in $CDCl_3$ or D_2O at 300 MHz and 75 MHz, respectively (M300, Varian).

2. 1 VAST search (Vector alignment search tool)

Protein structures similar to homoserine transacetylase (2b61) were identified by Vast[13] search at the non-identical sequence level and sorted by

aligned length. Proteins of similar structures are arranged by their aligned length from high to low.

2. 3 Superimposion of crystal structures.

Extra subunits were removed for each crystal structure and only Chain A remained. Cα atoms of catalytic histidine and serine and the two residues before and after nucleophilic Ser were pair-fitting using the software PyMol to get superimposed structures. (http://www.pymol.org)

2. 4 Comparison of dihedral angles of first oxyanion residue between hydrolases and acyltransferases.

All the hydrolases of carboxylesterase (lipase/esterase), amidase/peptidase, thioesterase with Ser-His-Asp/Glu catalytic triad were picked from SCOP database[14] of α/β hydrolase superfamily. For each enzyme I picked the crystal structure with highest resolution and some indication that is corresponds to a catalytically active conformation. For example, the structure may contain a substrate analog or inhibitor. In particular we avoided closed conformations of lipases (e. g., *Bacillus stearothermophilus* lipase, 1ku0) because the oxyanion loop orientation adopts a catalytically non-productive orientation in most of these structures. For acyltransferases, besides all SCOP database defined structures, we also added several structures (fengycin thioesterase, 2cb9 and homoserine *O*-acetyltransferase from *Leptospira interrogans*, 2pl5) identified by VAST search. Dihedral angles of oxyanion residues are measured in Pymol.

2. 5 Thioacetic acid (±)-*S*-sec-butyl ester.

Thioacetic acid (±)-*S*-sec-butyl ester was prepared by modifying the literature procedure[15] for preparing (*S*)-1-phenylethyl thioacetate. Diisopropylazodicarboxylate (4.0 mL, 4.1 g, 20.2 mmol) was added dropwise to triphenylphosphine (5.3 g, 20.2 mmol) in THF (100 mL) at 0 °C. After stirring for 30 min at 0 °C, the cloudy white mixture was treated dropwise

with a solution of (±)-2-butanol (1.0 g, 13.5 mmol) and thiolacetic acid (1.4 mL, 1.5 g, 20.2 mmol) in THF (10 mL). After 30 min at 0 °C the resulting greenish-brown solution was warmed to 25 °C and stirred for an additional 1 h. The reaction mixture was washed with saturated $NaHCO_3$ (4 x 100 mL), dried over $MgSO_4$, and the solvent was evaporated. Hexane (100 mL) was added to the crude product and the resulting white precipitate was filtered. The product was purified by column chromatography using hexane/ethyl acetate eluent (50:1), providing the thioacetate as a yellow oil in 40% yield. R_f = 0.36 (hexane:ethyl acetate; 20:1); ^{1}H NMR (300 MHz, $CDCl_3$) δ 3.50-3.40 (1H, m); 2.26 (3H, s); 1.59-1.51 (2H, m); 1.26-1.23 (3H, d); 0.94-0.89 (3H, t). ^{13}C NMR (75 MHz, $CDCl_3$) δ 196.24, 41.40, 31.18, 29.80, 21.19, 11.83. MS (EI) *m/z* (rel. intensity) 132 (31, M^+), 89 (8, M^+-Ac), 43 (100, CH_3CO). Thioacetic acid (*S*)-*S*-sec-butyl ester was prepared with the same procedure starting from commercially available (*R*)-2-butanol (90% ee). The enantiomeric excess was determined to be 89% by GC analysis using Chromopak Chiralsil-Dex CB column (25 m x 0.25 mm, Raritan, NJ): 70 °C for 2 min and raised to 190 °C at a rate of 1.5 °C/min at 50 kPa. Retention times were 13.0 min for thioacetic acid (*S*)- *S*-sec-butyl ester and 13.5 min for thioacetic acid (*R*)- *S*-sec-butyl ester.

2. 6 (±)-Butane-2-sulfonyl chloride.

A solution of 30% H_2O_2 (3.7 mL) was added dropwise to a solution of thioacetic acid (±)-*S*-sec-butyl ester (1.0 g, 7.6 mmol) in acetic acid (10.5 ml) at 60 °C. After stirring overnight at 60 °C the mixture was cooled to 25 °C and the excess H_2O_2 was destroyed by the addition of 5% Pd/C (35 mg). The mixture was diluted with ether, dried over $MgSO_4$, and concentrated. After the excess acetic acid was removed azeotropically with heptane,[7] the residue was diluted with water (10 mL) and neutralized with 0.5 M aqueous NaOH. Evaporation of water yielded the sodium salt of (±)-butanesulfonic acid as a white solid. Toluene (20 ml) was added and evaporated to eliminate the remaining traces of H_20 yielding the salt in 96% yield (1.2 g, 7.3 mmol). ^{1}H

NMR (300 MHz, D_2O) δ 2.96-2.81 (1H, m); 2.10-1.96 (1H, m); 1.63-1.47 (1H, m); 1.38-1.36 (3H, d); 1.11-1.06 (3H, t). ^{13}C NMR (75 MHz, D_2O) δ 57.71, 24.75, 14.28, 11.26.

The sodium salt of (±)-butanesulfonic acid (0.1 g, 0.6 mmol) was added to 10 mL of thionyl chloride ($SOCl_2$) and the mixture was refluxed for 24 h. Evaporation of the excess $SOCl_2$ yielded 0.06g (64% yield) of the crude (±)-butane-2-sulfonyl chloride; ^1H NMR (300 MHz, $CDCl_3$) δ 3.65-3.57 (1H, m); 2.25-2.13 (1H, m); 1.85-1.74 (1H, m); 1.57-1.55 (3H, d); 1.15-1.10 (3H, t). ^{13}C NMR (75 MHz, $CDCl_3$) δ 63.22, 24.08, 14.17, 11.20.

2. 7 (±)-Butane-2-sulfonic acid 4-nitrophenyl ester.

The sodium salt of (±)-butanesulfonic acid (0.4 g, 2.5 mmole) was refluxed in thionyl chloride and the crude (±)-butane-2-sulfonyl chloride was derivatized with *p*-nitrophenol (0.35 g, 2.5 mmole) and triethylamine (0.1 mL, 0.07 g, 0.7 mmole) in CH_2Cl_2 (20 mL). (±)-butane-2-sulfonic acid *p*-nitrophenyl ester was obtained in 16% yield (0.11 g, 0.4 mmole) after purification by column chromatography using hexane/ethyl acetate eluent (4:1 hexane:ethyl acetate); R*f*=0.42 (4:1 hexane/ethyl acetate); ^1H NMR (300 MHz, $CDCl_3$) δ 8.17-8.14 (2H, d); 7.47-7.44 (2H, d); 3.60-3.48 (1H, m); 2.16-2.0 (1H, m); 1.85-1.68 (1H, m); 1.61-1.59 (3H, d); 1.17-1.12 (3H, t). ^{13}C NMR (75 MHz, $CDCl_3$) δ 125.69, 122.78, 60.02, 24.21, 14.28, 11.29; MS (EI) *m/z* (rel. intensity) 259 (4, M^+), 139 (100, pNP-OH).

2. 8 Protein expression and purification.

An overnight culture (20 mL) of recombinant *Escherichia coli* DH5α containing plasmid pJOE2792 was added to Luria-Bertani broth (2 L; ampicillin, 100 µg/mL) and grown at 37 °C and 200 rpm to an OD_{600} of 0.5. Protein expression was induced by addition of sterile rhamnose (20 mL; 20% w/v) and incubation for 6 h at 37 °C and 200 rpm. The cells were harvested by centrifugation (15 min, 3000 x g, 4 °C) and the supernatant was discarded. To

lyse the cells, the cell pellet was resuspended in 50 mL of Buffer A (NaH_2PO_4, 50 mM; NaCl, 300 mM; imidazole, 10 mM; adjusted to pH 8.0 with NaOH) containing lysozyme (1 mg/mL) and incubated at 37 °C and 200 rpm for 30 min. The suspension was frozen at –20 °C and then thawed at room temperature.

The viscosity of the lysate was broken by repeatedly passing the solution through a sterile 20-gauge syringe needle to shear DNA/RNA and the sample was centrifuged (45 min, 3000 x g, 4 °C). To the supernatant was added 20 mL of Ni-NTA agarose resin (50% slurry in 30% ethanol; Qiagen Inc, Mississauga, ON, Canada) and the mixture was stirred at 4 °C for 24 h. The mixture was loaded on ten Poly-Prep columns (BioRad Laboratories, Mississauga, ON), allowed to settle and then drained. Each column was then washed twice with 4 mL of Buffer B (NaH_2PO_4, 50 mM; NaCl, 300 mM; imidazole, 20 mM; adjusted to pH 8.0 with NaOH). The His_6-PFE enzyme was eluted from each column with 4 volumes of Buffer C (2 mL; NaH_2PO_4, 50 mM; NaCl, 300 mM; imidazole, 250 mM; adjusted to pH 8.0 with NaOH). Eluate from the Ni-NTA columns containing purified PFE was exchanged from Buffer C to BES (5 mM, pH 7.2) using a Centriplus centrifugal filter device with 10 kDa molecular-weight cutoff (Millipore Corporation, Bedford, MA). The protein solution was concentrated to 10 mg/mL, and used directly in crystallization trials.

2. 9 Inactivation of PFE by (±)-butane-2-sulfonic acid 4-nitrophenyl ester.

Wild-type PFE was dissolved in 10 mL BES buffer (5 mM, pH 7.2) to a final concentration of 20 μM. A 10-fold molar excess of (±)-butane-2-sulfonic acid 4-nitro-phenyl ester (0.6 mg, 2.0 μmole) was added to the enzyme solution and the mixture was stirred at room temperature for 24 hours. The rate of *p*-nitrophenyl acetate hydrolysis dropped to 5% for the inhibited esterase. The PFE-inhibitor complex was separated from excess inhibitor by washing three times with BES buffer (5 mM, pH 7.2) using a Centriplus

centrifugal filter device with 10 kDa molecular-weight cutoff (Millipore Corporation, Bedford, MA). The complex solution was concentrated to 10 mg/mL for crystallization trials. The unreacted inhibitor was extracted from the buffer wash solution with CH_2Cl_2 for GC analysis. The enantiomeric excess was determined to be 8% in favour of (*S*)-butane-2-sulfonic acid 4-nitro-phenyl ester, the transition-state analog of the slow-reacting enantiomer. This indicates that the (*R*)-enantiomer reacted preferentially with the enzyme.

2. 10 Crystallization, data collection, and structure determination.

Initial crystallization screens for the PFE-inhibitor complex were performed using the hanging-drop vapor-diffusion method in a 24-well plate. The precipitant solutions ranged in pH from 5.0 - 7.5 and contained between 1 and 2 M $(NH_4)_2SO_4$ and 0-4% PEG 400. Drops contained 3 μL of protein solution (10 mg/mL) and 5 μL precipitant solution. The best crystallization conditions varied for each protein solution and were 1.7 M $(NH_4)_2SO_4$, 3% PEG in 0.1 M $NaKH_2PO_4$ pH 7.5. Crystals were flash-frozen at 93 K after brief immersion in a cryoprotectant solution consisting of precipitant solution with 25% glycerol added. Data for the PFE-inhbitor complex were collected using a Rigaku Micromax 007 rotating-anode generator equipped with Osmic mirrors and an HTC image plate detector (Rigaku/MSC; The Woodlands, TX, USA). Data were reduced using d*TREK[16] or DENZO/SCALEPACK.[17] Crystals were isomorphous with crystals from wild type PFE (PDB ID: 1VA4). Models of the mutant protein were generated from wild type PFE using O.[18] Refinements were performed using Refmac version 5[19] of the CCP4 Suite of crystallographic programs (1994).[20] Rigid body refinements allowing each of the six polypeptide chains in the asymmetric unit to move independently were followed by restrained maximum likelihood refinement. Medium or loose NCS restraints were used throughout the refinement. Water molecules were placed using ARP/WARP.[21] Final fitting of the models was done in O using SigmaA weighted $2F_o$-F_c maps.[22] The structures were validated using PROCHECK.[23]

Table 1. Data-collection and refinement statistics.

Data Collection	
Space Group	$P3_2$
Unit cell	
a, b, c (Å)	146.22, 146.22, 129.96
α, β, γ (º)	90, 90, 120
No. Reflection	
Observations	1329492
Unique	364141
Resolution Range (Å)	48.57-1.65
Completeness	
Overall (highest shell, 1.71-1.65)	97.4 (91.2)
R_{sym} (%)	
Overall (highest Shell, 1.71-1.65)	5.6 (34.3)
I/σI	
Overall (highest shell, 1.71-1.65)	13.2 (3.0)
Refinement	
R_{work} (highest shell, 1.693-1.65)	19.8 (31.1)
R_{free} (highest shell, 1.693-1.65)	20.7 (31.7)
R.m.s. deviations from ideality	
Bond lengths (Å)	0.003
Bond angles (º)	0.776
Ramachandran analysis	
Most favored (%)	91.6
Allowed (%)	7.6
Generously allowed (%)	0.8
Disallowed (%)	0.1
Final model	
No. of atoms	

Protein	13040
Solvent (H_2O, glycerol, SO_4)	1631
Ligand	42
Mean B factor	
Protein	21.668
Solvent	33.198
Ligand	31.531

3. Results

3. 1 Structure differences between *Haemophilus influenzae* homoserine acyltransferase (*Hi*HAT) and *Pseudomonas fluorescens* esterase (PFE).

Although the amino acid sequences of *Haemophilus influenzae* homoserine acyltransferase (*Hi*HAT) and *Pseudomonas fluorescens* esterase (PFE) differ signficantly (only 14% sequence identity), their three dimensional structures (protein data bank codes 2b61 and 1va4, respectively) are very similar. The Z-score for the structural overlay is 17.9 and root mean square deviation between the atoms in the two structures is 3.0 Å.

The major difference in the active sites is the oxyanion loop conformation. This loop occurs after strand β3 in the α/β-hydrolase fold and contains one residue that donates a main chain N-H to stabilize the oxyanion intermediate during catalysis, see Scheme 3 above. This residue, called the first oxyanion residue in this paper, is Leu49 in *Hi*HAT and Trp28 in PFE. In *Hi*HAT this loop adopts a type I β turn, while in PFE it adopts a type II β turn.

β-Turns reverse the direction of the peptide chain and consist of four amino acid residues where the first and last residues (*i* and *i* + 3) form a hydrogen bond between C=O (*i*) to N–H (*i* + 3)[24] Figure 4. This hydrogen bond is similar to the one between adjacent antiparallel beta strands; hence the name β turn. The two central residues in a β turn (second and third residues

called *i* + 1 and *i* + 2, respectively) lack hydrogen bonds between the main chain carbonyl and N–H groups. This lack of hydrogen bond is critical for catalysis in ester hydrolysis and acyl transfer since the *i* + 1 N–H group stabilizes the oxyanion intermediate by donating a hydrogen bond.

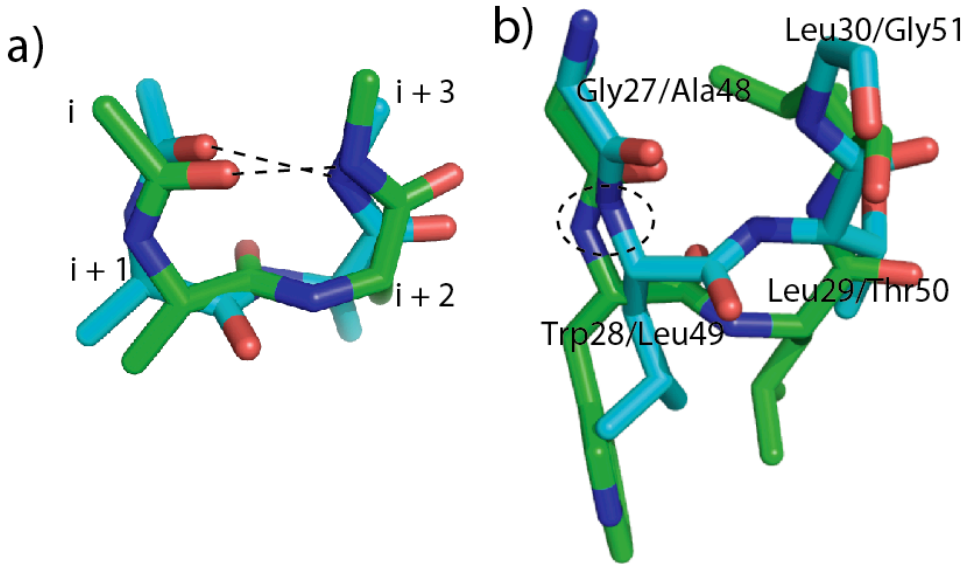

Figure 4. β-turns. a) Idealized type I β turn (cyan carbons) overlaid on an idealized type II β turn (green carbons). The amino acids are XxxAlaAlaXxx, where Xxx indicates an incompletely specified residue since only part of the *i* and *i* + 3 residues are shown. The labels are near the C_α of each residue; dotted lines indicate hydrogen bonds between the carbonyl of residue *i* and the N-H of residue *i* + 3. b) Superimposed x-ray crystal structures of the oxyanion loop regions of PFE (green carbons, a type II β turn) and *Hi*HAT (cyan carbons, a type I β turn). The structures were superimposed by pair fitting of the active site serine and histidine (not shown). In this view the active site lies behind the plane of the paper so the carbonyl of *i* + 1 in PFE (green) points toward the active site, while for *Hi*HAT (cyan carbons) the carbonyl of *i* + 1 points away from the active site. In both cases the N-H of *i* + 1 (circled with a dashed line) points toward the active site since it forms a hydrogen bond with the oxyanion intermediate.

The central residues in a β turn can adopt different conformations. The type I β turn contains $\Phi_{i+1} = -60°$, $\psi_{i+1} = -30°$, $\Phi_{i+2} = -90°$, $\psi_{i+2} = 0°$, while the type II β turn contains $\Phi_{i+1} = -60°$, $\psi_{i+1} = 120°$, $\Phi_{i+2} = 80°$, $\psi_{i+2} = 0°$. Variations of ±30° from these ideal values are still classified with these conformations. In PFE these angles are –66°, 135°, 87°, –21° and thus correspond to a type II turn (i + 1 = Trp28, i + 2 = Leu29). In *Hi*HAT, these angles are –48°, –49°, –109°, 14° and correspond to a type I turn (i + 1 = Leu49, i + 2 = Thr50. The consequence of this difference is that the carbonyl groups of PFE Trp28 and HAT Leu49 point in opposite directions: PFE Trp28 carbonyl points into the active site, while HAT Leu49 carbonyl points away from the active site.

3. 2 Different oxyanion loop conformation in GX-class hydrolases versus acyltransferases

I hypothesize that this difference in oxyanion turn orientation for PFE and *Hi*HAT is a common feature that distinguishes esterases from acyltransferases. To test this hypothesis we made a more extensive comparison of structures within closely related esterases/lipases and acyltransferases. For the hydrolases, we focused on esterases/lipases within the α/β hydrolase superfamily and further narrowed our comparison to those with a GX class oxyanion loop. The lipase engineering database subdivides lipases according the oxyanion loop orientation[25] into GX, GGGX and Y classes. G represents glycine, X represents any amino acid and Y represents tyrosine. The oxyanion loop orientation in acyltransferases (see below) is similar to GX family hydrolases, but the other two classes have significantly different orientations of the oxyanion loops. The GGGX class has a much larger space, while the Y class uses the tyrosine side chain to stabilize the oxyanion so the main chain orientation differs significantly. As mentioned above, we excluded any structures such as closed conformations of lipases where there was doubt whether it was a catalytically active conformation. We

used the SCOP database[26] to ensure that we included all examples that fit these criteria. We found thirty-two x-ray structures of hydrolases that fit these criteria, Table 2.

The oxyanion loops in most of these hydrolases adopt a type II β turn and all but one point the carbonyl group of the $i + 1$ residue toward the active site, Table 2. Among thirty-two GX-class hydrolases, twenty-one have angles are within 30° of the ideal values defined above for type II β turns, three have angles deviate slightly more than 30° from the ideal values, seven are not type II β turn because the last two angles (Φ_{i+2}, ψ_{i+2}) deviate significantly from those for a type II β turn. In all thirty-one of these structures, the first two dihedral angles in the definition of a type II β turn (Φ_{i+1}, ψ_{i+1}) are similar. The Φ_{i+1} angles range between -82° and -44° and the ψ_{i+1} angles range between 112° and 155°. Because of this similarity in the dihedral angles for $i + 1$, the carbonyl group of this residue points toward the active site in all thirty-one structures. The backbone N-H of this residue, whose catalytic role is stabilization of the oxyanion, also points toward the active site. The one exception to this generalization is human fatty acid synthetase thioesterase domain, which shows a type I β-turn for the oxyanion turn.[24] This exception is rationalized in the later paragraph.

Acyltransferases fall into several superfamilies within the structural classification of proteins database (SCOP), but only acyltransferases that have the α/β-hydrolase fold were included in this comparison. For example, homoserine *O*-succinyl transferase from *Bacillus cereus* (pdb code: 2ghr) is not included because its structure belongs to the class I glutamine amidotransferase-like superfamily. Similarly, histone acetylases are not included because most structures belong to the acyl-CoA *N*-acyltransferases superfamily. Three acyltransferases within the α/β-hydrolase fold superfamily are not included in Table 3 because their oxyanion loops are distorted. Two thioesterases of polyketide biosynthesis (erythromycin thioesterase and

pikromycin thioesterase) contain a two-amino-acid insertion in the oxyanion loop, which significantly changes its orientation, see the later paragraph for details. Myristoyl-ACP-specific thioesterase is also excluded because the x-ray structure[24] did not definitively identify the oxyanion loop. The most likely oxyanion loop is too far from active site: 8.6 Å from Oγ of Ser114 to the backbone nitrogen Phe44. (The corresponding distance in PFE is 4.8 Å.) Catalysis may require a conformational change or a bridging water molecule. Table 3 lists the eight acyltransferases in the α/β-hydrolase fold superfamily whose x-ray crystal structures have been solved. These include three mycolyl transferases (*Mycobacterium tuberculosis* antigens), two thioesterases from polyketide antibiotic biosynthesis that catalyze cyclization of surfactin or fengycin, two homoserine acyltransferases and an acetyl transferase from β-lactam antibiotic biosynthesis.

Table 2. Conformation of the oxyanion turn in thirty-one GX-class hydrolases within the α/β-hydrolase superfamily.[a]

Hydrolase	**PDB code**	**Oxyanion turn, sequence,Φ_{i+1}, ψ_{i+1}, Φ_{i+2}, ψ_{i+2}[b]**	**Hydrolyzed bond**
aclacinomycin methylesterase (RdmC) with bound product analog	1q0r[27]	GGNL (31-34) -67°, 140°, 59°, 19°	Carboxylester
Burkholderia cepacia lipase complexed with phosphonate	1ys2[28]	GLTG (16-19) -53°, 138°, 78°, -15°	Carboxylester
Pseudomonas aeruginosa lipase complexed with phosphonate	1ex9[29]	GMLG (15-18) -65°, 139°, 57°, 31° close to a type II β turn	Carboxylester
Burkholderia glumae lipase	1qge[30]	GLAG (16-19) -82°, 112°,-144°, 160° not a type II β turn	Carboxylester
Bacillus subtilis lipase A complexed with phosphonate	1r4z[31]	GIGG (11-14) -61°, 122°, 78°, 4°	Carboxylester
Pseudomonas fluorescens hydrolase complexed with sulfonate	this work	GWLL (27- 30) -65°, 139° 86°, -26°	Carboxylester
Aureobacterium species γ-lactamase complexed with carbonate	1hl7[32]	GYPL (31- 34) -71°, 145°, -108°, 44° not a type II β turn	Carboxylester
Tobacco salicylic acid-binding protein 2	1y7h[33]	GACH (12- 15) -67°, 145°, 67°, 6°	Carboxylester

Saccharomyces cerevisiae S-formylglutathione hydrolase	1pv1[34]	GLTC (57- 60) -44°, 129°, 73°, -2°	Thioester
Bacillus stearothermophilus carboxylesterase	1r1d[35]	GFTG (23-26) -63°, 126°, 77°, -1°	Carboxylester
Alcaligenes sp. hydrolase	1qlw[36]	GCCL (70-73) -67°, 155°, 67°, 14°	Carboxylester
Dog gastric lipase complexed with phosphonate	1k8q[37]	GLLA (66-69) -53°, 135°, 57°, 21°	Carboxylester
Human gastric lipase	1hlg[38]	GLLA (66-69) -50°, 134°, 51°, 24°	Carboxylester
Palmitoyl-protein thioesterase 1 precursor complexed with palmitate	1eh5[39]	GMGD (40-43) -59°, 131°, 79°, -6°	Thioester
Human palmitoyl-protein thioesterase 2	1pja[40]	GLFD (44-47) close to a type II β turn -55°, 140°, 44°, 43°	Thioester
Rat pancreatic lipase-related protein 2	1bu8[41]	GFLD (76-79) not a type II β turn -58°, 126°, -116°, 110°	Carboxylester
Horse pancreatic lipase	1hpl[42]	GFID (76-79) -71°, 134°, -119°, 118° not a type II β turn	Carboxylester
Human pancreatic lipase	1lpa[43]	GFID (76-79) -58°, 140°, 68°, -36° close to a type II β turn	Carboxylester
Pseudomonas fluorescens carboxylesterase	1auo[44]	GLGA (22-25) -65°, 130°, 86°, -17°	Carboxylester
Human acyl protein thioesterase 1	1fj2[45]	GLGD (24-27) not a type II β turn -66°, 134°, 85°, -58°	Carboxylester

Rhizomucor miehei lipase complexed with phosphonate	4tgl[46]	G<u>S</u>SS (81-84) not a type II β turn -57°, 127°, -144°, -12°	Carboxylester
Humicola lanuginosa lipase (open form)	1dt5[47]	G<u>S</u>RS (82-85) not a type II β turn -78°, 151°, -73°, -21°	Carboxylester
Candida antarctica lipase B	1tca[48]	G<u>T</u>GT (39-42) -59°, 135°, 82°, 16°	Carboxylester
Aspergillus niger ferulate esterase	2hl6[49]	G<u>T</u>GS (67-70) not a type II β turn -69°, 125°, -134°, 23°	Carboxylester
Streptomyces exfoliates lipase	1jfr[50]	G<u>F</u>TA (62-65) -56°, 130°, 63°, 17°	Carboxylester
Bacillus subtilis cephalosporin-C deacetylase	1l7a[51]	G<u>Y</u>NA (90-93) -62°, 118°, 55°, 28°	Carboxylester
Clostridium thermocellum endo-1,4-β-xylanase Z precursor	1jjf[52]	G<u>I</u>GG (89-92) -52°, 135°, 70°, -7°	Carboxylester
Fusarium solani cutinase	1agy[53]	G<u>S</u>TE (41-44) -63°, 134°, 73°, 7°	Carboxylester
Penicillium purpurogenum acetylxylan esterase[c]	2axe[54]	E<u>T</u>TA(12-15) -64°, 132°, 72°, -3°	Carboxylester
Trichoderma reesei acetyl xylan esterase[c]	1qoz[55]	E<u>T</u>TV(12-15) -60°, 146°, 72°, -12°	Carboxylester
Clostridium thermocellum feruloyl esterase module of xylanase 10B[d] complexed with carboxylic acid	1gkl[56]	G<u>G</u>GE (865-868) -62°, 139°, 79°, 0°	Carboxylester

Human fatty acid synthase thioesterase domain	1xkt[57]	PIEG (2249-2252) a type I β-turn[e] -63°, -29°, -72°, -3°	Thioester

[a] The table includes all GX-class hydrolases whose x-ray crystal structures have been solved. In the cases where more than one x-ray crystal structure is available, we chose the structure most likely to represent the catalytically active form; that is, those structures containing a transition-state analog or in the open conformation in the case of lipases.

[b] The GX class hydrolases have four amino acid residues in the oxyanion turn. The first residue, called *i*, is a glycine. The second residue, underlined and called the i+1 residue donates the main chain N–H to stabilize the oxyanion. The numbers in parentheses indicate the amino acid numbering of the oxyanion turn. The four angles are the Φ and ψ dihedral angles of the *i*+1 and *i* + 2 residues. All the oxyanion turns adopt a type II β turn conformation, except where noted. The examples that do not fit a type II β turn still point the carbonyl oxygen of the *i*+1 residue toward the active site. The Φ and ψ dihedral angles for this *i*+1 residue are similar to those for a type II β turn, but the dihedral angles for the third residues differ from a type II β turn.

[c] Although these two enzymes do not belong to GX class because the first residue is not a glycine, we include them in this table because their peptide backbones orient as a type II β turn and are similar to GX class hydrolases.

[d] This hydrolase could be classified into either the GGGX class or the GX class based on the amino acid sequence of the oxyanion turn. The structure show that the oxyanion turn conformation is a type II β turn typical of the GX-class hydrolases so it is included in this Table.

[e]This exception uses an alternative mechanism to activate water for hydrolysis - the side chain of the *i*+2 residue, glutamate. See text for details.

Table 3. Conformation of the oxyanion turn in eight acyltransferases within the α/β-hydrolase superfamily.[a]

Acyltransferase	**PDB code**	**Oxyanion turn, sequence, Φ_{i+1}, ψ_{i+1}, Φ_{i+2}, ψ_{i+2}[b]**	**Reaction catalyzed**
Mycobacterium tuberculosis Antigen 85-C[c] with diethyl phosphate inhibitor	1dqy[58]	GLRA (39-42) -49°, -40°, -96°, 30°	transfer of mycolyl group
Mycobacterium tuberculosis Antigen 85-A[c]	1sfr[59]	GLRA (41-44) -51°, -40°, -98°, 42° close to type I β turn	transfer of mycolyl group
Mycobacterium tuberculosis Antigen 85-B[c]	1f0n[60]	GLRA (41-44) -50°, -44°, -90°, 39° close to type I β turn	transfer of mycolyl group
Bacillus subtilis surfactin synthetase thioesterase domain	1jmk[61]	PVLG (26-29) -54°, -24°,-63°, -28°	macrolactonization of peptide
Bacillus subtilis fengycin synthetase thioesterase domain[d]	2cb9[62]	PISG (29-32) -60°, -24°, -52°, -32° close to type I β turn	macrolactonization of peptide
Leptospira interrogans homoserine acyltransferase[d]	2pl5[63]	ALSG (54-57) -54°, -44°, -81°, -24°	transfer of acetyl group
Haemophilus influenzae homoserine acyltransferase[d]	2b61[64]	ALTG (48-51) -70°, -48°, -109°, 14°	transfer of acetyl group

Acremonium chrysogenum deacetylcephalosporin C acetyltransferase [d] with *O*-acetyl serine and acceptor deacetylcephalosporin C	2vav[65]	TLTS (58-61) (-46°, -52°, -111°, 11°)	transfer of acetyl group

[a] The table includes all acyltransferases whose x-ray crystal structures have been solved. Only the first three acyltransferases have a GX signature sequence. The remaining five are included because their oxyanion residues are positioned similar to GX hydrolases.

[b] Acyltransferases have four amino acid residues in the oxyanion turn. The second residue, underlined and called the *i* +1 residue donates the main chain N–H to stabilize the oxyanion. The numbers in parentheses indicate the amino acid numbering of the oxyanion turn. The four angles are the Φ and ψ dihedral angles of the *i*+1 and *i* + 2 residues. All the oxyanion turns adopt a type I β turn conformation.

[c] Antigen 85 A, B and C are homologous proteins that catalyze the transfer of mycolic acid from one molecules of trehalose monomycolate to another to form trehalose dimycolate or from trehalose monomycolate to cell wall arabinogalactan to form cell wall arabinogalactan-mycolate.

[d] These acyltransferases were not included in the SCOP classification, but a structure-based search (VAST) identified them in the protein data bank.

The oxyanion turns in all eight acyltransferases in Table 3 are either type I β turns or very close to a type I β turn. In particular, the dihedral angles of the oxyanion residue are similar in each case: the Φ_{i+1} angles range from -70˚ to -46˚ and the ψ_{i+1} angles range from -52˚ to -24˚. The conformation of the oxyanion residues maintains the catalytically essential N-H in position to hydrogen bond to the oxyanion intermediate. However, this conformation points the carbonyl oxygen of this residue away from the active site and this orientation of the carbonyl group is the major structural difference between hydrolases and acyltransferases.

A graphic comparison of conformations of the oxyanion residue (i + 1 of the β turn) shows a dramatic difference between the hydrolases and the acyltransferases, Figure 5. The Φ_{i+1} angles are similar for both: an average of –62 ± 8° for the hydrolases in Table 2 (excluding hydrolase 1xkt) and and average of –54 ± 8° for the acyltransferases in Table 3. This similarity places the backbone amide N-H and the Cα of i + 1 in similar orientations and allows this amide N-H to contribute to catalysis in both classes of enzymes. In contrast, the ψ_{i+1} angles differ. For hydrolases this angle averages 134 ± 9°, while for acyltransferases it averages –40 ± 10°. This 174° difference corresponds to an opposite orientation for the carbonyl oxygen of this residue.

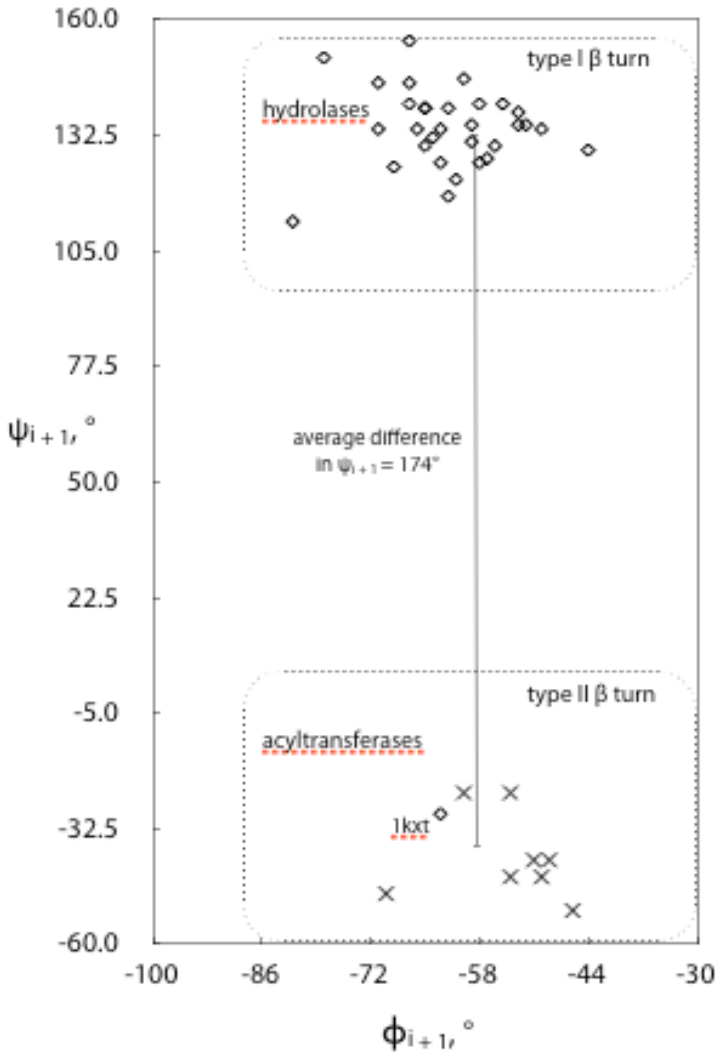

Figure 5. Dihedral angles of the oxyanion residue (*i* + 1 in the turn) in hydrolases and acyltransferases. The hydrolases (diamonds) have Φ_{i+1} = –62 ± 8°, ψ_{i+1} =134 ± 9°, which points the carbonyl oxygen of these residues *toward* the active site. The acyltransferases (crosses) have Φ_{i+1} = –54 ± 8°, ψ_{i+1} = –40 ± 10°, which points the carbonyl oxygen of these residues *away from* the active site. The average difference in ψ_{i+1} is 174°, which corresponds to an opposite orientation for the carbonyl oxygen of these residues. One hydrolase, labelled 1xkt, lies among the acyltransferases and is not included in the averages. The supporting information suggests an explanation for this exception. The dotted lines indicate angles within 30° of the ideal values for β turns.

3. 3 Why fatty acid synthase thioesterase is an exception in Table 2

Human fatty acid synthase thioesterase (hFAS TE) is an exception to the generalization that hydrolases contain a type II oxyanion turn because it contains a type I turn, Table 2 above. This acyl-transferase-like turn prevents activation of the attacking water by the mechanism detailed in the main text. The x-ray structure of hFAS TE suggests an alternative mechanism for activation of water, Figure 6. The side chain of another amino acid residue in the oxyanion turn Glu2251 lies in a similar position as the $i + 1$ carbonyl oxygen in the oxyanion turn of hydrolases. One carboxylate oxygen on the side chain of Glu2251 lies 6.16 Å from nucleophilic Ser as compared to 6.32 Å for the Trp28 carbonyl oxygen to Ser94 in PFE. Superimposition of PFE and hFAS TE indicates similar positions of PFE Trp28 backbone carbonyl group and hFAS TE Glu2251 side chain carboxylic group. Thus, Glu2331 in hFAS TE may activate a water molecule for nucleophilic attack. The sequence alignment of hFAS TE with fatty acid synthetase thioesterases from four other organisms indicated around conserved 35 residues,[66] including catalytic residues and Glu2251, which suggests that it has a catalytic role.

A

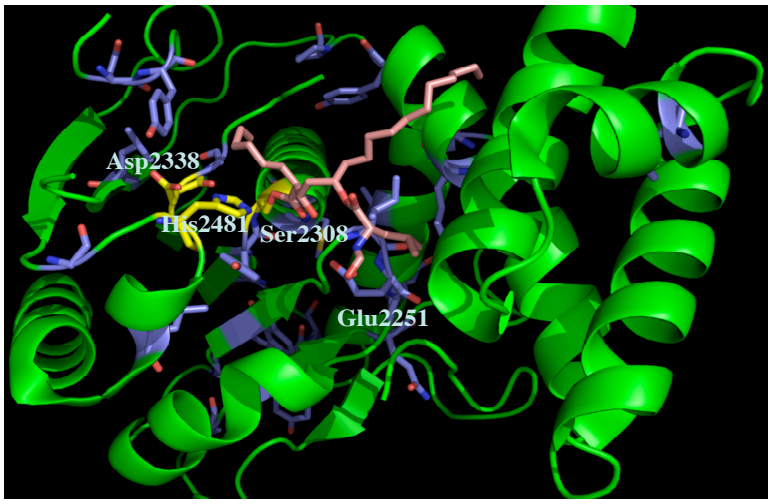

B

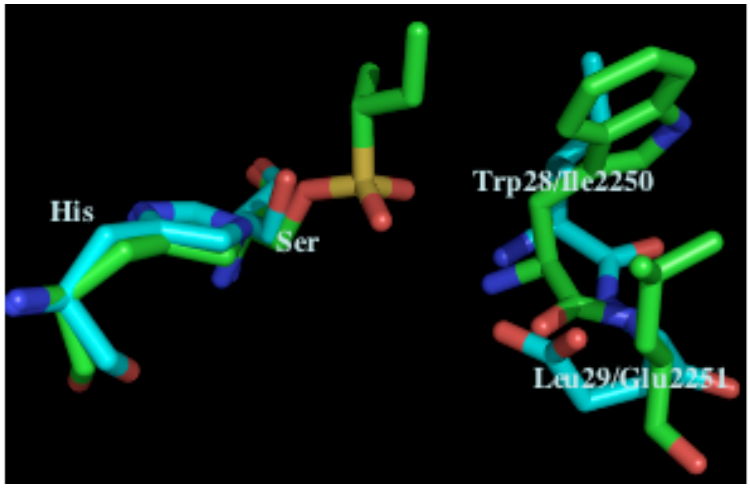

Figure 6. X-ray crystal structure of hFAS TE. A. Entire structure as a green ribbon showing the catalytic residues in yellow sticks, other conserved residues in purple sticks and the covalently bound ligand in pink. B. Superimposed active site of PFE (green carbons) and hFAS TE (cyan carbons). Catalytic residues Ser, His, oxyanion residues (PFE Trp28, HumanfasnTE Ile2250) and the next residues (PFE Leu29, HumanfasnTE Glu2251). The bound acyl group in humanfasnTE was removed to show the oxyanion hole more clear.

3. 4 Why Table 3 lacks the thioesterases from polyketide biosynthesis

Table 3 omits two thioesterases whose x-ray structures have been solved, both from polyketide biosynthesis: pikromycin thioesterase[67] and 6-deoxymethynolide B synthase thioesterase.[68] Both thioesterases catalyze a macrolactonization, Scheme 2. PikTE catalyzes a macrolactonization to make two natural products - the 12-membered lactone 10-deoxymethynolide and 14-membered narbonolide, while DEBS catalyzes macrolactonization of the 14-membered core of the antibiotic erythromycin, Figure 7.

Although these thioesterases adopt the α/β-hydrolase fold, their oxyanion loops contain a two-amino-acid insertion that prevents the loop from directly stabilizing the oxyanion. An x-ray structure containing a bound phosphonate transition-state analog[67] shows that the N-H bonds on the oxyanion loop are all too far from the oxyanion to make a hydrogen bond, Figure 8. Instead, a bridging water molecule hydrogen bonds to an N–H bond on the oxyanion loop and to the oxyanion. The x-xay structure of DEBS TE shows a similarly distorted oxyanion loop. Due to this distortion of the oxyanion loop, we cannot directly compare the oxyanion loop conformation of these to thioesterases with carboxylesterases. The x-ray structures of thiolase, which catalyzes a Claisen condensation of two acetyl-CoA molecules, also show an oxyanion hole made from a water molecule and a histidine side chain.[69]

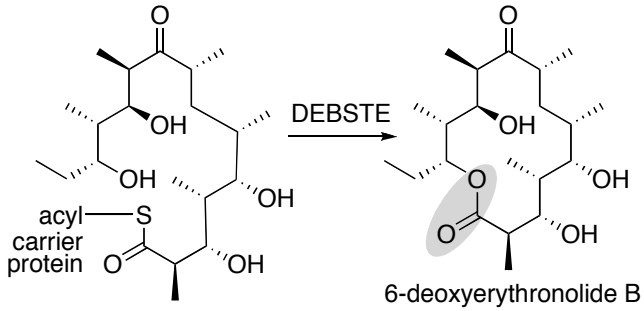

Figure 7. 6-Deoxymethynolide B synthase thioesterase domain (DEBS TE, also known as erythromycin polyketide synthase domain) catalyzes a macrolactonization to form precursor of the macrolactide antibiotic erythromycin.

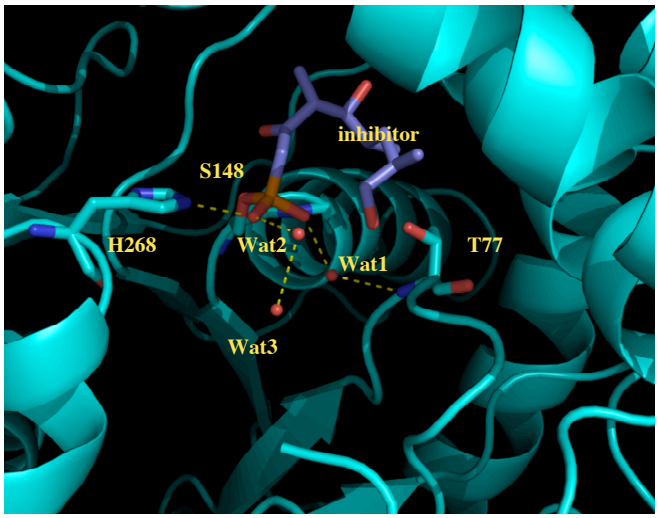

Figure 8. **X-ray crystal structure of pikromycin thioesterase containing a covalently bound phosphonate transition state analog (blue sticks) bound to active site (pdb id: 2hfj).** A cyan ribbon represents the main chain of the protein. The side chains of the active site serine (S148), histidine (H268) and a key residue on the oxyanion loop, threonine 77 are shown as cyan sticks. The N–H of Thr77 is too far from the oxyanion to make a direct hydrogen bond, but a water molecule (Wat1) bridges between them to stabilize the oxyanion. Two other molecules in the active site (Wat2 and Wat3) lie too from from the protien to make direct hydrogen bonds. Wat2 hydrogen bonds to a phosphonate oxygen.

3. 5 X-ray crystal structure of a sulfonate transition state analog bound to PFE to mimic hydrolysis

To identify the mechanistic significance of the different orientation of the type I versus type II β-turn in the oxyanion loop, we solved the x-ray crystal structure of a sulfonate transition state analog bound to the active site of PFE. The key difference between hydrolysis and acyl transfer is the choice between water or alcohol as the nucleophile. A phosphonate transition state analog mimics the attack of alcohol on the acyl enzyme, while a sulfonate transition state analog mimics the attack of water on the acyl enzyme. Phosphonates contain an –OR moiety, which mimics the alcohol of the ester, while sulfonates contain an –OH moiety to mimic the attacking water. Crystallographers have solved many x-ray crystal structures of lipases and esterases containing bound phosphonate transition state analogs, but not of a sulfonate transition state analog bound to a GX-class hydrolase. For this reason, we synthesized an irreversible inhibitor of PFE based on a sulfonate and solved its x-ray crystal structure.

p-Nitrophenyl sulfonate esters react with esterases and lipases to mimic the tetrahedral intermediate for attack of water on the acyl enzymes. The key step in making the α-substituted sulfonate in Figure 9 is the Mitsunobu reaction of the secondary alcohol, 2-butanol, with thiolacetic acid to form the thioacetate.[70] The thioacetate is then oxidized to the sulfonic acid and isolated as the sodium salt.[71] Chlorination with thionyl chloride and addition of *p*-nitrophenol and triethylamine yields the desired *p*-nitrophenyl sulfonate ester. The Supporting Information contains synthetic details.

Inactivation of wild-type PFE with 10-fold excess of (±)-butane-2-sulfonic acid 4-nitrophenyl ester inhibited 95% of the hydrolytic activity of PFE toward *p*-nitrophenyl acetate after 24 hours. The X-ray crystal structure of the complex contained only the (*R*)-enantiomer covalently linked to the Oγ of the catalytic serine (Ser94). This (*R*)-enantiomer corresponds the fast

reacting enantiomer of the corresponding ester substrate methyl (*R*)-2-methylbutanoate.[72] PFE favors the (*R*)-enantiomer of the ester 32-fold over the (*S*)-enantiomer and it is likely that PFE shows a similar enantiopreference toward the nitrophenyl sulfonate enantiomers.

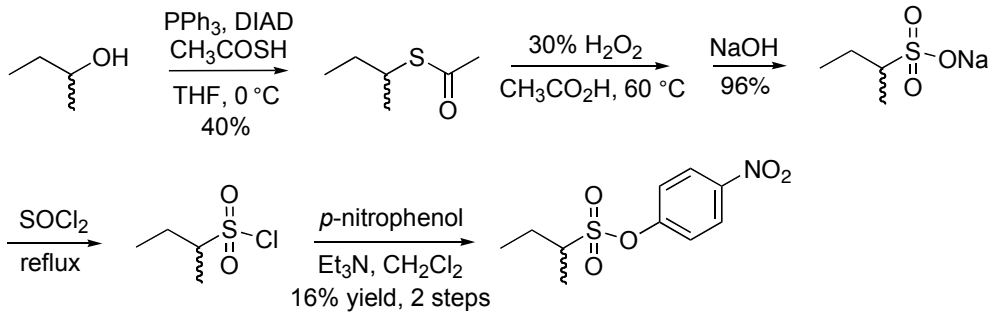

Figure 9. **Synthesis of *p*-nitrophenyl ester of racemic butane-2-sulfonic acid**. DIAD = diisopropylazodicarboxylate; THF = tetrahydrofuran.

The PFE-inhibitor complex and mutants formed single crystals under conditions similar to those for wild-type PFE.[73] Crystallizations used the hanging drop method with reservoir solution ranging in pH from 5.4 - 7.5 and containing between 1.2 and 1.8 M $(NH_4)_2SO_4$ and 0-4% PEG 400. The PFE-inhibitor complex and mutant protein crystals were isomorphous with those for wild-type PFE (PDB ID: 1va4) and contained six protein molecules with no significant deviation from the polypeptide backbone conformation of wild-type PFE. The structure is high quality (R_{work} = 19.8%, R_{free} = 20.7%) with a resolution of 1.65 Å, Table 3.

Alignment of the complex and wild-type structures reveals only minor changes to the active site. The ethyl substituent of the inhibitor is oriented between residues Phe198, Phe143, and Trp28, while the methyl substituent points toward Val121 and Phe125. Detailed analysis of the implication of this orientation on enantioselectivity will be reported elsewhere. The inhibitor mimics a catalytically productive orientation because it contains all the five hydrogen bonds necessary for catalysis, Figure 3. The sulfonyl oxygen in the oxyanion hole is hydrogen bonded to the N-H of both Met95 and Trp28 (2.9 and 3.0 Å, respectively), while the second sulfonyl oxygen is weakly hydrogen bonded to His251 Nε2 (3.3 Å) and to the bridging water molecule (3.2 Å). This bridging water molecule also hydrogen bonds to the main chain carbonyl oxygen of Trp28 (2.5 Å). The catalytic Ser94 Oγ is hydrogen bonded to the His251 Nε2 (3.2 Å) and Asp222 Oδ2 is hydrogen bonded to His251 Nδ1 (2.8 Å; also not shown in Figure 3 for clarity). Panel b of Figure 3 shows a schematic of the hydrogen bonds between the sulfonate transitions state analog and the protein, while panel c shows how these hydrogen bonds would look in the tetrahedral intermediate during hydrolysis. The x-ray crystal structure does not reveal the positions of the hydrogen atoms; all hydrogen bonds are inferred from the close distances of the oxygens or nitrogens.

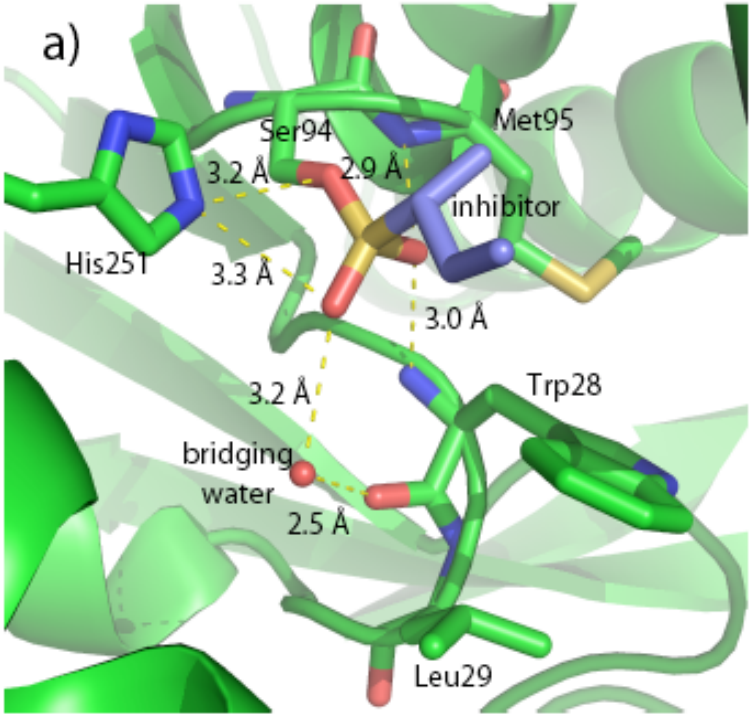
a)
Ser94
Met95
3.2 Å
2.9 Å
inhibitor
His251
3.3 Å
3.0 Å
3.2 Å
Trp28
bridging
water
2.5 Å
Leu29

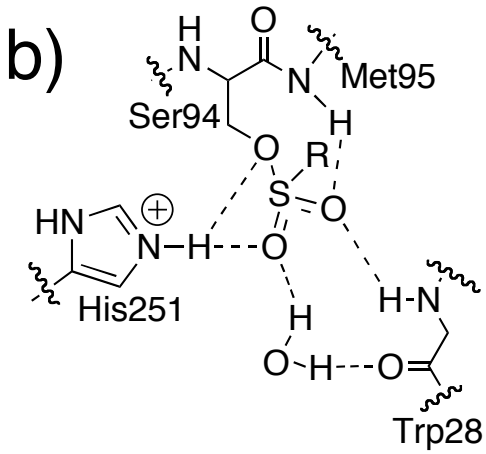
b)
Met95
Ser94
His251
Trp28

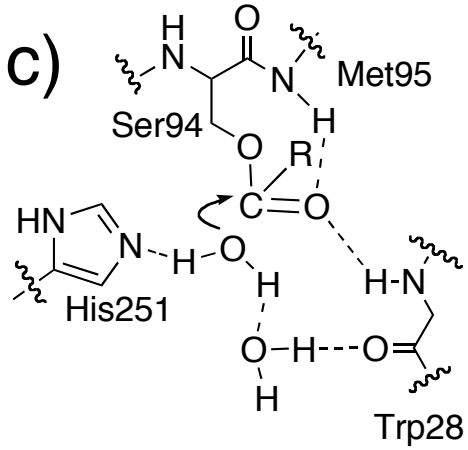
c)
Met95
Ser94
His251
Trp28

Figure 10. X-ray crystal structure of a sulfonate transition state analog bound to the catalytic serine of esterase from *Pseudomonas fluorescens* suggests a mechanistic role for a main chain carbonyl oxygen of the oxyanion loop. a) The active site of PFE showing key hydrogen bonds to the sulfonate transition state analog covalently linked to serine 94. One sulfonyl oxygen, partly obscured by the R group of the sulfonate in this view, mimics the oxyanion oxygen and accepts hydrogen bonds from the main chain N–H of methionine 95 and tryptophan 28 (2.9 and 3.0 Å, respectively). Another sulfonyl oxygen mimics the attacking water molecule and accepts hydrogen bonds from the catalytic histine 251 and a bridging water molecule (red ball; 3.3 and 3.2 Å, respectively). This bridging water molecule also hydrogen bonds to the main chain carbonyl oxygen of tryptophan 28 (2.5 Å). b) A schematic diagram of the x-ray crystal structure in panel a showing the hydrogen bonding pattern. c) Schematic diagram of the tetrahedral intermediate that corresponds to the sulfonate mimic in panel a and b. The attacking water molecule (bonded to the reacting carbon) makes hydrogen bonds to both the active site histidine 251 and the bridging water molecule.

3. 6 Mechanistic significance of the type I versus type II orientation of the oxyanion turn

The interaction with the bridging water molecule may contribute to catalysis Figure 8. By accepting a hydrogen bond from the attacking water molecule, the bridging water molecule acts as a base and may increase the reactivity of the attacking water molecule. The role of the active site histidine as a base is well established, the current proposal is that bridging water molecule can act as an additional base. Although a water molecule can serve as a hydrogen bond donor or acceptor, the interaction of this bridging water molecule with the carbonyl oxygen of Trp28 sets its role as a base. The carbonyl oxygen of Trp28 can only accept a hydrogen bond, thus, the bridging water donates a hydrogen bond. Since its partial negative charge has increased, the bridging water molecule will now accept a hydrogen bond from the attacking water.

A corresponding x-ray crystal structure of a sulfonate transition state analog bound to an acyltransferase shows a similar bridging water molecule.[74] Samel SA et al. inhibited fengycin thioesterase, which catalyzes the macrocyclization of a peptide, with phenylmethyl sulfonyl fluoride and solved the x-ray crystal structure. The phenylmethylsulfonyl moiety bound to the active site serine, but imperfectly mimicked the transition state, likely because the phenylmethyl moiety imperfectly mimicked the substrate peptide. One sulfonyl oxygen formed the expected two hydrogen bonds in the oxyanion hole, but the active site histidine adopted a catalytically non productive orientation. A bridging water molecule accepted a hydrogen bond from the N-H of the oxyanion loop (Ser31; N-O distance 3.3 Å). The bridging water molecule did not donate a hydrogen bond the sulfonate oxygen, which mimics the attacking water (O-O distance 4.2 Å).

I hypothesize that the bridging water molecule in acyltransferases does not promote hydrolysis as in the esterases, but hinders hydrolysis by positioning the attacking water molecule too far from the active site and by donating a hydrogen bond to reduce the nucleophilicity of the attacking water, Figure 8. The bridging water accepts a hydrogen bond from the N-H of the oxyanion loop as suggested by the x-ray crystal structure of the sulfonate bound to fengycin thioesterase. This interaction places the bridging water molecule too far away to interact with the attacking water molecule. Alternately, if it does interact, it positions the attacking water molecule too far from the carbonyl carbon to attack effectively. In addition the bridging water donates a hydrogen bond to the attacking water. This acidic interaction decreases the nucleophilicity of the attacking water and should slow down hydrolysis.

During acyl transfer, the acceptor alcohol or amine displaces the bridging water molecule from the active site, so it does not aid or hinder catalysis, Figure 8. The acceptors are larger than a water molecule and therefore displace the bridging water molecule. X-ray crystal structures of phosphonates bound to the active site of both hydrolases (e.g., *Burkholderia cepacia* lipase,[75] *Pseudomonas aeruginosa* lipase,[76] *Bacillus subtilis* lipase A,[77] dog gastric lipase[78] and *Rhizomucor miehei* lipase[79]) and acyltransferases (e.g., *Mycobacterium* antigen[80]) show either no water molecule or a water molecule that is too far to form a hydrogen bond to the alcohol oxygen.

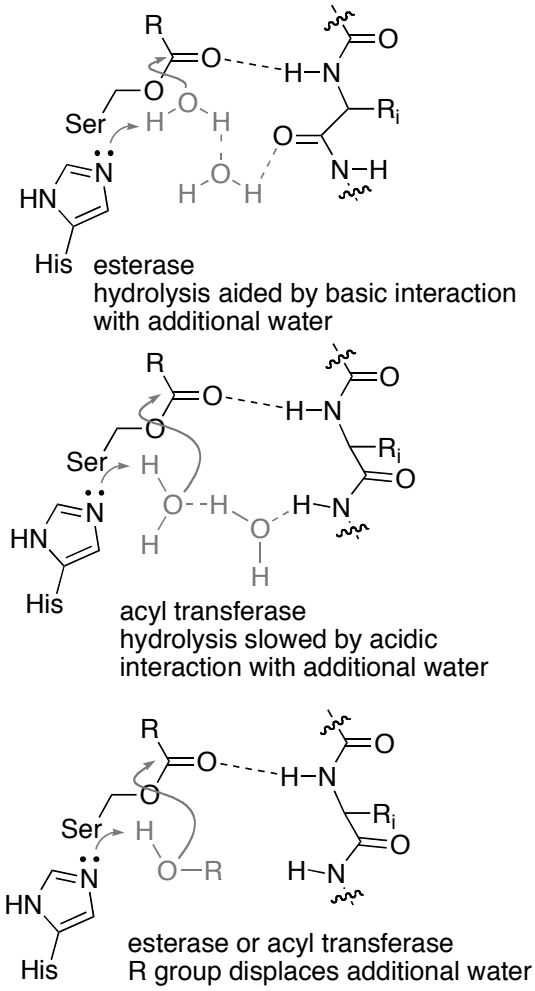

Figure 11. The different conformation of the oxyanion loop in esterases and acyltransferases can activate or deactivate the attacking water via a second water molecule. In esterases, the main chain carbonyl oxygen acts as a base via a bridging water molecule to activate the attacking water molecule. In acyltransferases, the N–H acts as an acid via a bridging water molecule to deactivate the attacking water molecule. For the acyl transfer reaction, the attacking nucleophile is an alcohol, which is larger than water. This alcohol displaces the bridging water molecule thereby eliminating any activating or deactivating effects.

4. Discussion

Comparison of the x-ray crystal structures of the GX class hydrolases with acyltransferases revealed a different oxyanion turn conformation. The oxyanion turn in the α/β hydrolase superfamily contributes to catalysis by donating a hydrogen bond from a backbone amide N–H to the oxyanion intermediate. In both the GX-class hydrolases (defined by a GX sequence at the start of the oxyanion turn, where X is the oxyanion residue and by a range of dihedral angles for the oxyanion turn residues) and the related acyltransferases the oxyanion turn positions the amide backbone N–H of the *i* + 1 residue so that it points toward the active site and can hydrogen bond to the oxyanion intermediate. However the orientation of the central amide bond in the oxyanion turn (between the *i* + 1 and *i* + 2 residues) differs in the two classes of enzymes. The oxyanion turn in the GX class hydrolases of the α/β hydrolase superfamily adopts a type II β turn conformation. This conformation points the backbone carbonyl oxygen of the *i* + 1 residue towards active site and the amide N–H of the *i* + 2 residue away from the active site. In contrast, the oxyanion turn in acyltransferases of the α/β hydrolase superfamily adopts a type I β turn conformation. This conformation points backbone carbonyl oxygen of the *i* + 1 residue away from active site and the amide N–H of the *i* + 2 residue toward the active site.

Some hydrolases and acyltransferases in the α/β hydrolase superfamily do not fit in this generalization because their oxyanion turns differ significantly from the GX-class hydrolases. The oxyanion turn in GGGX class hydrolases adopts a different conformation, but the oxyanion loop still donates a hydrogen bond from a main chain N–H. Consistent with the notion of a different oxyanion loop orientation in the GGGX hydrolases, this class of hydrolases catalyzes hydrolysis of tertiary alcohol esters, while the GX class of lipases do not.[81] Placing the oxyanion loop further away in the GGGX class creates more space for the alcohol moiety and thus allows tertiary alcohols to

fit in this region. The oxyanion stabilization in the Y class hydrolase is much different since the hydroxyl group of Tyr side chain stabilizes the oxyanion. The main chain is far away from the active site. Some plant acyltransferases do not use acyl-CoA thioesters, but 1-*O*-β-glucose esters as acyl donors. The amino acid sequences of these acyltransferases are ~36% identical to plant serine carboxypeptidases, which are α/β-hydrolase fold enzymes like lipases.[82] There are no structures of these acyltransferases available, so it is unclear how the oxyanion turn orients.

The x-ray structure of the sulfonate transition state analog bound to a GX-class hydrolase identifies a bridging water molecule that can enhance the nucleophilicity of the attacking water molecule. Although many x-ray crystal structures of lipases and esterases have been solved, including structures containing bound transition state analogs, most of these transition state analogs are phosphonates. These transition state analogs contain an –OR moiety, which mimics the alcohol of the ester, not an –OH moiety to mimic the attacking water. The x-ray structure of a sulfonate bound to the active site revealed a bridging water molecule between the sulfonate oxygen that mimics the attacking water and the carbonyl oxygen of the oxyanion loop. (The x-ray structure of phosphonate transition state analogs bound to the active site did not show this bridging water molecule because the alcohol moiety occupies this space.) This bridging water molecule may enhance the nucleophilicity of the attacking water molecule by acting as a base. The bridging water molecule donates a hydrogen bond to the carbonyl oxygen of the oxyanion loop and thus, can accept a hydrogen bond from the attacking water molecule. Thus, the bridging water molecule can act as a base toward the attacking water molecule. This interaction is in addition to the basic interaction with the catalytic histidine, so the effect of the bridging molecule is as a secondary base.

Other crystal structures of hydrolases have also identified secondary base interactions to the attacking water molecule including several that involve a bridging water molecule. In the glutamic peptidase family, the hydrolytic water hydrogen bonds to the catalytic glutamate base and to the carbonyl oxygen Oε1 of a nearby glutamine.[83] In a glycoside hydrolase, the hydrolytic water hydrogen bonds both the catalytic aspartate and an adjacent tyrosine phenolic oxygen that helps position the water molecule.[84] Three examples involve a bridging water molecule. Potato epoxide hydrolase and haloalkane dehalogenase, which both have the same α/β-hydrolase fold as esterases and acyltransferases, show a bridging interaction is the same as the one proposed for esterases in the current paper. In epoxide hydrolase, a bridging water molecule hydrogen bonds to the main chain carbonyl oxygen of Phe 33 and the attacking water,[85] while in the haloalkane dehalogenase this bridge is between main chain carbonyl oxygen of Asn38 and the attacking water.[86] In the second case, molecular dynamics simulations also suggest that this bridging water molecule has an important role in catalysis. In a penicllinase, the attacking water hydrogen bonds to both the base (Oγ of Ser87) and a bridging water molecule linked to Oγ of Ser110.[87] Recent modeling and mutagenesis indicated that a water network contributes to the amidase activity of a *Bacillus* esterase.[88]

Secondary base interaction is not essential for hydrolases activity since some hydrolases show no evidence of a secondary base interaction. One previous x-ray crystal structure of a lipase did contain a sulfonate transition state analog,[89] but this was not a GX-class hydrolase. *Candida rugosa* lipase belongs to the GGGX class of lipases, whose oxyanion loop is farther from the active site serine and tetrahedral intermediate to interact with them directly or by way of a bridging water molecule. There was no evidence of a bridging water molecule in this structure, so the proposed secondary base interaction may not be essential for catalysis. Similarly, the x-ray crystal structures proteases show no evidence for any secondary of acyl enzyme intermediates

in several serine proteases have identified the likely hydrolytic water.[90] It hydrogen bonds to Nε2 of the catalytic histidine, but not to anything else.

If a secondary base interaction can activate a water for reaction, then a secondary acid interaction should deactivate a water for reaction. In acyltransferases the oxyanion turn orients the central amide bond in an opposite manner so an N–H, not a carbonyl oxygen point toward the active site. Although no structural information is available on the attacking water molecule in these enzyme, we hypothesize that the situation is similar to GX-class hydrolases. However, the N–H donate a hydrogen bond to the bridging water, which in turn donates a hydrogen bond to the attacking water. This donation of a hydrogen decreases the nucleophilicity of the attacking water. This interaction may be partly responsible for the different chemical reactivity of the hydrolases versus acyltransferases.

Previous research had identified that the oxyanion loop can contribute, but had not identified how. Site directed mutagenesis in the oxyanion loop of surfactin thioeserase increased the relative amount of hydrolysis over acyl transfer.[91] Wild type enzyme showed 71% acyl transfer, but the Pro29Gly variant showed only 23% acyl transfer, the rest hydrolysis. This amino acid substitution likely changed the conformation of the oxyanion turn due to the different conformational preferences of proline versus glycine, but the nature of the conformational change was not established. In cyclization reactions, the higher effective molarity of nucleophile due to the folded conformation of peptide or polyketide can favor acyl transfer over hydrolysis. This effect cannot contribute to acyl transfers that do not involve cyclization.

The proposed molecular basis involve main chain interactions, which are difficult to find using amino acid sequence comparisons. There is no clear

link between amino acid sequence and the type I or II conformation in a β-turn.

References

1. Reviews: Grünewald, J., Marahiel, M.A. (2006) Chemoenzymatic and template-directed synthesis of bioactive macrocyclic peptides. *Microbiol Mol. Biol. Rev.* 70: 121-146; Kopp F, Marahiel MA (2007) Macrocyclization strategies in polyketide and nonribosomal peptide biosynthesis. *Nat. Prod. Rep.* 24: 735-749.
2. Mirza, I.A., Nazi, I., Korczynska, M., Wright, G.D., Berghuis, A.M. (2005) Crystal structure of homoserine transacetylase from *Haemophilus influenzae* reveals a new family of α/β-hydrolases *Biochemistry* 44 15768-15773.
3. Born, T.L., Franklin, M., Blanchard, J.S. (2000) Enzyme-catalyzed acylation of homoserine: mechanistic characterization of the *Haemophilus influenzae* met2-encoded homoserine transacetylase *Biochemistry* 39: 8556-8564.
4. Stubbe, J., Tian, J., He, A., Sinskey, A.J., Lawrence, A.G., Liu, P. (2005) Nontemplate-dependent polymerization processes: polyhydroxyalkanoate synthases as a paradigm. *Ann. Rev. Biochem.* 74: 433-480.
5. Wältermann, M., Stöveken, T., Steinbüchel, A. (2007) Key enzymes for biosynthesis of neutral lipid storage compounds in prokaryotes: properties function and occurrence of wax ester synthases/acyl-CoA: diacylglycerol acyltransferases. *Biochimie* 89: 230-242.
6. Trauger, J.W., Kohli, R.M., Mootz, H.D., Marahiel, M.A., Walsh, C.T. (2000) Peptide cyclization catalysed by the thioesterase domain of tyrocidine synthase. *Nature* 407: 215-218; Kohli, R.M., Burke, M.D., Tao, J., Walsh, C.T. (2003) Chemoenzymatic route to macrocyclic hybrid peptide/polyketide-like molecules. *J. Am. Chem. Soc.* 125: 7160-7161.
7. Kruger, R.G., Lu, W., Oberthür, M., Tao, J., Kahne, D., Walsh, C.T. (2005) Tailoring of glycopeptide scaffolds by the acyltransferases from the teicoplanin and A-40926 biosynthetic operons. *Chem. Biol.* 12: 131-140.

8. Xie, X., Watanabe, K., Wojcicki, W.A., Wang, C.C.C., Tang ,Y. (2006) Biosynthesis of lovastatin analogs with a broadly specific acyltransferase. *Chem Biol* 13: 1161-1169; Xie, X., Tang, Y. (2007) Efficient synthesis of simvastatin by use of whole-cell biocatalysis. *Appl. Environ. Microbiol.* 73: 2054-2060.
9. Bornscheuer, U.T., Kazlauskas, R.J. (2004) *Hydrolases in Organic Synthesis: Regio- and Stereoselective Biotransformations,* 2nd ed Wiley-VCH Chapter 5.
10. Tseng, C.C., Bruner, S.D., Kohli, R.M., Marahiel, M.A., Walsh, C.T., Sieber, S.A. (2002) Characterization of the surfactin synthetase C-terminal thioesterase domain as a cyclic depsipeptide synthase. *Biochemistry* 41 13350-13359.
11. Sharma, K.K., Boddy, C.N. (2007) The thioesterase domain from the pimaricin and erythromycin biosynthetic pathways can catalyze hydrolysis of simple thioester substrates. *Bioorg. Med. Chem. Lett.* 17: 3034-3037.
12. Ollis, D.L., Cheah, E., Cygler, M., Dijkstra, B., Frolow, F., Franken, S.M., Harel, M., Remington, S.J., Silman, I., Schrag, J., Sussman, J.L., Verschueren, K.H.G., Goldman, A. (1992) The α/β hydrolase fold. *Prot. Eng.* 5: 197-211; Holmquist, M. α/β-Hydrolase fold enzymes: structures functions and mechanisms. *Curr. Protein Pept. Sci.* 2000 1: 209-235.
13. Gibrat, J.F., Madej, T., Bryant, S.H. (1996) Surprising similarities in structure comparison. *Curr. Opin. Struct. Biol.* 6: 377-385; Madej, T., Panchenko, A.R., Chen, J., Bryant, S.H. (2007) Protein homologous cores and loops: important clues to evolutionary relationships between structurally similar proteins. *BMC Struct. Biol.* 7: 23.
14. Murzin, A.G., Brenner, S.E., Hubbard, T., Chothia, C. (1995) SCOP: a structural classification of proteins database for the investigation of sequences and structures. *J. Mol. Biol.* 247: 536-540.

15. Corey, E. J., Cimprich, K. A. (1992) Enantioselective routes to chiral benzylic thiols, sulfinic esters and sulfonic acids illustrated by the l-phenylethyl series. *Tet. Lett.* 33, 4099-4102.
16. Pflugrath, J.W. (1999) The finer things in diffraction data collection. *Acta. Crystallogr. Sect D Biol. Crystallogr.* 55: 1718-1725.
17. Otwinowski, Z., Minor, V. (1997) Processing of diffraction data collected in oscillation mode. *Methods Enzymol* 276: 307-326.
18. Jones, T.A., Zou, J.Y., Cowan, S.W., Kjeldgaard, M. (1991) Improved methods for building models in electron density maps and location of errors in these models. *Acta. Crystallogr. Sect. A Found Crystallogr.* 47: 110-119.
19. Murshudov, G.N., Vagin, A.A., Dodson, E.J. (1997) Refinement of macromolecular structures by the maximum-likelihood method. *Acta Crystallogr Sect D Biol Crystallogr* 53: 240-255.
20. Collaborative Computational Project, Number 4. (1994) The CCP4 suite: Programs for protein crystallography. *Acta Crystallogr Sect D Biol Crystallogr* 50: 760-763.
21. Perrakis, A., Morris, R., Lamzin, V.S. (1999) Automated protein model building combined with iterative structure refinement. *Nature Struct. Biol. 6*: 458-463.
22. Read, R.J. (1986) Improved Fourier coefficients for maps using phases from partial structures with errors. *Acta Crystallogr Sect A Found Crystallogr* 42: 140-149.
23. Laskowski, R.A. (1993) PROCHECK: A program to check the stereochemical quality of protein structures. *J. Appl. Crystallogr.* 26: 283-291.
24. a) Rose, G.D., Glerasch, L.M., Smith, J.A. (1985) Turns in peptides and proteins. *Adv. Prot. Chem.* 37: 1-109; Creighton TE *Proteins: Structure and Molecular Properties* 2nd ed Freeman: New York 1993 pp 225-227.

b) Wilmot, C.M., Thornton, J.M. (1988) Analysis and prediction of the different types of β-turns in proteins. *J. Mol. Biol.* 203: 221-232.

25. Pleiss, J., Fisher, M., Peiker, M., Thiele, C., Schmid, R.D. (2000) Lipase engineering database: Understanding and exploiting sequence–structure–function relationships. *J. Mol. Catal. B Enzym.* 10: 491-508; Fischer, M., Pleiss, J. (2003) The Lipase Engineering Database: a navigation and analysis tool for protein families. *Nucl. Acid. Res.* 31: 319-321.
26. Chakravarty, B., Gu, Z., Chirala, S.S., Wakil, S.J., Quiocho, F.A. (2004) Human fatty acid synthase: structure and substrate selectivity of the thioesterase domain. *Proc. Natl. Acad. Sci. USA* 101: 15567-15572.
27. Jansson, A., Niemi, J., Mantsala, P., Schneider, G. (2003) Crystal structure of aclacinomycin methylesterase with bound product analogues: implications for anthracycline recognition and mechanism. *J. Biol. Chem.* 278: 39006-39013.
28. Mezzetti, A., Schrag, J.D., Cheong, C.S., Kazlauskas, R.J. (2005) Mirror-image packing in enantiomer discrimination molecular basis for the enantioselectivity of *B cepacia* lipase toward 2-methyl-3-phenyl-1-propanol. *Chem. Biol.* 12: 427-437.
29. Nardini, M., Lang, D.A., Liebeton, K., Jaeger, K.E., Dijkstra, B.W. (2000) Crystal structure of *Pseudomonas aeruginosa* lipase in the open conformation The prototype for family I1 of bacterial lipases. *J. Biol. Chem.* 275: 31219-31225.
30. Lang, D.A., Stadler, P., Kovacs, A., Paltauf, F., Dijkstra, B.W. (1999) Structural and kinetic investigations of enantiomeric binding mode of subclass I lipases from the family of *Pseudomonadaceae* To be Published
31. Droege, M.J., Boersma, Y.L., van Pouderoyen, G., Vrenken, T.E., Rueggeberg, C.J., Reetz, M.T., Dijkstra, B.W., Quax, W.J. (2005) Directed evolution of *Bacillus subtilis* lipase A by use of enantiomeric phosphonate inhibitors: crystal structures and phage display selection. *ChemBioChem* 7: 149-157.

32. Line, K., Isupov, M.N., Littlechild, J.A. (2004) The crystal structure of a (-) γ-lactamase from an *Aureobacterium* species reveals a tetrahedral intermediate in the active site. *J. Mol .Biol.* 338: 519-532.
33. Forouhar, F., Yang, Y., Kumar, D., Chen, Y., Fridman, E., Park, S.W., Chiang, Y., Acton, T.B., Montelione, G.T., Pichersky, E., Klessig, D.F., Tong, L. (2005) Structural and biochemical studies identify tobacco SABP2 as a methyl salicylate esterase and implicate it in plant innate immunity. *Proc. Natl. Acad. Sci. USA* 102: 1773-1778.
34. Legler, P.M., Kumaran, D., Swaminathan, S., Studier, F.W., Millard, C.B. (2008) Structural characterization and reversal of the natural organophosphate resistance of a D-type esterase *Saccharomyces cerevisiae S*-formylglutathione hydrolase. *Biochemistry* 47: 9592-9601.
35. Cuff, M.E., Zhou, M., Collart, F., Joachimiak, A. (2005) Structure of a carboxylesterase from *Bacillus stearothermophilus*. To be published.
36. Bourne, P.C., Isupov, M.N., Littlechild, J.A. (2000) The atomic-resolution structure of a novel bacterial esterase. *Structure Fold Des* 8: 143-151.
37. Roussel, A., Miled, N., Berti-Dupuis, L., Riviere, M., Spinelli, S., Berna, P., Gruber, V., Verger, R., Cambillau C (2002) Crystal structure of the open form of dog gastric lipase in complex with a phosphonate inhibitor. *J. Biol. Chem.* 277: 2266-2274.
38. Roussel, A., Canaan, S., Egloff, M.P., Riviere, M., Dupuis, L., Verger, R., Cambillau, C. (1999) Crystal structure of human gastric lipase and model of lysosomal acid lipase two lipolytic enzymes of medical interest. *J. Biol. Chem.* 274: 16995-17002.
39. Bellizzi, J.J. 3rd, Widom, J., Kemp, C., Lu, J.Y., Das, A.K., Hofmann, S.L., Clardy, J. (2000) The crystal structure of palmitoyl protein thioesterase 1 and the molecular basis of infantile neuronal ceroid lipofuscinosis. *Proc. Natl. Acad. Sci. USA* 97: 4573-4578.
40. Calero, G., Gupta, P., Nonato, M.C., Tandel, S., Biehl, E.R., Hofmann, S.L., Clardy, J. (2003) The crystal structure of palmitoyl protein

thioesterase-2 (PPT2) reveals the basis for divergent substrate specificities of the two lysosomal thioesterases PPT1 and PPT2. *J. Biol. Chem.* 278: 37957-37964.

41. Roussel, A., Yang, Y., Ferrato, F., Verger, R., Cambillau, C., Lowe, M. (1998) Structure and activity of rat pancreatic lipase-related protein 2. *J. Biol. Chem.* 273: 32121-32128.
42. Bourne, Y., Martinez, C., Kerfelec, B., Lombardo, D., Chapus, C., Cambillau, C. (1994) Horse pancreatic lipase The crystal structure refined at 2.3 Å resolution. *J. Mol. Biol.* 238: 709-732.
43. van Tilbeurgh, H., Egloff, M.P., Martinez, C., Rugani, N., Verger, R., Cambillau, C. (1993) Interfacial activation of the lipase-procolipase complex by mixed micelles revealed by X-ray crystallography. *Nature* 362: 814-820.
44. Kim, K.K., Song, H.K., Shin, D.H., Hwang, K.Y., Choe, S., Yoo, O.J., Suh, S.W. (1997) Crystal structure of carboxylesterase from *Pseudomonas fluorescens* an α/β hydrolase with broad substrate specificity. *Structure* 5: 1571-1584.
45. Devedjiev, Y., Dauter, Z., Kuznetsov, S.R., Jones, T.L., Derewenda, Z.S. (2000) Crystal structure of the human acyl protein thioesterase I from a single X-ray data set to 1.5 Å. *Structure Fold Des* 8: 1137-1146.
46. Derewenda, U., Brzozowski, A.M., Lawson, D.M., Derewenda, Z.S. (1992) Catalysis at the interface: the anatomy of a conformational change in a triglyceride lipase. *Biochemistry* 31: 1532-1541.
47. Brzozowski, A.M., Savage, H., Verma, C.S., Turkenburg, J.P., Lawson, D.M., Svendsen, A., Patkar, S. (2000) Structural origins of the interfacial activation in *Thermomyces* (*Humicola*) *lanuginosa* lipase. *Biochemistry* 39: 15071-15082.
48. Uppenberg, J., Hansen, M.T., Patkar, S., Jones, T.A. (1994) The sequence crystal structure determination and refinement of two crystal forms of lipase B from *Candida antarctica. Structure* 2: 293-308.

49. Benoit, I., Asther, M., Sulzenbacher, G., Record, E., Marmuse, L., Parsiegla, G., Herpoel-Gimbert, I., Asther, M,. Bignon, C. (2006) Respective importance of protein folding and glycosylation in the thermal stability of recombinant feruloyl esterase A. *FEBS Lett* 580: 5815-5821.
50. Wei, Y., Swenson, L., Castro, C., Derewenda, U., Minor, W., Arai, H., Aoki, J., Inoue, K., Servin-Gonzalez, L., Derewenda, Z.S. (1998) Structure of a microbial homologue of mammalian platelet-activating factor acetylhydrolases: *Streptomyces exfoliatus* lipase at 1.9 Å resolution. *Structure* 6: 511-519.
51. Zhang, R., Koroleva, O., Collert, F., Joachimiak, A. (2002) 1.5-Å crystal structure of the cephalosporin C deacetylase. To be published.
52. Schubot, F..D, Kataeva, I.A., Blum, D.L. ,Shah, A.K., Ljungdahl, L.G., Rose, J.P., Wang, B.C. (2001) Structural basis for the substrate specificity of the feruloyl esterase domain of the cellulosomal xylanase Z from *Clostridium thermocellum. Biochemistry* 40: 12524-12532.
53. Longhi, S., Czjzek, M., Lamzin, V., Nicolas, A., Cambillau, C. (1997) Atomic resolution (1.0 Å) crystal structure of *Fusarium solani* cutinase: stereochemical analysis. *J. Mol. Biol.* 268: 779-799.
54. Ghosh, D., Erman, M., Sawicki, M., Lala, P., Weeks, D.R., Li, N., Pangborn, W., Thiel, D.J., Jornvall, H., Gutierrez, R., Eyzaguirre, J. (1999) Determination of a protein structure by iodination: the structure of iodinated acetylxylan esterase. *Acta Crystallogr Sect D Biol Crystallogr* 55: 779-784.
55. Hakulinen, N., Tenkanen, M., Rouvinen, J. (1998) Crystallization and preliminary X-ray diffraction studies of the catalytic core of acetyl xylan esterase from *Trichoderma reesei. Acta Crystallogr Sect D Biol Crystallogr* 54: 430-432.
56. Prates, J.A., Tarbouriech, N., Charnock, S.J., Fontes, C.M., Ferreira, L.M., Davies, G.J. (2001) The structure of the feruloyl esterase module of

xylanase 10B from *Clostridium thermocellum* provides insights into substrate recognition. *Structure* 9: 1183-1190.

57. Chakravarty, B., Gu, Z., Chirala, S.S., Wakil, S.J., Quiocho, F.A. (2004) Human fatty acid synthase: structure and substrate selectivity of the thioesterase domain. *Proc Natl Acad Sci USA* 101: 15567-15572.
58. Ronning, D.R., Klabunde, T., Besra, G.S., Vissa, V.D., Belisle, J.T., Sacchettini, J.C. (2000) Crystal structure of the secreted form of antigen 85C reveals potential targets for mycobacterial drugs and vaccines. *Nat Struct Biol* 7: 141-146.
59. Ronning, D.R., Vissa, V., Besra, G.S., Belisle, J.T., Sacchettini, J.C. (2004) *Mycobacterium tuberculosis* Antigen 85A and 85C structures confirm binding orientation and conserved substrate specificity. *J Biol Chem* 279: 36771-36777.
60. Anderson, D.H., Harth, G., Horwitz, M.A., Eisenberg, D. (2001) An interfacial mechanism and a class of inhibitors inferred from two crystal structures of the *Mycobacterium tuberculosis* 30 kDa major secretory protein (Antigen 85B) a mycolyl transferase. *J Mol Biol* 307 671-681.
61. Bruner, S.D., Weber, T., Kohli, R.M., Schwarzer, D., Marahiel, M.A., Walsh, C.T., Stubbs, M.T. (2002) Structural basis for the cyclization of the lipopeptide antibiotic surfactin by the thioesterase domain SrfTE. *Structure* 10: 301-310.
62. Samel, S.A., Wagner, B., Marahiel, M.A., Essen, L.O. (2006) The thioesterase domain of the fengycin biosynthesis cluster: a structural base for the macrocyclization of a non-ribosomal lipopeptide. *J Mol Biol* 359: 876-889.
63. Wang, M., Liu, L., Wang, Y., Wei, Z., Zhang, P., Li, Y., Jiang, X., Xu, H., Gong, W. (2007) Crystal structure of homoserine *O*-acetyltransferase from *Leptospira interrogans. Biochem Biophys Res Commun* 363: 1050-1056.
64. Mirza, I.A., Nazi, I., Korczynska, M., Wright, G.D., Berghuis, A.M. (2005) Crystal structure of homoserine transacetylase from *Haemophilus*

influenzae reveals a new family of α/β-hydrolases *Biochemistry* 44: 15768-15773.

65. Lejon, S., Ellis, J., Valegard, K. (2008) The last step in cephalosporin C formation revealed: crystal structures of deacetylcephalosporin C acetyltransferase from *Acremonium chrysogenum* in complexes with reaction intermediates. *J Mol Biol* 377: 935-944.
66. Chakravarty, B., Gu, Z., Chirala, S.S., Wakil, S.J., Quiocho, F.A. (2004) Human fatty acid synthase: structure and substrate selectivity of the thioesterase domain. *Proc Natl Acad Sci U S A* 101:15567-15572.
67. Akey, D.L., Kittendorf, J.D., Giraldes, J.W., Fecik, R.A., Sherman, D.H., Smith, J.L. (2006) Structural basis for macrolactonization by the pikromycin thioesterase. *Nat Chem Biol* 2: 537-542.
68. Tsai, S-C., Miercke, L.J.W., Krucinski, J., Gokhale, R., Chen, JC-H., Foster, P.G., Cane, D.E., Khosla, C., Stroud, R.M. (2001) Crystal structure of the macrocycle-forming thioesterase domain of the erythromycin polyketide synthase: Versatility from a unique substrate channel. *Proc Natl Acad Sci USA* 98 14808-14813.
69. Kursula, P., Ojala, J., Lambeir, A.M., Wierenga, R.K. (2002) The catalytic cycle of biosynthetic thiolase: a conformational journey of an acetyl group through four binding modes and two oxyanion holes. Biochemistry 41: 15543-15556.
70. Corey, E.J., Cimprich, K.A. (1992) Enantioselective routes to chiral benzylic thiols sulfinic esters and sulfonic acids illustrated by the l-phenylethyl series. *Tetrahedron Lett* 33: 4099-4102.
71. Piątek, A., Chapuis, C., Jurczak, J. (2002) Synthesis of a six-membered-ring (2*R*)-10a-homobornane-10a,2-sultam and structural comparison with Oppolzer's Lang's and King's sultams. *Helv Chim Acta* 85: 1973-1988.
72. Park, S., Morley, K.L., Horsman, G.P., Holmquist, M., Hult, K., Kazlauskas, R.J. (2005) Focusing mutations into the *P fluorescens* esterase

binding site increases enantioselectivity more effectively than distant mutations. *Chem Biol* 12: 45-52.

73. Cheeseman, J.D., Tocilj, A., Park, S., Schrag, J.D., Kazlauskas, R.J. (2004) X-Ray crystal structure of an aryl esterase from *Pseudomonas fluorescens. Acta Crystallogr Sect D: Biol Crystallogr* 60: 1237-1243.
74. Samel, S.A., Wagner, B., Marahiel, M.A., Essen, L.O. (2006) The thioesterase domain of the fengycin biosynthesis cluster: a structural base for the macrocyclization of a non-ribosomal lipopeptide. *J Mol Biol* 359: 876-889.
75. Mezzetti, A., Schrag, J.D., Cheong, C.S., Kazlauskas, R.J. (2005) Mirror-image packing in enantiomer discrimination molecular basis for the enantioselectivity of *B cepacia* lipase toward 2-methyl-3-phenyl-1-propanol. *Chem Biol* 12: 427-437.
76. Nardini, M., Lang, D.A., Liebeton, K., Jaeger, K.E., Dijkstra, B.W. (2000) Crystal structure of *Pseudomonas aeruginosa* lipase in the open conformation The prototype for family I1 of bacterial lipases. *J Biol Chem* 275: 31219-31225.
77. Droege, M.J., Boersma, Y.L., van Pouderoyen, G., Vrenken, T.E., Rueggeberg, C.J., Reetz, M.T., Dijkstra, B.W., Quax, W.J. (2005) Directed evolution of *Bacillus subtilis* lipase A by use of enantiomeric phosphonate inhibitors: crystal structures and phage display selection. *ChemBioChem* 7: 149-157.
78. Roussel, A., Miled, N., Berti-Dupuis, L., Riviere, M., Spinelli, S., Berna, P., Gruber, V., Verger, R., Cambillau, C. (2002) Crystal structure of the open form of dog gastric lipase in complex with a phosphonate inhibitor. *J Biol Chem* 277: 2266-2274.
79. Derewenda, U., Brzozowski, A.M., Lawson, D.M., Derewenda, Z.S. (1992) Catalysis at the interface: the anatomy of a conformational change in a triglyceride lipase. *Biochemistry* 31: 1532-1541.

80. Ronning, D.R., Klabunde, T., Besra, G.S., Vissa, V.D., Belisle, J.T., Sacchettini, J.C. (2000) Crystal structure of the secreted form of antigen 85C reveals potential targets for mycobacterial drugs and vaccines. *Nat Struct Biol* 7: 141-146.

81. Henke, E., Pleiss, J., Bornscheuer, U.T. (2002) Activity of lipases and esterases towards tertiary alcohols: insights into structure-function relationships. *Angew Chem Intl Ed* 41 3211-3213.

82. Steffens, J.C. (2000) Acyltransferases in protease's clothing. *Plant Cell* 12: 1253-1256; Milkowski, C., Strack, D. (2004) Serine carboxypeptidase-like acyltransferases. *Phytochemistry* 65: 517-524.

83. Pillai, B., Cherney, M.M., Hiraga, K., Takada, K., Oda, K., James, M.N.G. (2007) Crystal structure of scytalidoglutamic peptidase with its first potent inhibitor provides insights into substrate specificity and catalysis. *J Mol Biol* 365 343-361.

84. Collins, T., De Vos, D., Hoyoux, A., Savvides, S.N., Gerday, C., Van Beeumen, J., Feller, G. (2005) Study of the active site residues of a glycoside hydrolase family 8 xylanase. *J Mol Biol* 354: 425-435.

85. Thomaeus, A., Carlsson, J., Åqvist, J., Widersten, M. (2007) Active site of epoxide hydrolases revisited: a noncanonical residue in potato StEH1 promotes both formation and breakdown of the alkylenzyme intermediate. *Biochemistry* 46: 2466–2479.

86. Negri, A., Marco, E., Damborsky, J., Gago, F. (2007) Stepwise dissection and visualization of the catalytic mechanism of haloalkane dehalogenase LinB using molecular dynamics simulations and computer graphic.s *J Mol Graph Model* 26: 643-651.

87. Nicola, G., Peddi, S., Stefanova, M.E., Nicholas, R.A., Gutheil, W.G., Davies, C. (2005) Crystal structure of *Escherichia coli* penicillin-binding protein 5 bound to a tripeptide boronic acid inhibitor: a role for Ser-110 in deacylation. *Biochemistry* 44: 8207–8217.

88. Kourist, R., Bartsch, S., Fransson, L., Hult, L., Bornscheuer, U.T. (2008), Understanding promiscuous amidase activity of an esterase from *Bacillus subtilis*. *ChemBioChem* 9: 67–69.

89. Grochulski, P., Bouthillier, F., Kazlauskas, R.J., Serreqi, A.N., Schrag, J.D., Ziomek, E., Cygler, M. (1994) *Candida rugosa* lipase-inhibitor complexes simulating the acylation and deacylation transition states. *Biochemistry* 33: 3494-3500.

90. Wilmouth, R.C., Clifton, I.J., Robinson, C.V., Roach, P.L., Aplin, R.T., Westwood, N.J., Hajdu, J., Schofield, C.J. (1997) Structure of a specific acyl-enzyme complex formed between β-casomorphin-7 and porcine pancreatic elastase. *Nature Struct Biol* 4: 456-462; Wright, P.A., Wilmouth, R.C., Clifton, I.J., Schofield, C.J. (2001) Kinetic and crystallographic analysis of complexes formed between elastase and peptides from β-casein. *Eur J Biochem* 268: 2969-2974; Radisky, E.S., Lee, J.M., Lu, C-JK., Koshland, D.E. Jr (2006) Insights into the serine protease mechanism from atomic resolution structures of trypsin reaction intermediates. *Proc Natl Acad Sci USA* 103: 6835-6840.

91. Tseng, C.C., Bruner, S.D., Kohli, R.M., Marahiel, M.A., Walsh, C.T., Sieber, S.A. (2002), Characterization of the surfactin synthetase C-terminal thioesterase domain as a cyclic depsipeptide synthase. *Biochemistry* 41: 13350-13359.

Chapter 4. Protein engineering to improve synthetic efficiency of PFE

In a previous chapter, the structural difference between hydrolases and acyltransferases of α/β hydrolase superfamily were identified as different orientations of a carbonyl group. In hydrolases, the carbonyl group points toward the active site and is located in a type II β turn. In acyltransferases the carbonyl group points away from the active site and is located in a type I β turn. Herein, we try to improve *Pseudomonas fluorescens* esterase (PFE) synthetic efficiency by switching oxyanion loop from a type II β turn to a type I β turn. Replacing PFE oxyanion turn peptide GWLL with several acyltransferases type I β turn peptides yielded several mutants, among which only PFE-GLRA yielded soluble protein. However PFE-GLRA doesn't show activity in either phenyl acetate and benzyl alcohol or isopropenyl acetate and *n*-propanol reactions. I also used saturation mutagenesis at position W28 and L29, which are next to the critical carbonyl group and were expected to affect its orientation. The screening by using phenyl acetate and benzyl alcohol reaction identified the best Trp28X mutant as Try28Leu, which has the A/H ratio 1.01 fold of wild type, and several better mutants at Leu29X, including L29I, L29T, L29V, L29W, with acyltransfer/hydrolysis (A/H) ratios 2.2, 2.5, 2.5, 4 fold of that of the wild type. X-ray crystal structure of L29I in another research indicates a flipping main chain between type I and II β turn. Activity of PFE wild type and Leu29Ile are same in the crystallization buffer and screening buffer. The screening of Leu29X in isopropenyl acetate and *n*-propanol reaction identified decreased relative A/H ratio comparing to wild type, with only Leu29Trp having slight improvement, which is 1.08 fold of wild type. Double mutants W28L/L29I, W28L/L29T, W28L/L29V combining improved mutations at position 28 and 29, are made. However, they don't show better performance than the corresponding Leu29 single mutants. As a

conclusion, PFE synthetic efficiency can be improved by mutating residues oxyanion turn.

1. Introduction

Acyltransfer reactions play an important role in pharmaceutical, polyester, oleochemicals and biodiesel synthesis. Acyltransferases that catalyze antibiotic and other drug synthesis can form macrolactones and show high stereo selectivity. However natural acyltransferases have very narrow substrate specificity and do not efficiently catalyze their unnatural substrates, which limits their application [1, 2]. Moreover, natural acyltransferases use expensive acyl-CoA as acyl donor, which limits their application in industry. Esterases and lipases have broad substrate specificity, excellent stereo-selectivity and can use cheap isopropenyl or vinyl esters as acyl donors [2-4]. However esterase/lipases catalyzed acyltransfer reactions require an organic medium to avoid hydrolysis in presence of water. Since acyltransfer reactions are used for synthesis and hydrolysis is the reverse reaction of synthesis, hydrolysis reaction directly affects efficiency of synthetic reaction. Acyltransfer/hydrolysis ratio is used to evaluate the enzyme synthetic efficiency. Esterases/lipases with high synthetic efficiency are desirable in industry process.

To improve the synthetic efficiency of a lipase or esterase, there are two strategies: improving acyltransfer activity and decreasing hydrolysis activity. Optimizing alcohol (or acyl acceptor)-binding site can efficiently improve enzyme synthetic efficiency. Penicillin acylases (PA) are a group of enzymes distributed in microorganisms. They are used for semi synthesis of β-lactam antibiotics due to their ability to hydrolyze natural penicillin to 6-amino-penicillanic acid (6-APA) and the reverse reaction, which is often used for condensation of 6-APA with a new acyl donor to generate new β-lactam

antibiotics. In the condensation reaction, transfer of 6-APA to a water molecule decreases the synthetic efficiency. Crystal structure of *E.coli* PA has been solved and falls into N-terminal nucleophile hydrolase family. The natural PA has modest acyltransfer capability and needs to be improved. Saturation mutagenesis at active site R145 and F146, aimed at better binding of β-lactam, revealed the best mutants R145S and R145G obtaining a $(\upsilon_{acyl}/\upsilon_{hydro})_{ini}$ 4-5 fold that of the wild-type. This improvement comes from both the increased acyltransfer reaction and decreased hydrolysis reaction [5]. The strategy of optimizing the substrate-binding site works for a specific substrate, but not the improvement the whole spectrum of substrates.

In this study, I am trying to improve esterases synthetic efficiency by decreasing hydrolysis reaction. Some acyltransferases belong to α/β hydrolase superfamily and have similar structures and catalytic mechanisms to esterases/lipases, which we also call hydrolases in this research. Detailed structural analysis and comparison identified the critical difference between these hydrolases and acyltransferases as a carbonyl group, which in hydrolases points to active site to activate nucleophilic water and in acyltransferases points away from active site. This carbonyl group is located at a type II β turn in lipases/esterases and a type I β turn in acyltransferases. In principle, by switching the type II β turn to type I β turn in hydrolases, I should be able to decrease the enzyme hydrolysis activity by deactivating nucleophilic water.

Tight turns are important protein secondary structures. Tight turns consist less than 6 consecutive amino acids in which the peptide backbone reverses direction by 180˚ and the distance of first and last C^{α} is less than 7 Å [6]. Tight turns are critical elements not only for protein structures but also functions, for example, tight turn structure in green fluorescent protein immature form can bring Gly67 amide nitrogen and Ser65 carbonyl carbon

close enough for the autocatalysis of chromophore formation [7]; conserved Gly in a tight turn in apoptosis inhibitor family proteins is required for binding apoptosis stimulators to regulate cell apoptosis process [8]. β turn belongs to a class of tight turns that comprise 4 consecutive residues. According to the ϕ, ψ dihedral angles of the two central residues, β turns are divided into several subclasses. Several methods have been developed for predicting β turn types corresponding to peptide sequences. A residue-coupled mode resulted in the correct prediction of β turn types I, I', II, II', VI, VIII and non-β turn at 68.54%, 93.60%, 85.19%, 97.75%, 100%, 88.75% and 61.02% accuracy [9]. The method "Betaturns" based on artificial neural network trained on position-specific scoring matrices obtained from PSI-BLAST predicted β turn types I, II, IV and VIII at the accuracy 74.5%, 93.5%, 67.9% and 96.5%. [10].

The central peptide-plane of type I or II β turn can undergo a large rotation and cause 180° difference of C_α-C=O (ψ_{i+1}) and N- C_α(ϕ_{i+2}), which result in type I→II or II→I conversion. This phenomenon has been observed in many proteins. These proteins have one type of β turn in one crystal structure and the other type of β turn in another crystal structure[11]. The amino acid propensity analysis of these turns indicate that Gly occurs frequently at i+2 residue. The energy barrier for central peptide-plane flip is low.
It is more complicated to switch a β turn within a protein because the introduced peptide interacts with other parts of the protein structure. In this research, we are trying to decrease the hydrolyase activity of *Pseudomonas fluorescens* aryl esterase (PFE) by switching the oxyanion turn to a type I β turn. The PFE contains the oxyanion turn GWLL, with W28 the oxyanion residue, which donate its amide backbone to stabilize the oxygen ion of tetrahedral intermediate during catalysis. I proposed that this type II β turn is determined by the peptide sequence of itself, especially the two center residues, and planning to switch it by either replacing the peptide from acyltransferases or randomly mutating the two center residues.

PFE prefers substrates with short chain carboxylic acids, short chain alcohols and aryl group [12]. Herein we are going to use phenyl acetate and vinyl acetate as donors, and benzyl alcohol and short chain alcohols as acyl acceptors to test these PFE variants.

2. Methods

2.1 Mutagenesis

PCR reactions was conducted to generate all mutants by using plasmid pJOE2792 [13] as template and AccuPrime™ p*f*x DNA polymerase (Invitrogen, Carlsbad, CA). Primer design was according to GeneTailor™ Site-Directed Mutagenesis System (Invitrogen, Carisbad, CA), in which only one of the primers contain the mutation site, in our case it was the forward primer. The upstream overlapping region of the mutation site is about 15~20 nucleotides and the down stream extended region is more than 10 nucleotides; the reverse primer has the complimentary overlapping region of that of forward primer and the extended region containing 10~15 nucleotides (Fig .1). To prevent the better annealing of the reverse primer than forward primer to the template, which generates wild type gene, primer pairs were adjusted to 3:1 in mole (forward primer: reverse primer). The reaction mixture is: pJOE2792 plasmid 30 ng, forward primer 7.5 *p*mol, reverse primer 2.5 *p*mol, AccuPrime™ p*f*x DNA polymerase 1.25 U, 10× AccuPrime™ P*f*x Reaction Mix 2.5 μl and add autoclaved, distilled water to 25 μl. Reaction conditions are: denature the template for 1 min at 95 °C, perform 25 cycles of 95 °C for 15 s, 58 °C for 30 s then 68 °C for 5.5 min. The PCR products were treated with *Dpn* I 20 U (Invitrogen, Carlsbad, CA) at 37 °C for 4 hours, transformed into *E.coli* BL21 by electroporation according to MicroPluser™ Electroporation Appparatus Operating Instructions and Applications Guide (Bio-Rad, Hercules, CA) and then 50 μl bacteria medium was spread on LB plate containing ampicillin 100

μg/ml. The plasmids were extracted by using QIAprep Spin Miniprep kit (QIAGEN Sciences Maryland, USA) from single colonies and subjected to Sanger method to determine DNA sequences by using sequencing primer: taa tga aca att ctt aag aag gag.

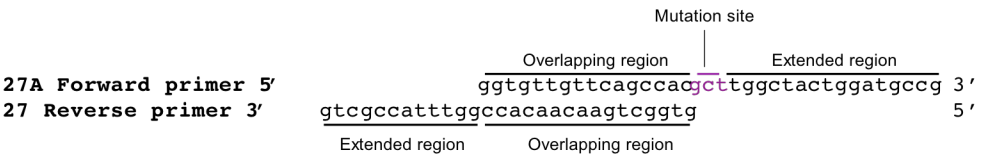

Figure 1. Primer pair of Gly27Ala mutation. The initial codon of Gly ggt was changed to Ala codon gct as shown at the mutation site. The overlapping region contains 16 nucleotides; extended region of forward primer contains 16 nucleotides and reverse primer 12 nucleotides.

2. 2 Protein purification

To determine the acyltransfer/hydrolysis ratio, pure PFE enzyme was desirable to avoid background noises. In pJOE plasmid, PFE is linked to a His_6 tag on the C terminus, which allowed easy purification with Ni-NTA agarose resin. For each PFE variants, 3 ml overnight culture was added to LB medium (300 ml; ampicillin, 100 μg/ml) and grown at 37 °C, 200 rpm for 3 hours to an OD_{600} around 0.5. Subsequently, protein expression was induced by adding sterile L-rhamnose (0.1% w/v of the final concentration) and incubated for 6 hours at 20 °C, 200 rpm. The cells were centrifuged (15 min, 5000 × g, 4 °C) and the pellet was resuspended in 5ml Buffer A (NaH_2PO_4, 50 mM; NaCl, 300 mM; imidazole, 10 mM; adjusted to pH 8.0 with NaOH), flash frozen and thawed, followed by adding lysozyme to 1 mg/ml and benzonase nuclease (Sigma, St Louis, MO) to 100 unit/ml. Cell sample was incubated at 4 °C overnight or until the viscosity all gone. The cell lysate was centrifuged (30 min, 10,000 × g, 4 °C) and the supernatant was purified by using Ni-NTA agarose resin according to the manufacturer's protocol (Qiagen Inc., Mississauga, ON). Purified protein was dialyzed (Spectrum Laboratories.

In, Rancho, Dominguez, CA) to exchange to BES buffer (100 mM, pH 7.2) and then concentrated by using Amicon Ultra Centrifugal Filters (Milllipore, Carrigtwohill, Co. Cork, Ireland).

Table1. Primers for PFE mutagenesis[a]

Primers	Primer sequences
Gly27Ala For[b]	ggtgttgttcagccacgcttggctactggatgccg
Gly27Pro For	ggtgttgttcagccacccttggctactggatgccg
PFE-ALTG For	ggtgttgttcagccacgctctaacaggtgatgccgacatgtggg
PFE-ALSG For	ggtgttgttcagccacgctctaagtggtgatgccgacatgtggg
PFE-ATSV For	ggtgttgttcagccacgctactagtgttgatgccgacatgtggg
PFE-AANG For	ggtgttgttcagccacgctgctaatggtgatgccgacatgtggg
PFE-PISG For	ggtgttgttcagccacgctatttctggtgatgccgacatgtggg
PFE-PVLG For	ggtgttgttcagccacgctgttctaggtgatgccgacatgtggg
PFE-GLRA For	gttgttcagccacggtcttcgtgctgatgccgacatgtgg
PFE-TLTS For	ggtgttgttcagccacactcttacttctgatgccgacatgtgg
Gly27 Rev[c]	gtggctgaacaacaccggtttaccgctg
Trp28X For	gttgttcagccacggtnnk[d]ctactggatgccgacatgtg
Trp28X Rev	gtcggcatccagtagmnn[d]accgtggctgaacaacacc
Trp28Leu/Leu29Ile	gttgttcagccacggtcttattctggatgccgacatgtg
Trp28Leu/Leu29Thr	gttgttcagccacggtcttactctggatgccgacatgtg
Trp28Leu/Leu29Val	gttgttcagccacggtcttgttctggatgccgacatgtg

Mutagenic sites are underlined in each primer.

[a]Trp28X mutant library is generated by using Trp28X For and Trp28X Rev primers. Gly27Ala, Gly27Pro, PFE-ALTG, PFE-ALSG, PFE-ATSV, PFE-AANG, PFE-PISG, PFE-PVLG, PFE-GLRA, PFE-TLTS, Trp28Leu/Leu29Ile, Trp28Leu/Leu29Thr and Trp28Leu/Leu29Val are generated by using corresponding forward primers and Gly27 Rev primer.

[b], [c] For stands for forward primer and Rev stands for reverse primer.

[d]Degenerate codon: 'n' stands for 25% A, T, C, and G mixture; 'k' stands for 50% of G and T mixture; 'm' stands for 50% of A and C mixture.

2. 3 Protein assay

Protein concentration was determined by Bio-Rad protein assay according to the manufacturer's protocol. (Bio-Rad. Hercules, CA) Protein purity, abundances in cell pellet and supernatant were determined by electrophoresis in SDS-PAGE gel (NuPAGE 4~12% Bis-Tis Gel, Invitrogen, Carisbad, CA).

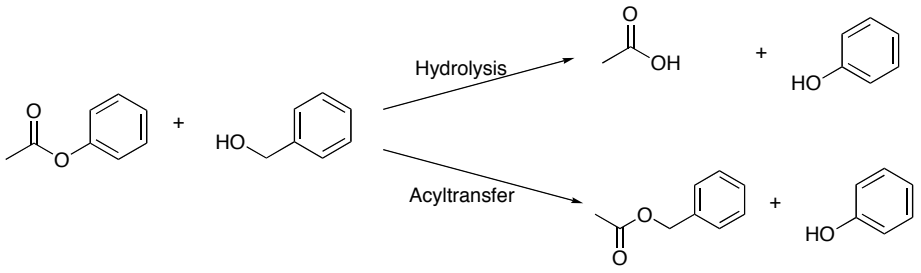

A

$$acyltransfer\ conversion = \frac{benzyl\ acetate}{phenyl\ acetate + phenol}$$

$$hydrolysis\ conversion = \frac{phenol - benzyl\ acetate}{phenyl\ acetaet + phenol}$$

B $$acyltransfer/hydrolysis = \frac{acyltransfer\ conversion}{hydrolysis\ conversion}$$

Figure 2. A/H assay of phenyl acetate and benzyl alcohol reaction A. PFE catalyzed phenyl acetate and benzyl alcohol reaction in aqueous solution. B. Formula for A/H ratio calculation.

2.4 PFE wild type acyltransfer reaction assay

Reactions were carried out by adding 1 μg PFE wild type to a mixture of 80 μl BES buffer (200 mM, pH 7.2) or BIS-TRIS buffer (0.1 M BIS-TRIS, 1.85 M ammonium sulfate, HCl adjust to pH 6.5), 10 μl phenyl acetate (3 M, dissolved in *t*-butanol) and 10 μl benzyl alcohol (900 mM as the final concentration) and the reaction was incubated at 25 °C, 650 rpm. Reactions were quenched at 10, 20, 30, 40, 50 and 60minutes by adding 15 μl 1 N HCl

and 900 μl MeCN and subjected to GC analysis to determine acyltransfer and hydrolysis conversion. Control reactions are also taken in the same way by adding no enzyme to the above mixture.

DB-FFAP column (Agilent, Santa Clara, CA), whose stationary phase is nitroterephthalic acid modified polyethylene glycol, was used for GC analysis. Temperature was held at 120 °C for 10 min, then was increased 5 °C /min to 200 °C and held for 2 min. The retention time for phenyl acetate was 7.5 minues, benzyl acetate was 10.9 minutes, phenol was 19.1 minutes. Response factor for phenyl acetate was 25.4 *p*mole^{-1}, benzyl acetate was 35.2 *p*mole^{-1}, phenol was 22.8 *p*mole^{-1}.

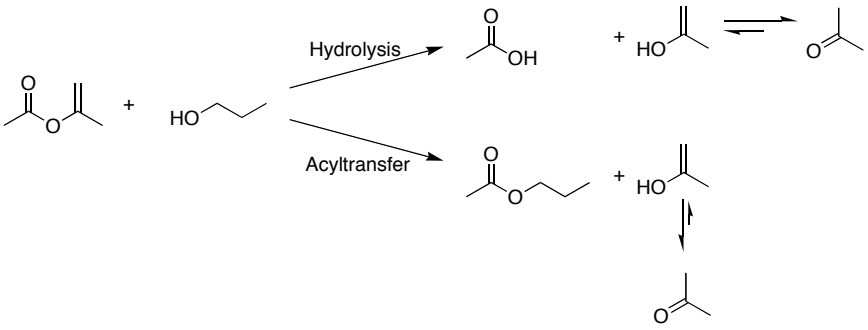

A

B

$$acyltransfer\ conversion = \frac{n-propyl\ acetate}{isopropenyl\ acetate + n-propyl\ acetate + acetic\ acid}$$

$$hydrolysis\ conversion = \frac{acetic\ acid}{isopropenyl\ acetate + n-propyl\ acetate + acetic\ acid}$$

$$acyltransfer/hydrolysis = \frac{acyltransfer\ conversion}{hydrolysis\ conversion}$$

Figure 3. A/H assay of isopropenyl acetate and *n*-propanol reaction. A. PFE catalyzed isopropenyl acetate and *n*-propanol reaction in aqueous solution. B. Formula for A/H ratio calculation.

2. 5 Screening method for PFE variants

The screening reaction for better mutants was the same as shown in Fig 2A. The substrates and buffer was mixed in the same way as PFE wild type acyltransfer reaction assay. The amount of enzyme varied in order to get the sum of acyltransfer conversion and hydrolysis conversion between 5%~20% when reaction was stopped at 40 minutes. The acyltransfer/ hydrolysis ratio was calculated (Fig .2B).

I also used isopropenyl acetate as acyl donor and *n*-propanol as acyl acceptor to test PFE Leu29X mutants acyltransfer/hydrolysis ratio (Fig .3). I mixed 90 μl BES buffer (200 mM, pH7.2), 3 μl isopropenyl acetate (324 mM as the concentration), 7 μl *n*-propanol (931 mM as the concentration) and PFE variants. After incubated at 25 °C and shaking at 650 rpm for 40 min, reactions were quenched by adding 15 μl1N HCl and 900 μl acetone.

DB-FFAP column (Agilent, Santa Clara, CA) was also used for this analysis. Temperature was held at 50 °C for 6 min, then increased 5 °C /min to 120 °C. The retention time for isopropenyl acetate was 4.2 min, propyl acetate was 3.8 min and acetic acid was 18 min. Response factor for isopropenyl acetate was 1.3 $p$mole^{-1}, *n*-propyl acetate was 2.3 $p$mole^{-1} and acetic acid was 0.53 $p$mole^{-1}.

3. Results

3.1 PFE wild type acyltransfer activity assay

I used isopropenyl acetate as acyl donor and *n*-propanol as acyl acceptor to test the synthetic efficiency of PFE variants. This esterase-catalyzed process in aqueous solution included an acyltransfer reaction, which transfers the acetyl group from isopropenyl acetate to *n*-propanol, and a hydrolysis reaction, which transfers acetyl group from phenyl acetate to water (Fig 3A). The hydrolysis reaction is irreversible, because it is an energy

favorable process and there are much more water molecules than phenol. However, the acyltransfer reaction is not so simple. The process from isopropenyl acetate to *n*-propanol acetate is energy favorable, but the product of *n*-propanol acetate can be hydrolyzed. Therefore it is necessary determine a region where enzyme catalyzed acyltransfer and hydrolysis reactions followed the first-order kinetics so that the accumulated products can reflect the reaction velocities. The pure PFE wild type was used to catalyze this reaction. Samples quenched at 0, 10, 20, 30, 40, 50, and 60 minutes were analyzed on GC to determine conversions. Control reactions without enzyme were analyzed in the same way. The result in Fig 4 indicated that both reactions follow first order rate kinetics before their conversion reached 35% when starting from high substrate concentrations: 300 mM isopropenyl acetate and 900 mM *n*-propanol. In the control reaction, there were also hydrolysis and acyltransfer reactions.

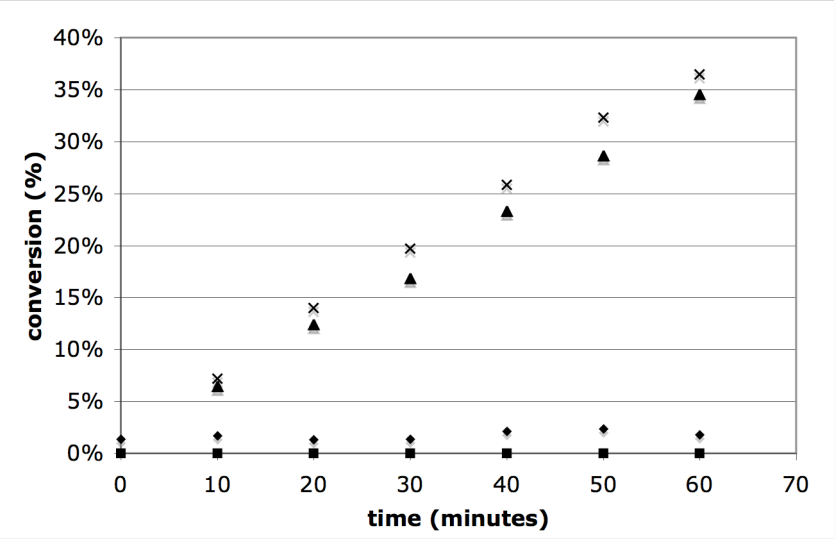

Figure 4. PFE wild type catalyzed vinyl acetate and benzyl alcohol assay. PFE catalyzed acyltransfer reaction is shown as "×"; PFE catalyzed hydrolysis reaction is shown as "▲"; hydrolysis conversion of control reaction are shown as "◆"; acyltransfer conversion of control reaction are shown as "■".

3. 2 PFE variants with replaced oxyanion turn

Previous structural analysis of acyltransferases of α/β hydrolase superfamily, which are *Mycobacterium tuberculosis* Antigen 85-A, B and C, *Bacillus subtilis* surfactin synthetase thioesterase domain, *Bacillus subtilis* fengycin synthetase thioesterase domain, *Leptospira interrogans* homoserine acyltransferase, *Haemophilus influenzae* homoserine acyltransferase and *Acremonium chrysogenum* deacetylcephalosporin C acetyltransferase, identified oxyanion turn peptide sequences: GLRA, PVLG, PISG, ALSG, ALTG and TLTS. Another two acyltransferases, erythromycin thioesterase and pikromycin thioesterase, have significantly different oxyanion loop structures, also contain type I β turns at similar position with the peptide sequences AANG and ATSV. I replaced the whole oxyanion turn peptide in PFE from GWLL (27~30) to those from acyltransferases by site-directed mutagenesis using PCR and gained 8 corresponding mutants. These mutants were induced for overexpression at 37 °C in LB medium as described in the method section. All the eight overexpressed PFE proteins appeared in the cell pellet section instead of supernatant after centrifuging cell crude lysate, this implied that these PFE mutants cannot fold well and aggregate in cell inclusion body [14]. Then we tried other strategies to improve protein folding efficiency, such as coexpression with charperones [15], adding 3% ethanol to the LB medium [16], and inducing protein at lower temperatures (20°C). Fortunately, there was one mutant PFE-GLRA, which had PFE protein partially in supernatant when induced at 20°C.

The PFE Gly27 is conserved in esterases and lipases, because of limited space at this position [17].I hypothesized that mutations at this position cause protein insolubility. To test this hypothesis I made Gly27Ala, Gly27Pro and Gly27Thr, which are present in acyltransferases. The SDS-PAGE result indicated that only G27A was soluble and showing in supernatant, while G27P and G27T aggregated in cell pellet.

The A/H ratios of PFE-GLRA and G27A in phenyl acetate and benzyl alcohol reaction were measured and compared to that of wild type. I carried out each enzyme-catalyzed reaction for the same time, 40 minutes, to make sure that there are equal background acyltransfer and hydrolysis conversions. The conversion of each reaction (the sum of acyltransfer and hydrolysis conversion) was adjusted between 5%~20% by varying the enzyme amount. If the conversion is too low, the measurement is less reliable. If conversion is high, some of the product ester may undergo hydrolysis. In the control reaction, hydrolysis and acyltransfer conversions for 40 minutes were 0.72% and 0.27% respectively.

The wild type PFE was added in the reaction at the concentration of 4 μg/ml, which resulted in acyltransfer conversion 3.03%, hydrolysis conversion 4.68% and A/H ratio 0.65. PFE-GLRA showed very low catalytic activity in this reaction, 0 for acyltransfer conversion and 0.99% for hydrolysis conversion, by adding the protein at the concentration 1000 μg/ml. G27A also had a lower activity than wild type with the acyltransfer and hydrolysis conversions 0.49% and 3.46% respectively by adding enzyme 2400 μg/ml.

PFE-GLRA showed very poor catalytic activity in this reaction. I tested its activity in another reaction with isopropenyl acetate and *n*-propanol as substrates. At the concentration of 5 μg/ml, PFE wild type catalyzed acyltransfer conversion 6.71% and hydrolysis conversion 3.78%, with the corresponding A/H ratio 1.78. PFE-GLRA didn't show any catalytic activity in this reaction: 0 for both acyltransfer conversion and hydrolysis conversion, by adding protein at a concentration 1500 μg/ml.

3. 3 PFE variants of single mutants L29X and L28X

The introducing of foreign oxyanion turn into PFE caused folding problems. I wondered if fewer mutations could switch oxyanion turn from type II to type I β turn without affecting protein folding. Since Trp28 and Leu29 are closer to the differently oriented carbonyl group, I hypothesized that these two residues have more effect on the turn conformation.

Saturation mutagenesis at positions 28 and 29 got 38 PFE variants. These mutants were induced at 20 °C and purified as described in the method section. From PFETrp28X library, we got 7 soluble proteins Trp28Phe, Trp28His, Trp28Ile, Trp28Leu, Trp28Met, Trp28Val and Trp28Tyr. Almost all of the PFE Leu29X mutants were soluble, except Leu29Arg and Leu29Asp. The A/H ratios of these mutants were assayed and the results were shown in Table 2.

For all these mutants, more proteins were used than wild type. Nearly all the Trp28X mutants showed decreases in synthetic efficiency and very low catalytic capability, which can be seen from the large amount of enzyme been added. Trp28Leu had the highest A/H ratio, 0.66, which was similar to wild type PFE. Trp28Ile, Trp28Tyr, Trp28Ile and Trp28Met had the A/H ratio, 0.58, 0.49 and 0.41 respectively. Trp28His showed extremely low A/H ratio 0.01, less than 1% that of wild type. Trp28Val didn't show acyltransfer conversion at all and its hydrolysis activity was also close to 0, although I added much more protein (2200 μg/ml) than that of the wild type.
In Leu29X mutant library, there were several mutants that show improved A/H ratio: Leu29His, Leu29Ile, Leu29Lys, Leu29Gln, Leu29Ser, Leu29Thr, Leu29Val and Leu29Trp show A/H ratio 0.82, 1.44, 0.78, 0.69, 0.84, 1.62, 1.60 and 2.61. Leu29Trp had the highest synthetic efficiency and showed an improvement of 4 fold from wild type PFE. Other L29X mutants showed lower A/H ratio. Leu29Pro didn't catalyze acyltransfer reaction at all and also showed very low hydrolysis activity.

Table 2. A/H ratio of PFE Trp28X and Leu29X variants catalyzed phenyl acetate and benzyl alcohol reaction[a].

PFE varients	Enzyme con [b] (μg/ml)	Acyltransfer conversion	Hydrolysis conversion	A/H ratio	Fold[d]
WT	4	3.03%	4.68%	0.65	1
Gly27Ala	2400	0.49%	3.34%	0.15	0.23
GLRA	1000	0	0.99%	0	0
Leu29Ala	50	8.55%	14.1%	0.61	0.93
Leu29Cys	50	10.72%	21.99%	0.49	0.75
Leu29Glu	90	4.18%	11.78%	0.35	0.55
Leu29Phe	4	2.00%	6.02%	0.33	0.51
Leu29Gly	40	2.45%	11.89%	0.21	0.32
Leu29His	400	5.00%	6.08%	0.82	**1.27**
Leu29Ile	20	10.21%	7.10%	1.44	**2.21**
Leu29Lys	75	2.53%	3.26%	0.78	**1.2**
Leu29Met	20	3.38%	10.01%	0.34	0.52
Leu29Asn	20	3.35%	9.62%	0.35	0.53
Leu29Pro	200	/	1.94%	0	0
Leu29Gln	50	5.02%	7.29%	0.69	**1.06**
Leu29Ser	50	8.81%	10.45%	0.84	**1.30**
Leu29Thr	40	9.33%	5.77%	1.62	**2.49**
Leu29Val	20	5.07%	3.17%	1.60	**2.46**
Leu29Trp	100	6.36%	2.43%	2.61	**4**
Leu29Tyr	4	2.75%	11.0%	0.25	0.38
Leu28Phe	300	1.53%	3.7%	0.41	0.63
Trp28His	150	0.08%	14.3%	0.01	0.008
Trp28Ile	460	2.23%	3.77%	0.58	0.88
Trp28Leu	1300	6.48%	9.76%	0.66	**1.01**
Trp28Met	880	2.69%	9.2%	0.29	0.45
Trp28Val	2200	0	0.5%	0	0
Trp28Tyr	420	4.85%	9.8%	0.49	0.76
Trp28Leu/Leu29Ile	105	8.33%	13.62%	0.61	0.94
Trp28Leu/Leu29Thr	260	7.52%	6.54%	1.15	**1.8**
Trp28Leu/Leu29Val	440	3.62%	2.58%	1.41	**2.2**
wt[c]	10	5.94%	9.63%	0.63	1
Leu29Ile[c]	40	11.8%	8.12%	1.37	2.17

Mutants with improved A/H ratios are shown in bold.

a Reaction condition: 300 mM phenyl acetate, 900 mM benzyl alcohol in 200 mM BES buffer, pH 7.2

b Different amounts of PFE variant were added.

c Reaction condition: 300 mM phenyl acetate, 900 mM benzyl alcohol in Bis-Tris buffer, pH7.2

d Fold indicates the improvements of A/H ratios of PFE variants over PFE wild type.

3. 4 PFE wild type and L29I show similar activity in crystallization buffer screening buffer.

The improved A/H ratio might have come from improved preference for alcohol group or decrease preference for water or the combination of both. I still had no idea if I got mutants containing a type I β turn. Another member in my lab was working on impoving PFE perhydrolysis activity. PFE Leu29Ile showed improved perhydrolysis specificity. Therefore he crystalized PFE Leu29Ile and solved the x ray structure, which indicated a flipping Trp28 carbonyl group, that is, the oxyanion turn switches between the states of type I and type II β turns. In the previous assay, Leu29Ile showed an A/H ratio 2.2 fold of wild type. I was wondering if Leu29Ile also flipped its Trp28 carbonyl backbone in BES buffer, which was the screening buffer. I performed the acyltransfer reaction of both PFE wild type (10 ug/ml) and L29I (40 ug/ml) in Bis-Tris buffer as used for Leu29Ile crystallization, and they showed A/H ratios 0.62 and 1.37 respectively. In BES buffer, their A/H ratios were 0.65 and 1.44. This result implied that the enzyme performances were similar in these two buffers. Leu29Ile should also have a flipping carbonyl backbone in BES buffer.

3. 5 PFE double mutants acyltransfer specificities

Since I got improved A/H ratios in PFE single mutants, I wondered if double mutations are better than single mutations. I choose the best mutant Trp28Leu from Trp28X library and combined it with Leu29Ile, Leu29Thr and Leu29Val from Leu29X library to create three double mutants. All the three

double mutants were soluble. These proteins were purified and synthetic efficiencies were assayed. Results are shown in Table 2. Trp28Leu/Leu29Ile showed the lowest A/H ratio 0.61 among these three mutants, which was even lower than wild type PFE. Trp28Leu/Leu29Thr and Trp28Leu/lle29Val had A/H ratio 1.15 and 1.41, which were higher than wild type PFE, but were still lower than single mutants Leu29Thr and Leu29Val respectively.

3. 6 PFE acyltransfer activity assay in isopropenyl acetate and n-propanol reaction

The acyltransfer activity is dramatically affected by acyl acceptor. Herein, I used different substrates, isopropenyl acetate and *n*-propanol, to test PFE Leu29X mutants. The A/H ratios were shown in Table 3. PFE wild type had an A/H ratio of 1.78 in this reaction, that is, the conversion of acyl group to *n*-propanol was 1.78 fold of the conversion to the water. For all these Leu29X mutants only Leu29Trp showed slightly higher A/H ratio than wild type, which was 1.92. For the Leu29Ile, Leu29Thr and Leu29Val mutants, their A/H ratios were lower than wild type, but still higher than other mutants. Leu29Pro still didn't show acyltransfer activity in this reaction.

Table 3. A/H ratios of PFE Leu29X mutants catalyzed isopropenyl acetate and *n*-propanol reaction

PFE variants	Enzyme con (ug/ml)	Acyltransfer conversion	Hydrolysis conversion	A/H ratio	Fold
WT	5	6.71%	3.78%	1.78	1
GLRA	1500	0	0	ND	ND
Leu29Ala	5	3.09%	10.26%	0.30	0.17
Leu29Cys	50	10.72%	21.99%	0.49	0.28
Leu29Phe	4	13.72%	10.51%	1.31	0.74
Leu29Gly	2	2.57%	7.90%	0.33	0.19
Leu29His	100	3.71%	4.21%	0.88	0.49
Leu29Ile	20	10.21%	7.10%	1.44	0.81
Leu29Met	20	3.38%	10.01%	0.34	0.19
Leu29Asn	3	3.24%	6.59%	0.49	0.28

Leu29Pro	10	0	7.58%	0	0.00
Leu29Gln	10	10.18%	20.17%	0.50	0.28
Leu29Ser	50	8.81%	10.45%	0.84	0.47
Leu29Thr	40	9.33%	5.77%	1.62	0.91
Leu29Val	20	5.07%	3.17%	1.60	0.90
Leu29Trp	100	10.69%	5.56%	1.92	**1.08**
Leu29Tyr	4	2.75%	11.0%	0.25	0.14

The relative synthetic efficiencies of PFE Leu29X mutants over wild type in both reactions were compared (Fig 5). The synthetic efficiencies of wild type were set to 1 for both reactions. For most mutants, they had higher improvement in the 1st reaction than in the 2nd reaction, except Leu29Phe, which was 0.51 fold in reaction 1 and 0.74 fold in reaction 2. Leu29Trp showed improvement in both reactions. Leu29Ile, Leu29Thr and Leu29Val were the next mutants after Leu29Trp that showed relative synthetic efficiency in both reactions. Leu29Pro showed 0 A/H ratio in both reactions, which implied that it could catalyze neither acyltransfer reaction. Generally, most variants showed better performance in phenyl acetate and benzyl alcohol reaction compared to wild type than the other reaction.

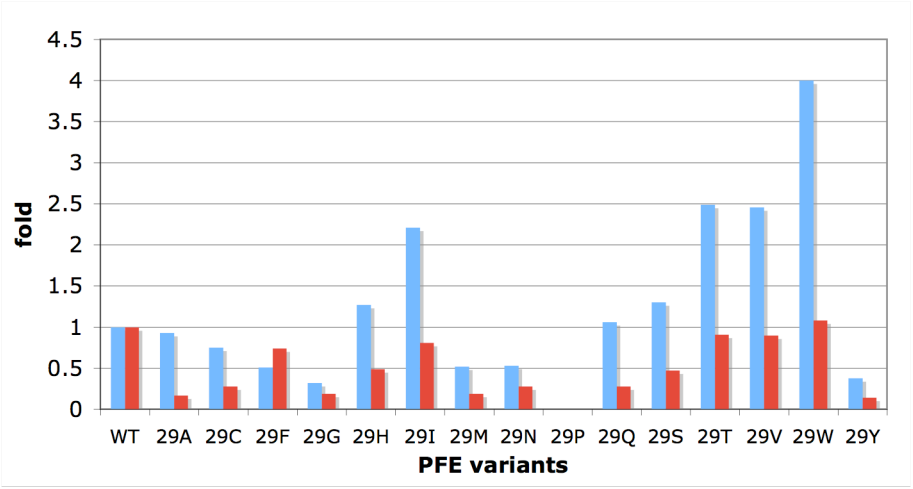

Figure 5. PFE Leu29X mutant A/H in both reactions compared to wild type. Blue bars represent phenyl acetate and benzyl alcohol reactions. Red bars represent isopropenyl acetate and n-propanol reactions.

Discussion

PFE mutants with Gly27~Leu30 peptide changed to acyltransferase oxyanion turns yield 8 mutants and 7 of which are insoluble. Apparently, mutations of this area affected protein stability significantly. Gly27 is the conserved residue in esterases/lipases of α/β hydrolyase superfamily and other residues with big side chains might disrupt the protein structure. The solubilities of PFE single mutants Gly27Ala, Gly27Pro and Gly27Thr were reasonable. Ala had a very small side chain and therefore Gly27Ala was soluble. Pro and Thr havd bigger side chains and therefore Gly27Pro and Gly27Thr aggregated. Trp28X mutation was also critical for protein stability because only 7 out of 19 Trp28X mutants are soluble. Nearly all Leu29X mutants, except Gly29Asp and Gly29Arg, were soluble and therefore this position was much less important for protein stability. PFE-GLRA was the only soluble mutant with changed acyltransferase oxyanion. Compared to other mutants, PFE-GLRA had only 3 mutations: the critical Gly27 wasn't changed, Trp28Leu mutation was tolerable, Leu29Arg was likely to have negative effect, which was insoluble as single mutation. PFE-GLRA was destabilized by the substitution of 3 amino acids and the protein can only be induced at low temperature. Induction at 37°C did not yield any soluble protein.

PFE-GLRA showed very poor activity in both reactions. The peptide GLRA came from the oxyanion turn of *Mycobacterium tuberculosis* Antigen 85 complex, which contains 3 homologous proteins: A, B, and C, which all catalyze the transfer of mycolyl group from trehalose dimycolate or trehalose monomycolate to C5 position of arabinofuranosides on the peptidoglycan matrix of cell wall. Substrate specificity of Antigen 85C was characterized by using different acyl donor and acceptors [18] (Fig 6). Antigen 85 proteins favor hydrophobic fatty acids as acyl moiety and hydrophilic sugars as alcohol part.

There are two possible reasons that PFE-GLRA cannot catalyze the two reactions: 1. The mutant doesn't obtain catalytic activity; 2. The mutant has catalytic activity, but we didn't use correct substrates. Analysis of both PFE and antigen 85C structures identified that the W28 position in PFE mainly affects the acyl moiety of the substrate. Therefore, I think phenyl acetate and isopropenyl acetate might not be good substrate due to their acyl group. Compared to the original GWLL in PFE, GLRA introduced a hydrophilic residue Arg at position 29, which might also change the preference for the alcohol group.

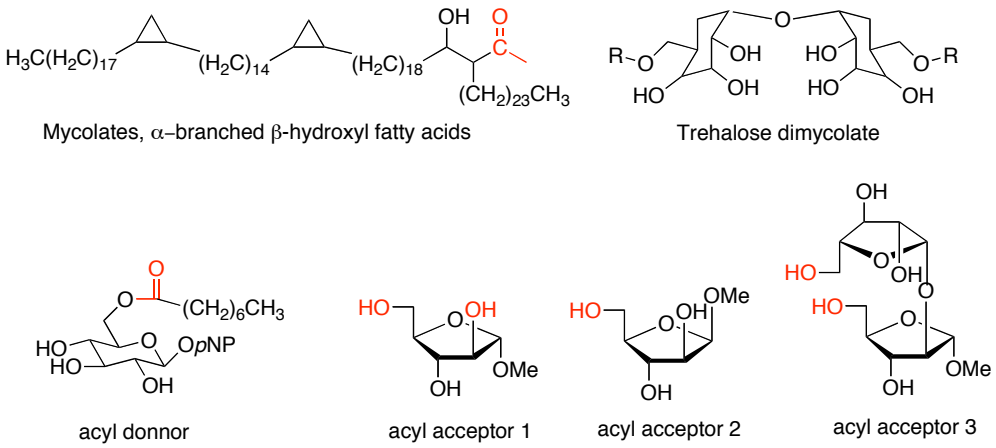

Figure 6. Substrates of *Mycobacterium tuberculosis* Antigen 85C. Tehalose dimycolate is the natural acyl donor. Mycolate represents the structure of the R group. The acyl donor and acyl acceptors at the bottom are not natural substrates, but they can also be catalyzed by Antigen 85C. The groups shown in red are the targets of chemical conversion.

Several Leu29X mutants, such as Leu29Ile, Leu29His, Leu29Thr, Leu29Val and Leu29Trp show improved synthetic efficiency in phenyl acetate and benzyl alcohol reaction. Among Trp28X mutants, the best one, Trp28Leu, had the synthetic efficiency similar to wild type.

The goal of the mutagenesis was to switch the carbonyl group of oxyanion residue to a type I β turn and therefore decrease the hydrolysis activity. I suppose the desired mutants should have less hydrolysis activity while the acyltransfer activity won't change too much. However, these mutants affect the substrate bind efficiency through changed side chains, and both hydrolysis and acyltransfer activity would be affected. We cannot see if we get any mutant with type I β turn. Fortunately, the resolution of the PFE Leu29Ile crystal structure shows a flipping carbonyl group, which is switching between type I and II β turn. The A/H ratio of Leu29Ile in phenyl acetate and benzyl alcohol reaction is slightly higher than wild type. PFE wild type and Leu29Ile get similar activity and A/H ratio in both the BES buffer, which we used for the mutants screening, and Bis-Tris buffer, which is used for PFE Leu29ILe crystallization. This result indicates that Leu29Ile might also have a flipping oxyanion turn in the screening buffer.

In the screening with isopropenyl acetate and n-propanol reaction, most Leu29X mutants show lower acyltransfer specificity than the other reaction. Leu29Trp is the only one that shows higher synthetic efficiency than wild type in both reactions. The acyltransfer specificities of some mutants, like Leu29Thr and Leu29Val, are lower than wild type in isopropenyl reaction, but are higher than most other mutants. These mutants with relatively high A/H ratio in both reactions, such as Leu29Thr, Leu29Val and Leu29Trp, are suspected to obtain a type I β turn or a flipping carbonyl group l like Leu29ILe.

Trp28X mutants have very poor catalytic activity, which can be seen from the amount of enzyme added into reactions. Among these mutants, Trp28Leu has the highest A/H ratio, which is similar to wild type. Other mutants have lower A/H ratio and Trp28Val has nearly 0 activity. It is hard to say if they have type I β turn. Trp28L, Trp28I are interesting, because they

show relatively higher A/H ratio comparing to other mutants. Trp28Val didn't show any activity, like PFE-GLRA, it might do not have any catalytic activity or just do not catalyze the substrates we added. The double mutants Trp28Leu/Leu29Ile, Trp28Leu/Leu29Thr and Trp28Leu/Leu29Val didn't show higher synthetic efficiency than their Leu29 single mutant as we expected. It might because the substrates are not perfect for these double mutants.

PFE wild type prefers esters with small acyl group, which might be caused by the bulky Trp28 side chain. Now the Trp28Leu side chain might gives more space and allows bigger substrate to fit in. I need to try more esters with PFE-GLRA, Trp28Leu and Trp28Val to determine their best substrates and their acyltransfer specificities.

Acyltransferation is a useful reaction in biosynthesis. This research is dedicated to elucidate the structural principle between hydrolases and acyltransferases and guide the design of interesting acyltransferases which might be used for drug synthesis, polymer synthesis and biodiesel synthesis.

References

1. Born, T.L., Franklin, M., Blanchard, J.S. (2000) Enzyme-catalyzed acylation of homoserine: mechanistic characterization of the *Haemophilus influenzae* met2-encoded homoserine transacetylase. *Biochemistry* 39, 8556-8564.
2. He, W., Wu, J., Khosla, C., Cane, D.E.(2006) Macrolactonization to 10-deoxymethynolide catalyzed by the recombinant thioesterase of the picromycin/methymycin polyketide synthase. *Bioorg. Med. Chem. Lett.* 16, 391-394.
3. Snellman, E.A., Colwell, R.R. (2008) Transesterification activity of a novel lipase from *Acinetobacter venetianus* RAG-1. *Antonie Van Leeuwenhoek* 94, 621-625.
4. Singh, M., Singh, S., Singh, R.S., Chisti, Y., Banerjee, U.C. (2008) Transesterification of primary and secondary alcohols using *Pseudomonas aeruginosa* lipase. *Bioresour. Technol.* 99, 2116-2120.
5. Jager, S.A., Shapovalova, I.V., Jekel, P.A., Alkema, W.B., Svedas, V.K., Janssen, D.B. (2008) Saturation mutagenesis reveals the importance of residues alphaR145 and alphaF146 of penicillin acylase in the synthesis of beta-lactam antibiotics. *J. Biotechnol.* 133, 18-26.
6. Chou, K.C. (2000) Prediction of tight turns and their types in proteins. *Anal. Biochem.* 286, 1-16.
7. Lemay, N.P., Morgan, A.L., Archer, E.J., Dickson, L.A., Megley, C.M., Zimmer, M. (2008) The role of the tight-turn, broken hydrogen bonding, Glu222 and Arg96 in the post-translational green fluorescent protein chromophore formation. *Chem. Phys.* 348, 152-160.
8. Luque, L.E., Grape, K.P., Junker, M. (2002) A highly conserved arginine is critical for the functional folding of inhibitor of apoptosis (IAP) BIR domains. *Biochemistry* 41, 13663-13671.
9. Chou, K.C., Blinn, J.R. (1997) Classification and prediction of beta-turn types. *J. Protein. Chem.* 16, 575-595.
10. Kaur. H., R., G.P. (2004) A neural network method for prediction of beta-turn types in proteins using evolutionary information. *Bioinformatics* 20, 2751-2758.
11. Gunasekaran, K., Gomathi, L., Ramakrishnan, C., Chandrasekhar, J., Balaram, P. (1998) Conformational interconversions in peptide beta-turns: analysis of turns in proteins and computational estimates of barriers. *J. Mol. Biol.* 284, 1505-1516.
12. Liua, A.M.F., Somersa, N.A., Kazlauskas, R.J., Brushb, T.S., Zocherc, F., Enzelbergerc, M.M., Bornscheuerc, U.T., Horsmana, G.P., Mezzettia, A., Schmidt-Dannertc, C., Schmidc, R.D. (2001) Mapping the substrate selectivity of new hydrolases using colorimetric screening: lipases from *Bacillus thermocatenulatus* and *Ophiostoma*

piliferum, esterases from *Pseudomonas fluorescens* and *Streptomyces diastatochromogenes*. *Tetrahedron: Asymmetry* 12, 545-556.
13. Horsman, G.P., Liu, A.M., Henke, E., Bornscheuer, U.T., Kazlauskas, R.J. (2003) Mutations in distant residues moderately increase the enantioselectivity of *Pseudomonas fluorescens* esterase towards methyl 3-bromo-2-methylpropanoate and ethyl 3phenylbutyrate. *Chem. Eur.J.* 9, 1933-1939.
14. Calloni, G., Zoffoli, S., Stefani, M., Dobson, C.M., Chiti, F. (2005) Investigating the effects of mutations on protein aggregation in the cell. *J. Biol. Chem.* 280, 10607-10613.
15. Ikura, K., Kokubu, T., Natsuka, S., Ichikawa, A., Adachi, M., Nishihara, K., Yanagi, H., Utsumi, S. (2002) Co-overexpression of folding modulators improves the solubility of the recombinant guinea pig liver transglutaminase expressed in *Escherichia coli*. *Prep. Biochem. Biotechnol.* 32, 189-205.
16. Thomas, J.G., Baneyx, F., (1997) Divergent effects of chaperone overexpression and ethanol supplementation on inclusion body formation in recombinant *Escherichia coli*. *Protein. Expression. Purif.* 11, 289-296.
17. Fischer, M., Pleiss, J. (2003) The lipase engineering database: a navigation and analysis tool for protein families. *Nucleic Acids Res.* 31, 319-321.
18. Sanki, A.K., Boucau, J., Ronning, D.R., Sucheck, S.J. (2009) Antigen 85C-mediated acyl-transfer between synthetic acyl donors and fragments of the arabinan. *Glycoconjugate. J.* 26, 589-596.

Comprehensive References

References for Chapter 1

1. Anastas, P.T., Warner, J.C. (1998). *Green Chemistry: Theory and Practice.* Oxford University Press, USA
2. Theil, F. (1995). Lipase-supported synthesis of biologically active compounds. *Chem. Rev.* 95, 2203-2227.
3. Shimada, Y., , Watanabe, Y., Samukawa, T., Sugihara, A., Noda, H., Fukuda, H., Tominaga, H. (1999). Conversion of vegetable oil to biodiesel using immobilized *Candida antarctica* lipase. *J. Am. Oil Chem. Soc.* 76, 789-793.
4. Chaudhary, A.K., Beckman, E.J., Russell, A.J. (1997). Biocatalytic polyester synthesis: Analysis of the evolution of molecular weight and end group functionality. *Biotechnol Bioeng.* 55, 227-239.
5. Bornscheuer, U.T. (2003). Immobilizing enzymes: how to create more suitable biocatalysts. *Angew. Chem. Int. Ed. Engl.* 42, 3336-3337.
6. Ishige, T., Honda, K., Shimizu, S. (2005). Whole organism biocatalysis. *Curr. Opin. Chem. Biol.* 9, 174-180.
7. Tao, J., Xu, J. H. (2009). Biocatalysis in development of green pharmaceutical processes. *Curr. Opin. Chem. Biol.* 13, 43-50.
8. Xie, X., Tang, Y. (2007). Efficient synthesis of simvastatin by use of whole-cell biocatalysis. *Appl. Environ. Microbiol.* 73, 2054-2060.
9. Xie, X., Watanabe, K., Wojcicki, W. A., Wang, C. C., Tang, Y. (2006). Biosynthesis of lovastatin analogs with a broadly specific acyltransferase. *Chem. Biol.* 13, 1161-1169.
10. Akoh, C.C., Chang, S. W., Lee, G. C., Shaw, J. F. (2007). Enzymatic approach to biodiesel production. *J. Agric. Food Chem.* 55, 8995-9005.
11. Kaiedaa, M., Samukawaa, T., Kondoa, A., Fukuda, H., (2001). Effect of methanol and water contents on production of biodiesel fuel from plant oil catalyzed by various lipases in a solvent-free system. *J. Biosci. Bioeng.* 91, 12-15.
12. Kaiedaa, M., Samukawaa, T., Matsumotoa, T., Ban, K., Kondoa, A., Shimadac, Y., Nodad, H., Nomotoe, F., Ohtsukae, K., Izumotof, E., Fukudab, H. (1999). Biodiesel fuel production from plant oil catalyzed by *Rhizopus oryzae* lipase in a water-containing system without an organic solvent. *J. Biosci. Bioeng.* 88, 627-631.
13. Lee, J.H., Lee, D. H., Lim, J. S., Um, B. H., Park, C., Kang, S. W., Kim, S. W. (2008). Optimization of the process for biodiesel production using a mixture of immobilized *Rhizopus oryzae* and *Candida rugosa* lipases. *J. Microbiol. Biotechnol.* 18, 1927-1931.
14. Duda, A., Kowalski, A., Penczek, S., Uyama, H., Kobayashi, S (2002). Kinetics of the ring-opening polymerization of 6-, 7-, 9-, 12-, 13-, 16-,

and 17-membered lactones. Comparison of chemical and enzymatic polymerizations *Macromolecules* 35, 4266-4270.
15. Patrick, C.C., Kimberly, M. M., Umeno, D. (2008). Generating mutant libraries using error-prone PCR. *Direct evolution library creation: Methods and Protocols.* Humana Press, 1st edition *231*, 3-9.
16. Cohen, J. (2001). How DNA shuffling works. *Science* 293, 237.
17. Hsu, C.C., Hong, Z., Wada, M., Franke, D., Wong, C. H. (2005). Directed evolution of D-sialic acid aldolase to L-3-deoxy-manno-2-octulosonic acid (L-KDO) aldolase. *Proc. Natl. Acad. Sci. U. S. A.* 102, 9122-9126.
18. Horsman, G.P., Liu, A. M., Henke, E., Bornscheuer, U. T., Kazlauskas, R. J. (2003). Mutations in distant residues moderately increase the enantioselectivity of *Pseudomonas fluorescens* esterase towards methyl 3bromo-2-methylpropanoate and ethyl 3phenylbutyrate. *Chemistry* 9, 1933-1939.
19. Park, S., Morley, K. L., Horsman, G. P., Holmquist, M., Hult, K., Kazlauskas, R. J. (2005). Focusing mutations into the P. *fluorescens* esterase binding site increases enantioselectivity more effectively than distant mutations. *Chem. Biol.* 12, 45-54.
20. Schmidt, M., Hasenpusch, D., Kähler, M., Kirchner, U., Wiggenhorn, K., Langel, W., Bornscheuer, U. T. (2005). Directed evolution of an esterase from *Pseudomonas fluorescens* yields a mutant with excellent enantioselectivity and activity for the kinetic resolution of a chiral building block. *Chembiochem* 7, 805-809.
21. Ivancic, M., Valinger, G., Gruber, K., Schwab, H. (2007). Inverting enantioselectivity of *Burkholderia gladioli* esterase EstB by directed and designed evolution. *J. Biotechnol.* 129, 109-122.
22. Reetz, M.T., Bocola, M., Carballleira, J. D., Zha, D. X., Vogel, A., (2005). Expanding the range of substrate acceptance of enzyme: combinatorial active-site saturation test. *Angew. Chem. Int. Ed. Engl.* 44, 4192-4196.
23. Kourist, R., María, P., Bornscheuer, U. T. (2008). Enzymatic synthesis of optically active tertiary alcohols: expanding the biocatalysis toolbox. *Chembiochem* 9, 491-498.
24. Qian, Z., Fields, C. J., Lutz, S. (2007). Investigating the structural and functional consequences of circular permutation on lipase B from *Candida antarctica*. *Chembiochem* 8, 1989-1996.
25. Pleiss, J., Fischer, M., Peiker, M., Thiele, C., Schmid, R. D. (2000). Lipase engineering database - Understanding and exploiting sequence-structure-function relationships. *J. Mol. Catal. B: Enzym.* 10, 491-508.
26. Fischer, M., Pleiss, J. (2003). The lipase engineering database: a navigation and analysis tool for protein families. *Nucleic. Acids. Res.* 31, 319-321.
27. Torres-Gavilán, A., Castillo, E., López-Munguía, A. (2006). The amidase activity of *Candida antarctica* lipase B is dependent on

specific structural features of the substrates. *J. Mol. Catal. B: Enzym.* 41, 136-140.
28. Bernhardt, P., Hult, K., Kazlauskas, R. J. (2005). Molecular basis of perhydrolase activity in serine hydrolases. *Angew. Chem. Int. Ed. Engl.* 44, 2742-2746.
29. Nakagawa, Y., Hasegawa, A., Hiratake, J., Sakata, K. (2007). Engineering of *Pseudomonas aeruginosa* lipase by directed evolution for enhanced amidase activity: mechanistic implication for amide hydrolysis by serine hydrolases. *Protein Eng., Des. Sel.* 20, 339-346.
30. Bornscheuer, U., Kazlauskas, RJ. (2004). Catalytic promiscuity in biocatalysis: using old enzymes to form new bonds and follow new pathways. *Angew. Chem. Int. Ed. Engl.* 43, 6032-6040.
31. Svedendahl, M., Hult, K., Berglund, P. (2005). Fast carbon-carbon bond formation by a promiscuous lipase. *J. Am. Chem. Soc*. 127, 17988-17989.
32. Jochens, H., Stiba, K., Savile, C., Fujii, R., Yu, J. G., Gerassenkov, T., Kazlauskas, R. J., Bornscheuer, U. T. (2009). Converting an esterase into an epoxide hydrolase. *Angew. Chem. Int. Ed. Engl.* 48, 3532-3535.

References for Chapter 2

1. Del Campo, J.A., García-González, M., Guerrero, M.G. (2007) Outdoor cultivation of microalgae for carotenoid production: current state and perspectives. *Appl. Microbiol. Biotechnol.* 74, 1163-1174.
2. Maoka, T. (2009) Recent progress in structural studies of carotenoids in animals and plants. *Arch. Biochem. Biophys.* 483, 191-195.
3. Suhnel, S., Lagreze, F., Ferreira, J.F., Campestrini, L.H., Maraschin, M. (2009) Carotenoid extraction from the gonad of the scallop *Nodipecten nodosus* (Linnaeus, 1758) (Bivalvia: Pectinidae). *Braz. Biol.* 69, 209-215.
4. Yurkov, V.V., Beatty, J.T. (1998) Aerobic anoxygenic phototrophic bacteria. *Microbiol. Mol. Biol. Rev.* 62, 695-724.
5. Britton, G. (1995) Structure and properties of carotenoids in relation to function. *FASEB J.* 9, 1551-1558.
6. Janata, J., josowicz, A. (2003) Conducting polymers in electronic chemical sensors. *Nat. Mater.* 2, 19-24.
7. Das, A., Yoon, S.H., Lee, S.H., Kim, J.Y., Oh, D.K., Kim, S.W. (2007) An update on microbial carotenoid production: application of recent metabolic engineering tools. *Appl. Microbiol. Biotechnol.* 77, 505-512.
8. Zhu, C., Naqvi, S., Capell, T., Christou, P. (2009) Metabolic engineering of ketocarotenoid biosynthesis in higher plants. *Arch Biochem. Biophys.* 483, 182-190.

9. Mijts, B.N., Lee, P.C., Schmidt-Dannert, C. (2005) Identification of a carotenoid oxygenase synthesizing acyclic xanthophylls: combinatorial biosynthesis and directed evolution. *Chem. Biol.* 12, 453-460.
10. Torres-Gavilán, A., Castillo, E., López-Munguía, A. (2008) The amidase activity of *Candida antarctica* lipase B is dependent on specific structural features of the substrates. *J. Mol. Catal. B: Enzym.* 41, 136.
11. Faber, K. Bitransformations in organic chemistry. Springer 2004. p434

References for Chapter 3

1. Reviews: Grünewald, J., Marahiel, M.A. (2006) Chemoenzymatic and template-directed synthesis of bioactive macrocyclic peptides. *Microbiol Mol. Biol. Rev.* 70: 121-146; Kopp F, Marahiel MA (2007) Macrocyclization strategies in polyketide and nonribosomal peptide biosynthesis. *Nat. Prod. Rep.* 24: 735-749.
2. Mirza, I.A., Nazi, I., Korczynska, M., Wright, G.D., Berghuis, A.M. (2005) Crystal structure of homoserine transacetylase from *Haemophilus influenzae* reveals a new family of α/β-hydrolases *Biochemistry* 44 15768-15773.
3. Born, T.L., Franklin, M., Blanchard, J.S. (2000) Enzyme-catalyzed acylation of homoserine: mechanistic characterization of the *Haemophilus influenzae* met2-encoded homoserine transacetylase *Biochemistry* 39: 8556-8564.
4. Stubbe, J., Tian, J., He, A., Sinskey, A.J., Lawrence, A.G., Liu, P. (2005) Nontemplate-dependent polymerization processes: polyhydroxyalkanoate synthases as a paradigm. *Ann. Rev. Biochem.* 74: 433-480.
5. Wältermann, M., Stöveken, T., Steinbüchel, A. (2007) Key enzymes for biosynthesis of neutral lipid storage compounds in prokaryotes: properties function and occurrence of wax ester synthases/acyl-CoA: diacylglycerol acyltransferases. *Biochimie* 89: 230-242.

6. Trauger, J.W., Kohli, R.M., Mootz, H.D., Marahiel, M.A., Walsh, C.T. (2000) Peptide cyclization catalysed by the thioesterase domain of tyrocidine synthase. *Nature* 407: 215-218; Kohli, R.M., Burke, M.D., Tao, J., Walsh, C.T. (2003) Chemoenzymatic route to macrocyclic hybrid peptide/polyketide-like molecules. *J. Am. Chem. Soc.* 125: 7160-7161.
7. Kruger, R.G., Lu, W., Oberthür, M., Tao, J., Kahne, D., Walsh, C.T. (2005) Tailoring of glycopeptide scaffolds by the acyltransferases from the teicoplanin and A-40926 biosynthetic operons. *Chem. Biol.* 12: 131-140.
8. Xie, X., Watanabe, K., Wojcicki, W.A., Wang, C.C.C., Tang ,Y. (2006) Biosynthesis of lovastatin analogs with a broadly specific acyltransferase. *Chem Biol* 13: 1161-1169; Xie, X., Tang, Y. (2007) Efficient synthesis of simvastatin by use of whole-cell biocatalysis. *Appl. Environ. Microbiol.* 73: 2054-2060.
9. Bornscheuer, U.T., Kazlauskas, R.J. (2004) *Hydrolases in Organic Synthesis: Regio- and Stereoselective Biotransformations,* 2nd ed Wiley-VCH Chapter 5.
10. Tseng, C.C., Bruner, S.D., Kohli, R.M., Marahiel, M.A., Walsh, C.T., Sieber, S.A. (2002) Characterization of the surfactin synthetase C-terminal thioesterase domain as a cyclic depsipeptide synthase. *Biochemistry* 41 13350-13359.
11. Sharma, K.K., Boddy, C.N. (2007) The thioesterase domain from the pimaricin and erythromycin biosynthetic pathways can catalyze hydrolysis of simple thioester substrates. *Bioorg. Med. Chem. Lett.* 17: 3034-3037.
12. Ollis, D.L., Cheah, E., Cygler, M., Dijkstra, B., Frolow, F., Franken, S.M., Harel, M., Remington, S.J., Silman, I., Schrag, J., Sussman, J.L., Verschueren, K.H.G., Goldman, A. (1992) The α/β hydrolase fold. *Prot. Eng.* 5: 197-211; Holmquist, M. α/β-Hydrolase fold enzymes: structures functions and mechanisms. *Curr. Protein Pept. Sci.* 2000 1: 209-235.

13. Gibrat, J.F., Madej, T., Bryant, S.H. (1996) Surprising similarities in structure comparison. *Curr. Opin. Struct. Biol.* 6: 377-385; Madej, T., Panchenko, A.R., Chen, J., Bryant, S.H. (2007) Protein homologous cores and loops: important clues to evolutionary relationships between structurally similar proteins. *BMC Struct. Biol.* 7: 23.
14. Murzin, A.G., Brenner, S.E., Hubbard, T., Chothia, C. (1995) SCOP: a structural classification of proteins database for the investigation of sequences and structures. *J. Mol. Biol.* 247: 536-540.
15. Corey, E. J., Cimprich, K. A. (1992) Enantioselective routes to chiral benzylic thiols, sulfinic esters and sulfonic acids illustrated by the l-phenylethyl series. *Tet. Lett.* 33, 4099-4102.
16. Pflugrath, J.W. (1999) The finer things in diffraction data collection. *Acta. Crystallogr. Sect D Biol. Crystallogr.* 55: 1718-1725.
17. Otwinowski, Z., Minor, V. (1997) Processing of diffraction data collected in oscillation mode. *Methods Enzymol* 276: 307-326.
18. Jones, T.A., Zou, J.Y., Cowan, S.W., Kjeldgaard, M. (1991) Improved methods for building models in electron density maps and location of errors in these models. *Acta. Crystallogr. Sect. A Found Crystallogr.* 47: 110-119.
19. Murshudov, G.N., Vagin, A.A., Dodson, E.J. (1997) Refinement of macromolecular structures by the maximum-likelihood method. *Acta Crystallogr Sect D Biol Crystallogr* 53: 240-255.
20. Collaborative Computational Project, Number 4. (1994) The CCP4 suite: Programs for protein crystallography. *Acta Crystallogr Sect D Biol Crystallogr* 50: 760-763.
21. Perrakis, A., Morris, R., Lamzin, V.S. (1999) Automated protein model building combined with iterative structure refinement. *Nature Struct. Biol. 6*: 458-463.

22. Read, R.J. (1986) Improved Fourier coefficients for maps using phases from partial structures with errors. *Acta Crystallogr Sect A Found Crystallogr* 42: 140-149.
23. Laskowski, R.A. (1993) PROCHECK: A program to check the stereochemical quality of protein structures. *J. Appl. Crystallogr.* 26: 283-291.
24. a) Rose, G.D., Glerasch, L.M., Smith, J.A. (1985) Turns in peptides and proteins. *Adv. Prot. Chem.* 37: 1-109; Creighton TE *Proteins: Structure and Molecular Properties* 2nd ed Freeman: New York 1993 pp 225-227. b) Wilmot, C.M., Thornton, J.M. (1988) Analysis and prediction of the different types of β-turns in proteins. *J. Mol. Biol.* 203: 221-232.
25. Pleiss, J., Fisher, M., Peiker, M., Thiele, C., Schmid, R.D. (2000) Lipase engineering database: Understanding and exploiting sequence–structure–function relationships. *J. Mol. Catal. B Enzym.* 10: 491-508; Fischer, M., Pleiss, J. (2003) The Lipase Engineering Database: a navigation and analysis tool for protein families. *Nucl. Acid. Res.* 31: 319-321.
26. Chakravarty, B., Gu, Z., Chirala, S.S., Wakil, S.J., Quiocho, F.A. (2004) Human fatty acid synthase: structure and substrate selectivity of the thioesterase domain. *Proc. Natl. Acad. Sci. USA* 101: 15567-15572.
27. Jansson, A., Niemi, J., Mantsala, P., Schneider, G. (2003) Crystal structure of aclacinomycin methylesterase with bound product analogues: implications for anthracycline recognition and mechanism. *J. Biol. Chem.* 278: 39006-39013.
28. Mezzetti, A., Schrag, J.D., Cheong, C.S., Kazlauskas, R.J. (2005) Mirror-image packing in enantiomer discrimination molecular basis for the enantioselectivity of *B cepacia* lipase toward 2-methyl-3-phenyl-1-propanol. *Chem. Biol.* 12: 427-437.
29. Nardini, M., Lang, D.A., Liebeton, K., Jaeger, K.E., Dijkstra, B.W. (2000) Crystal structure of *Pseudomonas aeruginosa* lipase in the open

conformation The prototype for family I1 of bacterial lipases. *J. Biol. Chem.* 275: 31219-31225.

30. Lang, D.A., Stadler, P., Kovacs, A., Paltauf, F., Dijkstra, B.W. (1999) Structural and kinetic investigations of enantiomeric binding mode of subclass I lipases from the family of *Pseudomonadaceae* To be Published
31. Droege, M.J., Boersma, Y.L., van Pouderoyen, G., Vrenken, T.E., Rueggeberg, C.J., Reetz, M.T., Dijkstra, B.W., Quax, W.J. (2005) Directed evolution of *Bacillus subtilis* lipase A by use of enantiomeric phosphonate inhibitors: crystal structures and phage display selection. *ChemBioChem* 7: 149-157.
32. Line, K., Isupov, M.N., Littlechild, J.A. (2004) The crystal structure of a (-) γ-lactamase from an *Aureobacterium* species reveals a tetrahedral intermediate in the active site. *J. Mol .Biol.* 338: 519-532.
33. Forouhar, F., Yang, Y., Kumar, D., Chen, Y., Fridman, E., Park, S.W., Chiang, Y., Acton, T.B., Montelione, G.T., Pichersky, E., Klessig, D.F., Tong, L. (2005) Structural and biochemical studies identify tobacco SABP2 as a methyl salicylate esterase and implicate it in plant innate immunity. *Proc. Natl. Acad. Sci. USA* 102: 1773-1778.
34. Legler, P.M., Kumaran, D., Swaminathan, S., Studier, F.W., Millard, C.B. (2008) Structural characterization and reversal of the natural organophosphate resistance of a D-type esterase *Saccharomyces cerevisiae S*-formylglutathione hydrolase. *Biochemistry* 47: 9592-9601.
35. Cuff, M.E., Zhou, M., Collart, F., Joachimiak, A. (2005) Structure of a carboxylesterase from *Bacillus stearothermophilus*. To be published.
36. Bourne, P.C., Isupov, M.N., Littlechild, J.A. (2000) The atomic-resolution structure of a novel bacterial esterase. *Structure Fold Des* 8: 143-151.
37. Roussel, A., Miled, N., Berti-Dupuis, L., Riviere, M., Spinelli, S., Berna, P., Gruber, V., Verger, R., Cambillau C (2002) Crystal structure of the open form of dog gastric lipase in complex with a phosphonate inhibitor. *J. Biol. Chem.* 277: 2266-2274.

38. Roussel, A., Canaan, S., Egloff, M.P., Riviere, M., Dupuis, L., Verger, R., Cambillau, C. (1999) Crystal structure of human gastric lipase and model of lysosomal acid lipase two lipolytic enzymes of medical interest. *J. Biol. Chem.* 274: 16995-17002.

39. Bellizzi, J.J. 3rd, Widom, J., Kemp, C., Lu, J.Y., Das, A.K., Hofmann, S.L., Clardy, J. (2000) The crystal structure of palmitoyl protein thioesterase 1 and the molecular basis of infantile neuronal ceroid lipofuscinosis. *Proc. Natl. Acad. Sci. USA* 97: 4573-4578.

40. Calero, G., Gupta, P., Nonato, M.C., Tandel, S., Biehl, E.R., Hofmann, S.L., Clardy, J. (2003) The crystal structure of palmitoyl protein thioesterase-2 (PPT2) reveals the basis for divergent substrate specificities of the two lysosomal thioesterases PPT1 and PPT2. *J. Biol. Chem.* 278: 37957-37964.

41. Roussel, A., Yang, Y., Ferrato, F., Verger, R., Cambillau, C., Lowe, M. (1998) Structure and activity of rat pancreatic lipase-related protein 2. *J. Biol. Chem.* 273: 32121-32128.

42. Bourne, Y., Martinez, C., Kerfelec, B., Lombardo, D., Chapus, C., Cambillau, C. (1994) Horse pancreatic lipase The crystal structure refined at 2.3 Å resolution. *J. Mol. Biol.* 238: 709-732.

43. van Tilbeurgh, H., Egloff, M.P., Martinez, C., Rugani, N., Verger, R., Cambillau, C. (1993) Interfacial activation of the lipase-procolipase complex by mixed micelles revealed by X-ray crystallography. *Nature* 362: 814-820.

44. Kim, K.K., Song, H.K., Shin, D.H., Hwang, K.Y., Choe, S., Yoo, O.J., Suh, S.W. (1997) Crystal structure of carboxylesterase from *Pseudomonas fluorescens* an α/β hydrolase with broad substrate specificity. *Structure* 5: 1571-1584.

45. Devedjiev, Y., Dauter, Z., Kuznetsov, S.R., Jones, T.L., Derewenda, Z.S. (2000) Crystal structure of the human acyl protein thioesterase I from a single X-ray data set to 1.5 Å. *Structure Fold Des* 8: 1137-1146.

46. Derewenda, U., Brzozowski, A.M., Lawson, D.M., Derewenda, Z.S. (1992) Catalysis at the interface: the anatomy of a conformational change in a triglyceride lipase. *Biochemistry* 31: 1532-1541.
47. Brzozowski, A.M., Savage, H., Verma, C.S., Turkenburg, J.P., Lawson, D.M., Svendsen, A., Patkar, S. (2000) Structural origins of the interfacial activation in *Thermomyces* (*Humicola*) *lanuginosa* lipase. *Biochemistry* 39: 15071-15082.
48. Uppenberg, J., Hansen, M.T., Patkar, S., Jones, T.A. (1994) The sequence crystal structure determination and refinement of two crystal forms of lipase B from *Candida antarctica. Structure* 2: 293-308.
49. Benoit, I., Asther, M., Sulzenbacher, G., Record, E., Marmuse, L., Parsiegla, G., Herpoel-Gimbert, I., Asther, M,. Bignon, C. (2006) Respective importance of protein folding and glycosylation in the thermal stability of recombinant feruloyl esterase A. *FEBS Lett* 580: 5815-5821.
50. Wei, Y., Swenson, L., Castro, C., Derewenda, U., Minor, W., Arai, H., Aoki, J., Inoue, K., Servin-Gonzalez, L., Derewenda, Z.S. (1998) Structure of a microbial homologue of mammalian platelet-activating factor acetylhydrolases: *Streptomyces exfoliatus* lipase at 1.9 Å resolution. *Structure* 6: 511-519.
51. Zhang, R., Koroleva, O., Collert, F., Joachimiak, A. (2002) 1.5-Å crystal structure of the cephalosporin C deacetylase. To be published.
52. Schubot, F..D, Kataeva, I.A., Blum, D.L. ,Shah, A.K., Ljungdahl, L.G., Rose, J.P., Wang, B.C. (2001) Structural basis for the substrate specificity of the feruloyl esterase domain of the cellulosomal xylanase Z from *Clostridium thermocellum. Biochemistry* 40: 12524-12532.
53. Longhi, S., Czjzek, M., Lamzin, V., Nicolas, A., Cambillau, C. (1997) Atomic resolution (1.0 Å) crystal structure of *Fusarium solani* cutinase: stereochemical analysis. *J. Mol. Biol.* 268: 779-799.
54. Ghosh, D., Erman, M., Sawicki, M., Lala, P., Weeks, D.R., Li, N., Pangborn, W., Thiel, D.J., Jornvall, H., Gutierrez, R., Eyzaguirre, J.

(1999) Determination of a protein structure by iodination: the structure of iodinated acetylxylan esterase. *Acta Crystallogr Sect D Biol Crystallogr* 55: 779-784.

55. Hakulinen, N., Tenkanen, M., Rouvinen, J. (1998) Crystallization and preliminary X-ray diffraction studies of the catalytic core of acetyl xylan esterase from *Trichoderma reesei. Acta Crystallogr Sect D Biol Crystallogr* 54: 430-432.
56. Prates, J.A., Tarbouriech, N., Charnock, S.J., Fontes, C.M., Ferreira, L.M., Davies, G.J. (2001) The structure of the feruloyl esterase module of xylanase 10B from *Clostridium thermocellum* provides insights into substrate recognition. *Structure* 9: 1183-1190.
57. Chakravarty, B., Gu, Z., Chirala, S.S., Wakil, S.J., Quiocho, F.A. (2004) Human fatty acid synthase: structure and substrate selectivity of the thioesterase domain. *Proc Natl Acad Sci USA* 101: 15567-15572.
58. Ronning, D.R., Klabunde, T., Besra, G.S., Vissa, V.D., Belisle, J.T., Sacchettini, J.C. (2000) Crystal structure of the secreted form of antigen 85C reveals potential targets for mycobacterial drugs and vaccines. *Nat Struct Biol* 7: 141-146.
59. Ronning, D.R., Vissa, V., Besra, G.S., Belisle, J.T., Sacchettini, J.C. (2004) *Mycobacterium tuberculosis* Antigen 85A and 85C structures confirm binding orientation and conserved substrate specificity. *J Biol Chem* 279: 36771-36777.
60. Anderson, D.H., Harth, G., Horwitz, M.A., Eisenberg, D. (2001) An interfacial mechanism and a class of inhibitors inferred from two crystal structures of the *Mycobacterium tuberculosis* 30 kDa major secretory protein (Antigen 85B) a mycolyl transferase. *J Mol Biol* 307 671-681.
61. Bruner, S.D., Weber, T., Kohli, R.M., Schwarzer, D., Marahiel, M.A., Walsh, C.T., Stubbs, M.T. (2002) Structural basis for the cyclization of the lipopeptide antibiotic surfactin by the thioesterase domain SrfTE. *Structure* 10: 301-310.

62. Samel, S.A., Wagner, B., Marahiel, M.A., Essen, L.O. (2006) The thioesterase domain of the fengycin biosynthesis cluster: a structural base for the macrocyclization of a non-ribosomal lipopeptide. *J Mol Biol* 359: 876-889.

63. Wang, M., Liu, L., Wang, Y., Wei, Z., Zhang, P., Li, Y., Jiang, X., Xu, H., Gong, W. (2007) Crystal structure of homoserine *O*-acetyltransferase from *Leptospira interrogans. Biochem Biophys Res Commun* 363: 1050-1056.

64. Mirza, I.A., Nazi, I., Korczynska, M., Wright, G.D., Berghuis, A.M. (2005) Crystal structure of homoserine transacetylase from *Haemophilus influenzae* reveals a new family of α/β-hydrolases *Biochemistry* 44: 15768-15773.

65. Lejon, S., Ellis, J., Valegard, K. (2008) The last step in cephalosporin C formation revealed: crystal structures of deacetylcephalosporin C acetyltransferase from *Acremonium chrysogenum* in complexes with reaction intermediates. *J Mol Biol* 377: 935-944.

66. Chakravarty, B., Gu, Z., Chirala, S.S., Wakil, S.J., Quiocho, F.A. (2004) Human fatty acid synthase: structure and substrate selectivity of the thioesterase domain. *Proc Natl Acad Sci U S A* 101:15567-15572.

67. Akey, D.L., Kittendorf, J.D., Giraldes, J.W., Fecik, R.A., Sherman, D.H., Smith, J.L. (2006) Structural basis for macrolactonization by the pikromycin thioesterase. *Nat Chem Biol* 2: 537-542.

68. Tsai, S-C., Miercke, L.J.W., Krucinski, J., Gokhale, R., Chen, JC-H., Foster, P.G., Cane, D.E., Khosla, C., Stroud, R.M. (2001) Crystal structure of the macrocycle-forming thioesterase domain of the erythromycin polyketide synthase: Versatility from a unique substrate channel. *Proc Natl Acad Sci USA* 98 14808-14813.

69. Kursula, P., Ojala, J., Lambeir, A.M., Wierenga, R.K. (2002) The catalytic cycle of biosynthetic thiolase: a conformational journey of an acetyl group through four binding modes and two oxyanion holes. Biochemistry 41: 15543-15556.

70. Corey, E.J., Cimprich, K.A. (1992) Enantioselective routes to chiral benzylic thiols sulfinic esters and sulfonic acids illustrated by the l-phenylethyl series. *Tetrahedron Lett* 33: 4099-4102.
71. Piątek, A., Chapuis, C., Jurczak, J. (2002) Synthesis of a six-membered-ring (2*R*)-10a-homobornane-10a,2-sultam and structural comparison with Oppolzer's Lang's and King's sultams. *Helv Chim Acta* 85: 1973-1988.
72. Park, S., Morley, K.L., Horsman, G.P., Holmquist, M., Hult, K., Kazlauskas, R.J. (2005) Focusing mutations into the *P fluorescens* esterase binding site increases enantioselectivity more effectively than distant mutations. *Chem Biol* 12: 45-52.
73. Cheeseman, J.D., Tocilj, A., Park, S., Schrag, J.D., Kazlauskas, R.J. (2004) X-Ray crystal structure of an aryl esterase from *Pseudomonas fluorescens. Acta Crystallogr Sect D: Biol Crystallogr* 60: 1237-1243.
74. Samel, S.A., Wagner, B., Marahiel, M.A., Essen, L.O. (2006) The thioesterase domain of the fengycin biosynthesis cluster: a structural base for the macrocyclization of a non-ribosomal lipopeptide. *J Mol Biol* 359: 876-889.
75. Mezzetti, A., Schrag, J.D., Cheong, C.S., Kazlauskas, R.J. (2005) Mirror-image packing in enantiomer discrimination molecular basis for the enantioselectivity of *B cepacia* lipase toward 2-methyl-3-phenyl-1-propanol. *Chem Biol* 12: 427-437.
76. Nardini, M., Lang, D.A., Liebeton, K., Jaeger, K.E., Dijkstra, B.W. (2000) Crystal structure of *Pseudomonas aeruginosa* lipase in the open conformation The prototype for family I1 of bacterial lipases. *J Biol Chem* 275: 31219-31225.
77. Droege, M.J., Boersma, Y.L., van Pouderoyen, G., Vrenken, T.E., Rueggeberg, C.J., Reetz, M.T., Dijkstra, B.W., Quax, W.J. (2005) Directed evolution of *Bacillus subtilis* lipase A by use of enantiomeric phosphonate inhibitors: crystal structures and phage display selection. *ChemBioChem* 7: 149-157.

78. Roussel, A., Miled, N., Berti-Dupuis, L., Riviere, M., Spinelli, S., Berna, P., Gruber, V., Verger, R., Cambillau, C. (2002) Crystal structure of the open form of dog gastric lipase in complex with a phosphonate inhibitor. *J Biol Chem* 277: 2266-2274.
79. Derewenda, U., Brzozowski, A.M., Lawson, D.M., Derewenda, Z.S. (1992) Catalysis at the interface: the anatomy of a conformational change in a triglyceride lipase. *Biochemistry* 31: 1532-1541.
80. Ronning, D.R., Klabunde, T., Besra, G.S., Vissa, V.D., Belisle, J.T., Sacchettini, J.C. (2000) Crystal structure of the secreted form of antigen 85C reveals potential targets for mycobacterial drugs and vaccines. *Nat Struct Biol* 7: 141-146.
81. Henke, E., Pleiss, J., Bornscheuer, U.T. (2002) Activity of lipases and esterases towards tertiary alcohols: insights into structure-function relationships. *Angew Chem Intl Ed* 41 3211-3213.
82. Steffens, J.C. (2000) Acyltransferases in protease's clothing. *Plant Cell* 12: 1253-1256; Milkowski, C., Strack, D. (2004) Serine carboxypeptidase-like acyltransferases. *Phytochemistry* 65: 517-524.
83. Pillai, B., Cherney, M.M., Hiraga, K., Takada, K., Oda, K., James, M.N.G. (2007) Crystal structure of scytalidoglutamic peptidase with its first potent inhibitor provides insights into substrate specificity and catalysis. *J Mol Biol* 365 343-361.
84. Collins, T., De Vos, D., Hoyoux, A., Savvides, S.N., Gerday, C., Van Beeumen, J., Feller, G. (2005) Study of the active site residues of a glycoside hydrolase family 8 xylanase. *J Mol Biol* 354: 425-435.
85. Thomaeus, A., Carlsson, J., Åqvist, J., Widersten, M. (2007) Active site of epoxide hydrolases revisited: a noncanonical residue in potato StEH1 promotes both formation and breakdown of the alkylenzyme intermediate. *Biochemistry* 46: 2466–2479.
86. Negri, A., Marco, E., Damborsky, J., Gago, F. (2007) Stepwise dissection and visualization of the catalytic mechanism of haloalkane dehalogenase

LinB using molecular dynamics simulations and computer graphic.s *J Mol Graph Model* 26: 643-651.

87. Nicola, G., Peddi, S., Stefanova, M.E., Nicholas, R.A., Gutheil, W.G., Davies, C. (2005) Crystal structure of *Escherichia coli* penicillin-binding protein 5 bound to a tripeptide boronic acid inhibitor: a role for Ser-110 in deacylation. *Biochemistry* 44: 8207–8217.
88. Kourist, R., Bartsch, S., Fransson, L., Hult, L., Bornscheuer, U.T. (2008), Understanding promiscuous amidase activity of an esterase from *Bacillus subtilis*. *ChemBioChem* 9: 67–69.
89. Grochulski, P., Bouthillier, F., Kazlauskas, R.J., Serreqi, A.N., Schrag, J.D., Ziomek, E., Cygler, M. (1994) *Candida rugosa* lipase-inhibitor complexes simulating the acylation and deacylation transition states. *Biochemistry* 33: 3494-3500.
90. Wilmouth, R.C., Clifton, I.J., Robinson, C.V., Roach, P.L., Aplin, R.T., Westwood, N.J., Hajdu, J., Schofield, C.J. (1997) Structure of a specific acyl-enzyme complex formed between β-casomorphin-7 and porcine pancreatic elastase. *Nature Struct Biol* 4: 456-462; Wright, P.A., Wilmouth, R.C., Clifton, I.J., Schofield, C.J. (2001) Kinetic and crystallographic analysis of complexes formed between elastase and peptides from β-casein. *Eur J Biochem* 268: 2969-2974; Radisky, E.S., Lee, J.M., Lu, C-JK., Koshland, D.E. Jr (2006) Insights into the serine protease mechanism from atomic resolution structures of trypsin reaction intermediates. *Proc Natl Acad Sci USA* 103: 6835-6840.
91. Tseng, C.C., Bruner, S.D., Kohli, R.M., Marahiel, M.A., Walsh, C.T., Sieber, S.A. (2002), Characterization of the surfactin synthetase C-terminal thioesterase domain as a cyclic depsipeptide synthase. *Biochemistry* 41: 13350-13359.

References for Chapter 4

1. Born, T.L., Franklin, M., Blanchard, J.S. (2000) Enzyme-catalyzed acylation of homoserine: mechanistic characterization of the

Haemophilus influenzae met2-encoded homoserine transacetylase. *Biochemistry* 39, 8556-8564.

2. He, W., Wu, J., Khosla, C., Cane, D.E.(2006) Macrolactonization to 10-deoxymethynolide catalyzed by the recombinant thioesterase of the picromycin/methymycin polyketide synthase. *Bioorg. Med. Chem. Lett.* 16, 391-394.
3. Snellman, E.A., Colwell, R.R. (2008) Transesterification activity of a novel lipase from *Acinetobacter venetianus* RAG-1. *Antonie Van Leeuwenhoek* 94, 621-625.
4. Singh, M., Singh, S., Singh, R.S., Chisti, Y., Banerjee, U.C. (2008) Transesterification of primary and secondary alcohols using *Pseudomonas aeruginosa* lipase. *Bioresour. Technol.* 99, 2116-2120.
5. Jager, S.A., Shapovalova, I.V., Jekel, P.A., Alkema, W.B., Svedas, V.K., Janssen, D.B. (2008) Saturation mutagenesis reveals the importance of residues alphaR145 and alphaF146 of penicillin acylase in the synthesis of beta-lactam antibiotics. *J. Biotechnol.* 133, 18-26.
6. Chou, K.C. (2000) Prediction of tight turns and their types in proteins. *Anal. Biochem.* 286, 1-16.
7. Lemay, N.P., Morgan, A.L., Archer, E.J., Dickson, L.A., Megley, C.M., Zimmer, M. (2008) The role of the tight-turn, broken hydrogen bonding, Glu222 and Arg96 in the post-translational green fluorescent protein chromophore formation. *Chem. Phys.* 348, 152-160.
8. Luque, L.E., Grape, K.P., Junker, M. (2002) A highly conserved arginine is critical for the functional folding of inhibitor of apoptosis (IAP) BIR domains. *Biochemistry* 41, 13663-13671.
9. Chou, K.C., Blinn, J.R. (1997) Classification and prediction of beta-turn types. *J. Protein. Chem.* 16, 575-595.
10. Kaur. H., R., G.P. (2004) A neural network method for prediction of beta-turn types in proteins using evolutionary information. *Bioinformatics* 20, 2751-2758.
11. Gunasekaran, K., Gomathi, L., Ramakrishnan, C., Chandrasekhar, J., Balaram, P. (1998) Conformational interconversions in peptide beta-turns: analysis of turns in proteins and computational estimates of barriers. *J. Mol. Biol.* 284, 1505-1516.
12. Liua, A.M.F., Somersa, N.A., Kazlauskas, R.J., Brushb, T.S., Zocherc, F., Enzelbergerc, M.M., Bornscheuerc, U.T., Horsmana, G.P., Mezzettia, A., Schmidt-Dannertc, C., Schmidc, R.D. (2001) Mapping the substrate selectivity of new hydrolases using colorimetric screening: lipases from *Bacillus thermocatenulatus* and *Ophiostoma piliferum*, esterases from *Pseudomonas fluorescens* and *Streptomyces diastatochromogenes*. *Tetrahedron: Asymmetry* 12, 545-556.
13. Horsman, G.P., Liu, A.M., Henke, E., Bornscheuer, U.T., Kazlauskas, R.J. (2003) Mutations in distant residues moderately increase the enantioselectivity of *Pseudomonas fluorescens* esterase towards

methyl 3-bromo-2-methylpropanoate and ethyl 3phenylbutyrate. *Chem. Eur.J.* 9, 1933-1939.

14. Calloni, G., Zoffoli, S., Stefani, M., Dobson, C.M., Chiti, F. (2005) Investigating the effects of mutations on protein aggregation in the cell. *J. Biol. Chem.* 280, 10607-10613.
15. Ikura, K., Kokubu, T., Natsuka, S., Ichikawa, A., Adachi, M., Nishihara, K., Yanagi, H., Utsumi, S. (2002) Co-overexpression of folding modulators improves the solubility of the recombinant guinea pig liver transglutaminase expressed in *Escherichia coli*. *Prep. Biochem. Biotechnol.* 32, 189-205.
16. Thomas, J.G., Baneyx, F., (1997) Divergent effects of chaperone overexpression and ethanol supplementation on inclusion body formation in recombinant *Escherichia coli*. *Protein. Expression. Purif.* 11, 289-296.
17. Fischer, M., Pleiss, J. (2003) The lipase engineering database: a navigation and analysis tool for protein families. *Nucleic Acids Res.* 31, 319-321.
18. Sanki, A.K., Boucau, J., Ronning, D.R., Sucheck, S.J. (2009) Antigen 85C-mediated acyl-transfer between synthetic acyl donors and fragments of the arabinan. *Glycoconjugate. J.* 26, 589-596.